Annual Report

Leibniz–Institut für Kristallzüchtung
im Forschungsverbund Berlin e.V.

2014

IKZ

Annual Report

Leibniz–Institut für Kristallzüchtung
im Forschungsverbund Berlin e.V.

2014

Preface

Liebe Leserinnen und Leser, liebe Kolleginnen und Kollegen,

Das Institut hat auch im zurückliegenden Jahr seine Aktivitäten erfolgreich weitergeführt. Der vorliegende Bericht gibt einen Überblick über die Themen, die 2014 am Institut bearbeitet wurden, sowie über die aktuellen Ergebnisse aus der Forschung.

Die Erforschung und Entwicklung von technischen Neuerungen beruht zu einem wesentlichen Teil auf der Verfügbarkeit von kristallinen Materialien. Diese Verfügbarkeit wird häufig vorausgesetzt – tatsächlich ist sie jedoch oftmals nur sehr eingeschränkt gegeben oder nur für Material mit limitierter Qualität. Durch die fachliche Kompetenz und die gute technische Ausstattung ist das IKZ in der Lage, zum Teil einzigartige kristalline Materialien exklusiv für Forschungs- und Anwendungszwecke zur Verfügung zu stellen. Das IKZ bleibt damit ein gefragter Kooperationspartner für Forschung und Wirtschaft.

Ein Beispiel dafür ist der vor kurzem beantragte Leibniz-WissenschaftsCampus zur Erforschung von Materialien für die Oxidelektronik. Der Campus vernetzt Leibniz-Institute und Universitäten aus Berlin, Leipzig und Magdeburg. Eine wesentliche Grundlage der Forschungsaktivitäten bilden dabei die am IKZ gezüchteten halbleitenden Oxide, die anderweitig nicht verfügbar sind.

Andere Materialien werden zwar bereits kommerziell angeboten, ihre Verfügbarkeit ist jedoch stark eingeschränkt. Ein Beispiel hierfür ist Aluminiumnitrid. Diese Einkristalle bilden im wahrsten Sinne des Wortes die Grundlage für Forschungsaktivitäten im Konsortium Advanced UV for Life. Das Konsortium, das im Rahmen der BMBF-Initiative Unternehmen Region: Zwanzig20 – Partnerschaft für Innovation gefördert wird, beschäftigt sich mit der Entwicklung von UV-Leuchtdioden als Ersatz für die derzeit verwendeten Strahler auf Quecksilber-Basis. In dem Konsortium arbeitet das IKZ gemeinsam mit 12 weiteren Forschungseinrichtungen und 18 Partnern aus der Industrie.

Die einzigartigen Kompetenzen des Instituts beziehen sich jedoch nicht nur auf die Züchtung von neuen Materialien, sondern auch auf die Entwicklung von Kristallzüchtungstechnologien und ihre Anwendung. Das prominenteste Beispiel ist sicher das von der Physikalisch-Technischen Bundesanstalt in Braunschweig geleitete Projekt zur Neubestimmung der Avogadro-Konstante. Diese Naturkonstante gibt die Zahl von Teilchen in einer bestimmten Stoffmenge an, die durch das „Zählen" von Atomen in einem perfekten Einkristall ermittelt werden soll. Die Züchtung von Silizium-Einkristallen aus isotopenreinem Ausgangsmaterial ist mit der erforderlichen höchsten Perfektion und Reinheit weltweit nur am IKZ möglich. Die genaue Bestimmung der Konstante könnte letztendlich auch zu einer Neudefinition des Kilogramm-Maßstabs führen und damit das Ur-Kilogramm in Paris ablösen.

Bei der Lektüre dieses Berichts werden sie auf weitere interessante Beispiele treffen, die sich an dieser Stelle leider nicht alle nennen lassen.

Am IKZ wird exzellente Forschung betrieben. Das Institut gilt international als einzigartiges Kompetenzzentrum für alle Fragestellungen der Kristallzüchtung. Dies verdankt es in erster Linie seinen kompetenten und engagierten Beschäftigten, also den Wissenschaftlerinnen und Wissenschaftlern, dem technischen Personal und der Verwaltung. An dieser Stelle möchten wir auch unseren Zuwendungsgebern aus dem Land Berlin und dem Bund danken, die unsere Forschung durch ihre finanzielle Unterstützung erst ermöglichen.

Ich wünsche Ihnen eine unterhaltsame Lektüre,

Ihr

Günther Tränkle

Preface

Dear readers,
dear colleagues,

The institute has continued its research activities successfully in 2014. This annual report will give you an overview on the topics addressed during the last year, as well as on current research results.

The availability of crystalline materials is a key prerequisite for research and development of technical innovations. This availability is usually taken for granted – but in fact, for many materials this does not hold true or only for material with limited quality. Thanks to the professional expertise and its good technical equipment, IKZ is able to provide unique crystalline materials exclusively for research or application. Therefore, the institute is in demand as partner for research and industry.

The Leibniz ScienceCampus, which has been proposed just recently, may be one example. This network of research institutions and universities from Berlin, Leipzig and Magdeburg deals with research on materials for oxide electronics. Semiconducting oxides grown at IKZ are providing the essential basis for these activities, since these crystals are otherwise not available.

Other materials may be commercially available, but access is severely restricted. Like aluminium nitride, which is literally the basis for research activities in the consortium Advanced UV for Life. Funded by the German Federal Ministry for Education and Research (BMBF) in the frame of the program Twenty20 – Partnership for Innovation, the consortium deals with the development of UV light emitting diodes as substitute for mercury based emitters based. The IKZ is involved in these activities together with 12 further research institutions and 18 partners from industry.

Not only the growth of new materials, but also the development of growth technologies and their application belong to IKZ's unique competences. Probably the most prominent example is the project led by the National Petrology Institute of Germany (PTB) on a more precise determination of the Avogadro constant. This natural constant gives the number of particles in a certain amount of substance and shall be determined by "counting" the atoms in a perfect single crystal. Indeed, worldwide only IKZ is capable to grow such a crystal from isotopically pure raw material with the required highest perfection and purity. Eventually, the determination of the constant could lead to a redefinition of the kilogram standard, superseding the kilogram prototype kept in Paris.

While reading this report, you will find further interesting examples, which cannot all be named at this point, unfortunately.

At IKZ, excellent research is performed. The institute is internationally acknowledged as competence center for all issues concerning crystal growth. We owe this success to the commitment and the competences of our employees, i.e. the scientists, the technicians and administrative personnel. We would also like to thank the State of Berlin and the Federal Government for enabling our research with their financial support.

I hope you will enjoy reading this report.

Yours sincerely,
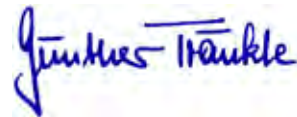
Günther Tränkle

Content

Classical Semiconductors

Dielectric & Wide Bandgap Materials

Layers & Nanostructures

Simulation & Characterization

The Institute

Foto: Lothar M. Peter

Leibniz-Institut für Kristallzüchtung im Forschungsverbund Berlin e.V.

FOUNDED 1992
PART of Forschungsverbund Berlin e.V.
MEMBER of the Leibniz Association (WGL)

STAFF	102
Scientists	58 (external funding: 21)
Ph.D. students	13
Technicians	40 (external funding: 6)
Trainees	4

BUDGET 2014	11.1 Mio €
Basic funding	8.9 Mio €
Third-party funding	2.2 Mio €

The Institute

Das Leibniz-Institut für Kristall-züchtung (IKZ)

ist eine staatliche Forschungs- und Service-Einrichtung, die sich experimentell und theoretisch mit den wissenschaftlich-technischen Grundlagen des Wachstums, der Züchtung, der Bearbeitung und der physikalischchemischen Charakterisierung von kristallinen Festkörpern beschäftigt. Dies reicht von der Grundlagenforschung bis hin zum Vorfeld industrieller Entwicklung. Die zurzeit entwickelten Materialien finden vorwiegend Verwendung in der Mikro-, Opto- und Leistungselektronik, der Photovoltaik, in Optik und Lasertechnik, in der Sensorik und Akustoelektronik.

Das Forschungsgebiet des IKZ umfasst Volumenkristalle, kristalline Schichten und Nanostrukturen sowie die Entwicklung von materialübergreifenden Kristallzüchtungstechnologien.

Arbeitsschwerpunkte des Institutes sind:

- *Entwicklung von Züchtungs-, Bearbeitungs- und Charakterisierungsverfahren für Massivkristalle sowie kristalline Gebilde mit Abmessungen im Mikro- und Nanometerbereich sowie von materialübergreifenden Kristallzüchtungstechnologien*

- *Bereitstellung von Kristallen mit speziellen Spezifikationen für Forschungs- und Entwicklungszwecke*

- *Modellierung und Erforschung der Kristallwachstums- und Kristallzüchtungsprozesse*

- *Experimentelle und theoretische Untersuchungen zum Einfluss von Prozessparametern auf Kristallzüchtungsvorgänge und Kristallqualität*

- *Erarbeitung von Verfahren zur Kristallbearbeitung und Erforschung der dabei ablaufenden Vorgänge*

- *Physikalisch-chemische Charakterisierung kristalliner Festkörper und damit verbunden die Entwicklung geeigneter Methoden; Untersuchung von Materialeigenschaften und den zugrundeliegenden Vorgängen*

- *Entwicklung und Bau von Anlagenkomponenten für die Züchtung, Bearbeitung und Charakterisierung von Kristallen*

Als Züchtungsverfahren werden Methoden der Züchtung aus der Schmelze, aus der Lösung, aus der Gasphase und davon abgeleitete Verfahren zur Herstellung kristalliner Schichten verwendet.

Durch die mögliche Synergie zwischen Volumenkristallzüchtung und der Abscheidung von Schichten verfügt das Institut über ideale Voraussetzung zur Herstellung von Substrat/Schicht-Kombinationen mit maßgeschneiderten Eigenschaften.

Materialien

- *Halbleiter mit großem Bandabstand (AlN- und GaN-Kristalle) für Hochtemperatur-, Leistungs- und Optoelektronik*

- *Oxidische und fluoridische Kristalle für Lasertechnik, Optik, Sensorik und Akustoelektronik*

- *Silizium-Kristalle für Leistungselektronik und Photovoltaik*

- *Silizium/Germanium Kristalle für Strahlungsdetektoren und Beugungsgitter*

- *Silizium Schichten auf amorphen Unterlagen für die Photovoltaik*

- *Kristalline Schichten mit Dimensionen im Mikro- und Nanometerbereich (epitaktische halbleitende oder ferroelektrische oxidische Schichten, SiGe-Mikrostrukturen und Si-Nanowhisker)*

The Leibniz Institute for Crystal Growth

is a governmental research and service institute, which is theoretically and experimentally investigating the scientific-technical fundamentals of crystal growth, processing and physico-chemical characterisation of crystalline solids. This ranges from explorative fundamental research to pre-industrial development. The materials presently in development are of fundamental importance in micro-, opto- and power electronics, in photovoltaics, in opto- and laser technology, in acousto-electronics and sensor technology as well as for fundamental research.

The research activities of the institute include bulk single crystals as well as crystalline layers and nanostructures, but also the development of comprehensive crystal growth technologies, which are suitable for different materials.

The Institute

The research and service tasks of the institute include:

- Development of technologies for growth, processing and characterization of bulk crystals and of crystalline structures with dimensions in the micro- and nanometer range and of comprehensive growth technologies

- Supply of crystals with non-standard specifications for research and development purposes

- Modelling and investigation of crystal growth processes

- Experimental and theoretical investigations of the influence of process parameters on crystal growth processes and crystal quality

- Development of technologies for the chemo-mechanical processing of crystalline samples and scientific investigation of related processes

- Physico-chemical characterisation of crystalline solids and development of suitable methods; investigation of the correlation between physical properties and related physical processes

- Development and construction of components for growth, processing and characterization of crystals

Crystals are grown from the melt, from solutions and from the vapour phase and new techniques are developed and improved for the preparation of crystalline layers.

With the combination of bulk crystal growth and layer deposition, the institute possesses ideal conditions to produce customized substrate/layer-combinations.

Materials presently in development

- Wide band gap semiconductors (crystalline AlN and GaN) for high temperature, power- and optoelectronics

- Oxide and fluoride crystals for acousto-electronics, laser-, opto- and sensor technology

- Si-crystals for power electronics and photovoltaics

- Si/Ge-crystals for radiation detectors and diffraction gratings

- Si layers an amorphous substrates for photovoltaics

- Crystalline layers with dimensions in the micro- and nanometer range (semiconducting or ferroelectric oxide layers, SiGe-microstructures and Si-nanowhisker)

Organisation Chart/Organigramm

Forschungsverbund Berlin e.V. Dr. M. Urban	Acting Director Prof. Dr. G. Tränkle	Scientific Advisory Board

Department **Classical Semiconductors** Acting Head: Dr. F.-M. Kießling	Department **Dielectric & Wide Bandgap Materials** Head: Prof. Dr. M. Bickermann	Department **Layers & Nanostructures** Acting Head: Dr. G. Wagner	Section **Simulation & Characterization** Coordinator: PD Dr. D. Klimm
Silicon & Germanium	Oxides/Fluorides	Semiconducting Oxide Layers	Physical Characterization
Multi-crystalline Silicon	Gallium Nitride	Si/Ge Nanocrystals	Electron Microscopy
Gallium Arsenide	Aluminium Nitride	Ferroelectrical Oxide Layers	Chemical & Thermodynamic Analysis
			Crystal Machining

General Service: Administration, Computing, Library, Technical Service

The Institute

Scientific Advisory Board 2014
Wissenschaftlicher Beirat 2014

Dr. Stefan Eichler (Chairman)
Freiberger Compound Materials GmbH, Freiberg

Dr. Lothar Ackermann
Forschungsinstitut für mineralische und metallische Werkstoffe,
Edelsteine/Edelmetalle – FEE GmbH, Idar-Oberstein

Dr. Hubert Aulich
SC Sustainable Concepts GmbH, Erfurt

Prof. Dr. Silke Christiansen
Helmholtz-Zentrum Berlin für Materialien und Energie HZB, Berlin

Prof. Dr. Knut Deppert
Department of Solid State Physics, Lund University, Sweden

Prof. Dr. Saskia Fischer
Department of Physics, Humboldt-Universität zu Berlin

apl. Prof. Dr.-Ing. Michael Heuken
Faculty of Electrical Engineering and Information Technology,
RWTH Aachen University & Vice President of Research and Development
AIXTRON AG, Aachen

Prof. Dr. Michael Kneissl
Institute of Solid State Physics, Technische Universität Berlin

Prof. Dr. Götz Seibold
Brandenburgische Technische Universität BTU, Cottbus-Senftenberg

Dr. Ulrich Steegmüller
Head of Research and Technology OSRAM Opto Semiconductors GmbH, Regensburg

Prof. Dr. Eicke Weber
Fraunhofer Institute for Solar-Energy-Systems ISE, Freiburg

Representative of the State of Berlin

Marie Trappiel
Senatsverwaltung für Wirtschaft, Technologie und Forschung, SenWTF Berlin

Representative of the Federal Republic

Dr. Fabian Kohler
Bundesministerium für Bildung und Forschung, BMBF Bonn / Berlin

Guests

Dr. Manuela Urban
Forschungsverbund Berlin e.V.

Prof. Dr. Martha Ch. Lux-Steiner
Helmholtz-Zentrum für Materialien und Energie HZB, Berlin

6. Internationaler Workshop on Crystal Growth Technology (IWCGT-6)

Von 15.–19. Juni 2014 trafen sich in Berlin die welt-weit führenden Experten zum sechsten Internationalen Workshop zur Kristallzüchtungstechnologie (IWCGT-6). Der Workshop wurde in diesem Format zum zweiten Mal durch das Leibniz-Institut für Kristallzüchtung in Berlin organisiert und stand erneut unter der Schirm-herrschaft der International Organization for Crystal Growth IOCG. Er bot eine einzigartige Gelegenheit für Forscher, Entwickler und Anwender aus der Industrie und den Forschungsinstituten, sich über Technologien und neue Entwicklungen in der angewandten Kristall-züchtung auszutauschen. Über 120 Teilnehmer aus 26 Staaten – viele Kollegen aus den USA, Japan, Russland, China, Frankreich, aber auch aus Tschechien, Polen, der Ukraine, Algerien oder Saudi Arabien – hörten sich an vier Tagen 28 Fachvorträge erfahrener Spezialisten an. Zudem stellten knapp 60 Teilnehmer ihre eigene Arbeit im Rahmen der beiden Posterpräsentationen vor, und sechs Firmen zeigten in einer Ausstellung oder mit Kurzvorträgen ihre aktuellen Entwicklungen.

Kristalline Materialien bilden die Grundlage für eine Vielzahl von modernen Anwendungen in den Bereichen Leistungs-, Opto- und Mikroelektronik, den optischen Technologien, der Photovoltaik, in Detektor- und Sen-sortechnik. Damit können diese Materialien einen be-deutenden Beitrag für die grundlegenden Herausforde-rungen der heutigen Gesellschaft leisten. Dazu zählen u.a. Bereiche wie Energieumwandlung und -speiche-rung, Sicherheit, Informations- und Kommunikations-technik, Mobilität. Dabei spielt nicht nur die Erforschung neuer kristalliner Verbindungen eine Rolle, sondern auch die Entwicklung von kostengünstigen Technologi-en für die Herstellung von Kristallen hoher Perfektion.

Vor diesem Hintergrund wurde während des Workshops der aktuelle Stand der Forschung und Technik themati-siert. Neben Sessions zu verschiedenen Materialkatego-rien wurden auch Fragestellungen der Qualitätskont-rolle oder des Ressourcenmanagements angesprochen. Nachdem der Workshop mit einer offenen Podiumsdis-kussion zum Thema „Die Zukunft der Kristallzüchtungs-technologie – wie bringt man neue Technologien zur industriellen Anwendung?" startete, schloss er mit ei-ner Session zu den aktuellen Herausforderungen der Kristallzüchtungstechnologie.

Die Tagung wurde von den Teilnehmern und den Orga-nisatoren als großer Erfolg gewertet. Auch das Format zwischen Schule und Konferenz, das den Teilnehmen-den viel Zeit zum fachlichen Austausch und zur Diskus-sion bot, wurde sehr positiv aufgenommen. Wir danken an dieser Stelle nochmals den Sponsoren der Veranstal-tung für ihre Unterstützung. Nähere Informationen finden sich unter http://iwcgt-6.ikz-berlin.de.

6th International Workshop on Crystal Growth Technology (IWCGT-6)

From 15–19 June 2014, the world's leading experts met in Berlin at the 6th International Workshop on Crystal Growth Technology (IWCGT-6) held under the auspices of the International Organization for Crystal Growth IOCG. For the second time, the IWCGT had been organized in this format by the Leibniz Institute for Crystal Growth, Berlin. The workshop provides a unique platform for researchers and users from industry and research ins-titutions to establish an open dialog on growth techno-logies as well as recent developments in crystal growth. More than 120 participants attended from 26 coun-tries, from USA, Japan, Russia, China, France, to Poland,

Events

Ukraine, Czech Republic, Algeria and Saudi Arabia. For four days, 28 talks were given by experienced specialists, 60 participants presented their results in two poster sessions and six companies showed their portfolio either as exhibition or as short oral presentation.

Many modern devices and applications from power-, opto- and microelectronics, optical technologies, photovoltaics and in detector and sensor technology are based on crystalline materials. This means, such materials will also contribute to the fundamental challenges of the modern society, including energy conversation and storage, security, information and communication or mobility. To this end, not only the research on new crystalline materials may play a crucial role, but also the development of cost-efficient technologies for the production of high perfection crystals.

Against this background, the state of the art in research and technology was discussed during the workshop. In addition to topical sessions on different types of materials, also issues like quality assurance or management of resources were addressed. Starting with an open panel discussion on "The future of crystal growth technology – bringing new technologies to industrial growth application", the event closed with a session on the "Frontiers in crystal growth technology".

The IWCGT-6 has been considered as great success by both participants and organizers. Especially the format of the workshop between school and conference, including many opportunities for discussion has been appreciated. At this point we would to thank again our sponsors for their support. More information may be found under http://iwcgt-6.ikz-berlin.de

Beruf und Familie

Die Vereinbarkeit von Beruf und Familie ist ein wichtiges Thema in der heutigen Arbeitswelt. Das Institut hat sich dazu entschlossen, sich dieser Fragestellung explizit anzunehmen und einen internen Diskussionsprozess zu starten. Ziel ist es, für alle Beschäftigten nachhaltig familienfreundliche Arbeitsbedingungen zu schaffen bzw. zu erhalten.

Unterstützt wird das Institut in diesem Prozess durch das audit berufundfamilie, bzw. von der berufundfamilie gGmbH. Nach Erfassung des Status Quo der bereits vorhandenen Maßnahmen wird das mögliche Entwicklungspotential in acht möglichen Handlungsfeldern ermittelt. Verbindliche Zielvereinbarungen sorgen für die Verankerung des Familienbewusstseins in der Institutskultur. Das Institut hat diesen Prozess in 2014 begonnen und strebt eine Zertifizierung durch das audit berufundfamilie in 2015 an. Das audit steht unter der Schirmherrschaft der Bundesfamilienministerin und des Bundeswirtschaftministers, nähere Informationen finden sich unter www.beruf-und-familie.de.

Work and life balance

The reconciliation of professional and family life is a relevant aspect in today's working environment. After the institute decided to take up this question explicitly, we started internal discussions on this topic. With this, we are aiming at providing a sustainable family-friendly working environment for all of IKZ's staff members.

The audit berufundfamilie, respectively the berufandfamilie gGmbH supports the institute through this process. After providing an overview on the already existing activities, possible measures are determined in eight different fields of action. Eventually, the awareness on family issues should be integrated in every days working life by defining binding procedures. This process has been initiated in 2014, aiming at the certification of IKZ by the audit berufundfamilie in 2015. This certificate is issued under the auspices of the German Federal Minister for Families and the German Federal Economics Minister. More information is available under www.beruf-und-familie.de

Classical Semiconductors
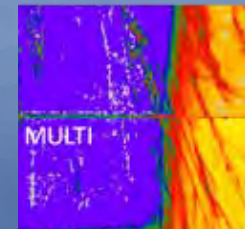
Classical Semiconductors

Acting head of department: Dr. Frank M. Kießling

Die Abteilung „Klassische Halbleiter" sieht sich als Teil eines führenden Instituts der Kristallzüchtung in Europa und Deutschland in der Verantwortung, Forschung und Entwicklung auf dem Gebiet der Massivkristallzüchtung weiter voranzutreiben. Obwohl die Mittelbeschaffung sehr anspruchsvoll ist, konnten wiederum fast 2/3 des wissenschaftlichen und technischen Personals der Abteilung über Drittmittel finanziert werden, u.a. auf der Basis verschiedener bilateraler Industrieprojekte. Die Arbeiten in der Abteilung umfassen die Züchtung von Volumenkristallen der elementaren Halbleiter Silicium, Germanium und deren Mischkristallen, sowie der klassischen Verbindungshalbleiter aus der Schmelze. Als Methoden werden im wesentlichen Floating Zone (FZ), Czochralski (CZ) und Vertical Gradient Freeze (VGF) eingesetzt. Alle VGF- und mehrerer CZ-Kristallzüchtungsanlagen sind mit speziellen KRISTMAG® Heizer-Magnet-Modulen zur Erzeugung von Wandermagnetfeldern ausgerüstet. Die Stärke und Richtung der wirkenden Lorentzkräfte werden so erzeugt, dass über diese kontaktlose Beeinflussungsmöglichkeit die Strömungen der Schmelze kontrolliert werden können.

In den Themengrupen „Multikristallines Silicium" und „Galliumarsenid" wird der Einfluss dieser nicht-stationären Magnetfelder auf die Züchtungsbedingungen und damit die Kristalleigenschaften erforscht. Nach der Methode der gerichteten Erstarrung werden Si-Blöcke verschiedener Größe gezüchtet. Die Prozessentwicklung zur Verringerung von rekombinationsaktiven Defektstrukturen in multikristallinem oder sogar quasi-einkristallinem Silicium für photovoltaische Anwendungen steht im Mittelpunkt der Arbeiten. Die Forschungsaktivitäten zum GaAs fokussieren sich insbesondere auf die Steigerung der Effizienz des VGF-Züchtungsprozesses. Zur Lösung dieser technologischen und wissenschaftlichen Herausforderung werden unterschiedliche Strategien verfolgt, z.B. die simultane Kristallisation in mehreren Tiegeln sowie die Erhöhung der Kristallisationsgeschwindigkeit. Das Material wird in Baugruppen der WLAN-Kommunikation sowie in der Mikrowellen- und Hochfrequenz-Technologie eingesetzt. In der Themengruppe „Silicium und Germanium" ist die Züchtung von Si-Kristallen und auch isotopenreinen Si-Kristallen mit der FZ Methode bis zu 150 mm im Durchmesser im Fokus. Ein zweiter Schwerpunkt der Forschungsarbeiten ist die Prozessentwicklung zur Züchtung von hochreinen Ge-Einkristallen. Es wird monokristallines Silizium für die Leistungselektronik, Germanium für Detektoren sowie $Si_{1-x}Ge_x$ für Strahlungsdetektoren und Beugungsgitter gezüchtet. SiGe-Kristalle wurden als Gradientenkristalle und als Mosaikkristalle mit kontrollierter Mosaizität gezüchtet.

Modellierer sind in die einzelnen Gruppen der Abteilung integriert und unterstützen die Prozessentwicklungen durch numerische Simulationen. Hauptsächlich werden globale Temperaturfelder berechnet und der Einfluss magnetischer Felder auf die Wachstumsbedingungen untersucht.

Der überwiegende Anteil der Forschungsarbeiten in der Abteilung wird durch eine Vielzahl nationaler und internationaler Projektpartner aus der Industrie eingefordert. So wurde u.a. unter der Federführung der Physikalisch-Technischen Bundesanstalt das internationale Projekt „Kilogramm-2" in der Gruppe „Silicium & Germanium" fortgeführt. Im Rahmen eines BMWi-Projektes wurden in der Gruppe „Multikristallines Silicium" Prozessentwicklungen unter Anwendung von magnetischen Wanderfeldern zur gerichteten Erstarrung in der in 2013 erworbenen G2-Anlage (75 kg) fortgesetzt. Auch wurde erfolgreich das Know-how der Beschichtungstechnologie für Quarzgut- und Kieselglastiegel in die Gruppe überführt. Der GaAs-Themengruppe gelang die Züchtung versetzungsarmer Kristalle nach dem VGF Verfahren unter Nutzung geeigneter Magnetfelder. Dabei konnten mehrere Kristalle simultan in einem Rezipienten gezüchtet werden.

The department „Classical Semiconductors" as part of a leading institute in crystal growth in Europe and Germany sees itself in the responsibility to advance research and development in the field of bulk crystal growth. Although the fund-raising is very demanding, again nearly 2/3 of the scientific and technical staff of the department could be financed by third-party funds and several bilateral industrial projects. The main task in the department is the growth of bulk crystals of the elementary semiconductors silicon, germanium and their solid solutions, as well as the classical semiconductor compound materials. Basically, Floating Zone (FZ), Czochralski (CZ) and Vertical Gradient Freeze (VGF) are the methods used. All the VGF- and several CZ-growth furnaces are equipped with special KRIST*MAG*® heater magnet modules in order to produce travelling magnetic fields. Applying this contactless interference method the strength and direction of acting Lorentz forces are generated in order to control melt flows.

In the groups „Multi-crystalline Silicon" and „Gallium Arsenide" the influence of these non-stationary magnetic fields on the growth conditions and hence, the crystal qualities are investigated. Silicon ingots of different sizes have been directionally solidified. Solidification processes have been developed to reduce recombination active defect structures in multi-crystalline or even quasi-mono silicon used for photovoltaic applications. The GaAs research activities focus themselves in particular on the efficiency increase of the VGF growth process. Different strategies are pursued to tackle these technological and scientific challenges, e.g. the simultaneous growth in several crucibles as well as an increase of the crystallization rate. The material is used in WLAN communication devices as well as in the microwave and high-frequency technology. The group „Silicon and Germanium" focused on the growth of Si crystals and also isotope-pure Si crystals applying the method FZ up to 150 mm in diameter. Furthermore, the process development of highly pure Ge single crystals is another main research project. Single crystalline silicon has been grown for power electronics, germanium for detectors as well as $Si_{1-x}Ge_x$ for radiation detectors and diffraction gratings. SiGe crystals have been grown as gradient crystals and as mosaic crystals with controlled mosacity.

Modelers are integrated in the different groups of the department to support the process developments by numerical simulations. Primarily, global temperature fields are simulated and the influence of magnetic fields on the growth conditions is studied.

Most of the research projects of the department are demanded by numerous national and international industry partners. For instance among others, the international project „Kilogramm 2" has been continued in the group "Silicon & Germanium" under the leadership of the German National Metrology Institute. Within the scope of a BMWi project process developments were continued in the group „Multi-crystalline Silicon" using magnetic travelling fields during directional solidification in the G2 arrangement acquired in 2013 (75 kg). Also the know-how of the coating technologies for quartz ceramic and fused silica crucibles were transferred successfully to the group. The group "GaAs" succeeded in growing dislocation-reduced crystals by the VGF method using suitable magnetic fields. In doing so, several crystals could be grown simultaneously in one furnace.

Classical Semiconductors:
Silicon & Germanium

Head   Dr. Nikolay Abrosimov
Team   M. Czupalla, J. Fischer, B. Hallmann-Seifert, S. Kayser, L. Lehmann, Dr. A. Lüdke, Dr. R. Menzel,
        Dr. W. Miller, Dr. M. Neubert, K. Reinhold, M. Renner, Dr. H. Riemann, Dr. H. Rost, T. Turschner

Übersicht

Silizium und Germanium sind die Halbleiter mit den meisten Anwendungen in der modernen Industrie wie zum Beispiel in der Mikroelektronik, Photonik und Photovoltaik. Die Themengruppe Silizium & Germanium konzentrierte sich wie Jahre zuvor auf die Float-Zone (FZ)-Züchtung von Silizium und die Czochralski (Cz)-Züchtung von Germanium. Unsere langjährige Erfahrung in der Züchtung von Si/Ge-Mischkristallen wird derzeit angefragt für die Züchtung von Kristallen, für die Untersuchung ihrer thermoelektrischen Eigenschaften (Kooperation mit dem Fraunhofer-Institut für Physikalische Messtechnik, IPM, Freiburg) oder für Leviations-Experimente zur Bestimmung von thermo-physikalischen Eigenschaften der Schmelzen (Universität Göttingen, ESA-Projekt SEMITERM).

Eines der Highlights in der Gruppe waren die Arbeiten im Rahmen des internationalen Projektes „Kilogramm 2" unter der Leitung und Finanzierung der Physikalisch-Technischen Bundesanstalt (PTB). Ziel dieses Projekts ist eine genauere Bestimmung der Avogadro-Konstante. Diese gibt die Zahl von Atomen einer festgelegten Stoffmenge an, in diesem Fall von einem Mol. Zu diesem Zweck bestimmt die PTB die Zahl der Atome in einer perfekten Silizium-Kugel, die aus dem stabilen Isotop mit der atomaren Masse 28 (^{28}Si) besteht. Diese Kugeln werden aus einem am IKZ gezüchteten Kristall höchster Perfektion und Reinheit präpariert, was erlaubt, das Volumen der Kugel mit der Zahl der Atome in der hochgeordneten Kristallstruktur zu verknüpfen.

Nach der Lieferung eines polykristallinen Stabs ^{28}Si aus Russland wurden zunächst fünf Float-Zone Durchgänge zur Reinigung des Materials durchgeführt. Durch die aufwändige und kostenintensive Herstellung steht nur eine begrenzte Menge des hoch mit ^{28}Si angereicherten Ausgangsmaterials zur Verfügung, in diesem Fall knapp unter 6 kg. Wir mussten entsprechend neue Techniken entwickeln, um selbst kleine Verluste an dem kostspieligen Material während der Züchtung zu minimieren. Insgesamt stand gerade ausreichend Material zur Verfügung, um daraus genau einen Einkristall zu züchten mit dem erforderlichen Volumen zur Präparation von zwei Kugeln.

Hoch isotopenangereicherte, ultrareine Materialien wie Silizium, aber auch Germanium sind Gegenstand weiterer Forschungsaktivitäten. Derzeit wird in unserer Gruppe eine Technologie zur Züchtung von hochreinen Germanium-Kristallen entwickelt, die für Detektoren im Projekt GERDA (GERmanium Detector Array) verwen- det werden sollen. Im Jahre 2014 wurden dazu Cz-Züchtungsversuche durchgeführt mit dem Ziel, die thermische Zone mit Hilfe der globalen Computersimulation zu optimieren. Der Schwerpunkt der vergangenen Arbeiten lag jedoch auf der Entwicklung und Konstruktion einer Zonenreinigungsanlage, mit der die bislang fehlende Verfügbarkeit von gut definiertem, polykristallinem Germanium als Ausgangsmaterial für die Cz-Züchtung sichergestellt werden soll. Diese Anlage wird derzeit in Betrieb genommen.

Eine weitere Herausforderung ist die Herstellung von Germanium-Einkristallen, die mit flüchtigen Elementen wie Phosphor dotiert sind, bzw. mit Elementen mit einem Verteilungskoeffizienten in Ge größer als 1, wie beispielsweise Bor mit $k_o \approx 12$. Für diese Zwecke wurde ein Züchtungsverfahren entwickelt, basierend auf der Dotierung aus der Gasphase unter Verwendung von Phosphin für Phosphor-Dotierung und Diboran für Bor-Dotierung. Die Kristalle werden nach dem mini-Cz-Verfahren hergestellt, das für die Züchtung von isotopenreinem Si und Ge aus extrem kleinen Mengen des Ausgangsmaterials entwickelt wurde. Weitere Germanium-Kristalle, undotiert oder dotiert mit anderen Elementen der Gruppe III oder V, wurden in verschiedenen kleinen Projekten und im Rahmen des BMBF-Projekts InTerFEL (Materialentwicklung für einen schnellen Terahertz-Detektor) gezüchtet.

Overview

Silicon and germanium are semiconductor materials with large areas of application in modern industry such as microelectronics, photonics and photovoltaics. The Silicon & Germanium group focuses its activities on Float-Zone (FZ) growth of silicon and Czochralski (Cz) growth of germanium. In addition, the experience in the crystal growth of SixGe1-x solid solutions is used to grow specific crystals provided for the investigation of thermo-electrical properties (e.g. in cooperation with Fraunhofer-Institut für Physikalische Messtechnik IPM, Freiburg) or for levitation experiments with the goal to investigate the thermo-physical properties of the semiconductor melts (University of Göttingen, ESA project SEMITHERM).

Classical Semiconductors: **Silicon & Germanium**

One of our highlights have been the activities in frame of the international project "Kilogramm-2" under the leadership of Physikalisch-Technische Bundesanstalt (PTB) – German National Metrology Institute. This project aims at a more precise determination of the Avogadro constant, which describes the number of atoms contained in a certain quantity of substance, for the constant this would be one mole. To accomplish this, the PTB counts the atoms in perfect spheres of silicon enriched with ^{28}Si – one of the stable Si isotops. These spheres are prepared from single crystals grown in our group at IKZ, giving a connection between the volume and the number of atoms in the highly ordered crystalline structure. In 2014, a rod of 6 kg polycrystalline ^{28}Si was delivered from Russia and the first 5 FZ-runs were carried out for additional purification. Due to the elaborate manufacturing process of the high isotopic enriched ^{28}Si, the starting material is extremely valuable and the amount of isotopically pure silicon was limited. This meant that we had to develop new techniques to achieve the highest yield possible for the crystal the spheres will be prepared of.

Highly isotopically enriched, ultra pure materials like silicon, but also germanium are in demand also for other research activities. Currently our group is developing a technology for the growth of germanium single crystals with high purity, to be used in the project GERDA – GERmanium Detector Array. In 2014, some Ge Cz-growth experiments based on thermal zone optimization using the global computer simulation were carried out. Because of the lack of polycrystalline high-purity germanium as starting material for Cz-growth, a zone refining furnace has been constructed, which is now made ready for operation.

Growth of Ge crystals doped with volatile impurities such as phosphorus or with impurities having distribution coefficients larger than 1 such as boron ($k_0 \approx 12$) is a challenge in crystal growth technology. To solve this problem a technique based on gas-doping using phosphin and diborane has been developed. Crystals are grown by the mini-Cz technique, which is used usually for the growth of isotopically pure Si and Ge crystals from extremely small quantities of raw material. Also Ge crystals both doped and co-doped with other elements of III- and V-group were grown in frame of InTerFEL project (Time resolved infrared and terahertz spectroscopy of carrier dynamics in semiconductors with free electron lasers) and as subcontracted work.

Results

The advancement in development of crystal growth techniques is based on understanding the influence of different growth parameters on crystal quality and process stability. This can be also used for the development of growth models for implementation in numerical computer simulations.

Within a cooperation of IKZ with the Siltronic AG some scientific investigations and experiments have been performed to support and verify the results of numerical simulations regarding the influence of some process parameters on melt convection and solid-liquid interface during Float-Zone (FZ) silicon single crystal growth. Therefore, a series of dislocation free 4" FZ Si single crystals were grown in IKZ using standard technology. The aim was the systematical investigation of the solid-liquid interface deflection and the radial resistivity variation in dependence on growth velocity, rotation speed and crystal rotation mode. Furthermore, for a given set of growth parameters the range of growth velocities should be determined where a reproducible 4"- dislocation free FZ single crystal growth is possible.

Beginning with standard conditions (v_g = 3.5 mm min^{-1}, rpm$_{crys}$ = 6 min^{-1}, phosphine doping for the visualization of the solid-liquid interface), after reaching the final crystal diameter (4") and waiting for a certain time to establish the quasi-stationary state, the growth velocity was in situ changed in steps of 0,3 mm min^{-1} and 0,5 mm min^{-1}, respectively (either increased or reduced until the end of the feed rod was reached (Fig 1).

Fig.1
4" Fz-Si crystal grown with pulling rate varying from 3.5 to 2.0 mm min^{-1}
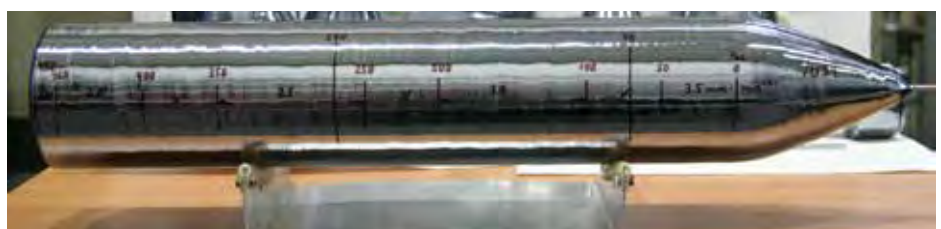
Classical Semiconductors: **Silicon & Germanium**

Additionally, the crystal rotation mode (mono and alternating rotational direction) was changed in situ for a certain rotational speed value (16 min^{-1}). The values of the solid–liquid interface deflection and the radial resistivity variation were measured on crystal plates cut parallel to the growth direction at the end of each growth interval using LPS and 4–point probe measurements across the crystal diameter.

As a result, it could be shown that using the above described set of parameters reproducible growth of 4 inch dislocation free Si single crystals is possible at a growth velocity between 1.7 mm min^{-1} and 4.0 mm min^{-1} as maximum. We could not verify the asserted lower limit of 1.7 mm min^{-1} because the end of the feed rod was reached. Passing the upper limit, dislocations were introduced. In the range of the growth velocity investigated (2.0 – 4.5 mm min^{-1}) the deflection of the solid–liquid interface in the 4" Si crystal increased nearly linear from 12.5 to 24 mm (Fig.2). The enlargement of the solid–liquid interface deflection correlates with growing radial temperature gradients and consequently increasing thermo–mechanical stresses which can be made responsible for the generation of dislocations.
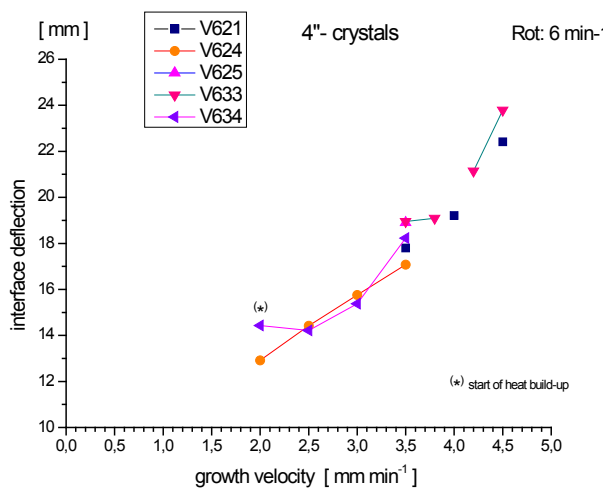
Fig.2

Deflection of the solid–liquid interface vs. pulling rate for 4" FZ–Si crystal

For the radial resistivity variation in dependence on the growth velocity a tendency to the radial homogenization of the resistivity values and a reduced mean variation between the minimum and maximum values with decreasing the growth velocity has been found. The typical W–profile seems to be more leveled (Fig.3).
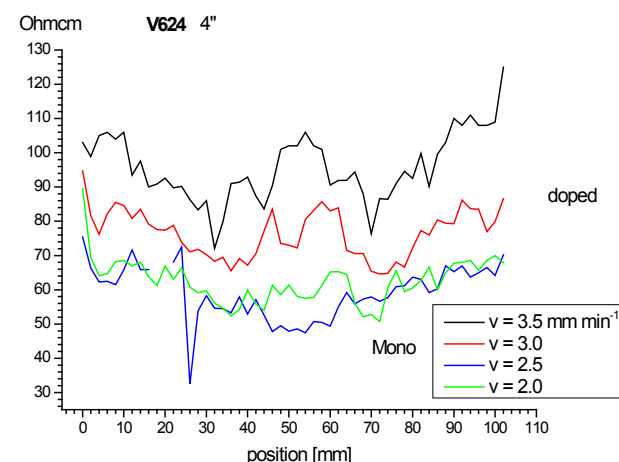
Fig.3

Radial resistivity in 4" FZ–Si crystal grown with different pulling rates

The dependence of the solid–liquid interface deflection on the rotation speed (alternating rotational mode) was not homogeneous. The values strongly vary with increasing rotational speed, probably due to disturbance of the convection in the melt zone using alternating rotational modes. This should result in a better mixing of the melt and therefore in a lower radial resistivity variation as was confirmed by our measurements.

The impact of the mono– and alternating rotational mode for the same rotation speed in situ, e.g. during the same crystal growth run, was compared. It was found that the deflection of the solid–liquid interface for the alternating rotational mode were about 14–16% higher than those of the mono rotational mode. Regarding the radial resistivity variation no essential difference between the two rotational modes for the same rotation speed was found. Compared with the standard rotation speed at 6 min^{-1} the variation of resistivity in the central parts of the crystal was lower in both cases due to the better mixing at higher rotation speed.

Currently one of the main goals within the GERDA project is the reduction of the dislocation density in Ge crystals. Because the multiplication of dislocations is driven by thermal stress, numerical simulations have been applied to study and improve the thermal field and eventually reduce the thermal stress. Numerical simulations give us the advantage to check the effect of geometrical changes without great efforts. We used the software CrysMAS from IISB Erlangen to compute the thermal field and stress for various configurations by axi–symmetric calculations.

Classical Semiconductors: **Silicon & Germanium**

As an example we show the von Mises stress in three different cases in particular at the end of the process (see Fig. 4). Case A is without modification, case B includes one extra shield, and case C two extra shields. The impact on the thermal stress can be clearly seen. The modification will be realized in a next step.

In the next step the dislocation densities should be computed and be compared to the EPD measurements on wafers of crystals from the various experiments. For such calculations it is necessary to calculate the dynamics of the growth process rather than to perform quasi-steady state calculations at different stages of it. For this reason we tested the software tool CGsim from STR Ltd., which includes the computation of dislocation densities employing the Alexander-Haasen-Sumino model. First runs with a simplified geometry of the furnace used in the GERDA project have been performed to check the capabilities of CGsim.
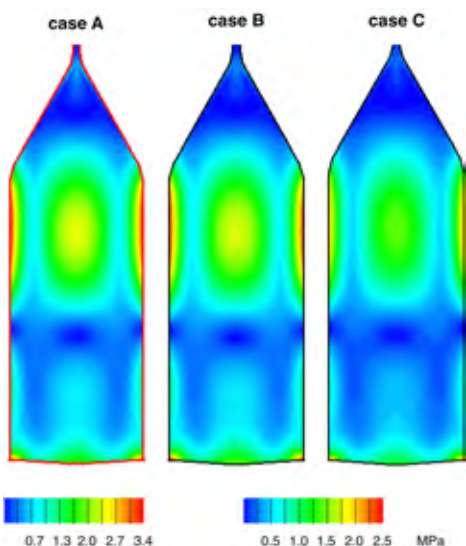
Fig.4
Numerical simulation of von Mises stress for three cases.
A: without heat shield,
B: with simple heat shield,
C: with double heat shield. Please note the different scale
for case A and B & C.

One on the topics of BMBF-Project InTerFEL – Time-resolved infrared and terahertz spectroscopy of carrier dynamics in semiconductors with free electron lasers– is the development of the fast l-He-cooled detector to cover wavelengths up to 240 µm. Instead of conventional photoconductive Ge detectors, relatively lightly doped with Ga or Sb ($\sim 10^{14}$cm^{-3}) it was decided to use highly doped and highly compensated Ge. N-type and p-type Ge crystals co-doped with Ga and Sb were grown by Czochralski technique (Fig.5). The total doping level of $N_{Ga}+N_{Sb}\sim(5\text{-}9)\times 10^{16}$ cm^{-3} which is just below the critical metal-insulating transition density of $\sim 10^{17}$ cm^{-3} was

chosen both for n-type (more Sb than Ga) and for p-type (more Ga than Sb) crystals. Because of different segregation coefficients of Ga ($k_0=0.087$) and Sb ($k_0=0.003$) different samples with different compensation level, i.e. different amounts of Ga acceptors and Sb donors could be produced. All crystals of 30 mm in diameter were grown in <100>-direction.

Fig.5
Highly compensated p-type Ga and Sb co-doped <100> Ge crystal grown for use as photoconductive Ge detectors

10×10×0.5 mm^3 Ge samples from crystals with high compensation were investigated with pump- probe technique. The recombination time of the free charge carriers measured varies between 30 and 300 ps. The higher the compensation level and the higher the pump power, the shorter is the recombination time. A photodetector made from compensated material grown in this project has a typical rise time of ˜60 ps and a FWHM of ˜150 ps [1]. This is more than one order of magnitude less than the fastest Ge photodetector demonstrated so far [2].

References

[1] N. Deßmann, S.G. Pavlov, A. Pohl,
    N.V. Abrosimov, S. Winnerl, M. Mittendorff, R.Kh. Zhukavin, V.V. Tsyplenkov,
    D.V. Shengurov, V.N. Shastin, H.-W. Hübers;
    Appl. Phys. Lett. 106 (2015) 171109

[2] F. A. Hegmann, J. B. Williams, B. Cole,
    M. S. Sherwin, J. W. Beeman, E. E. Haller;
    Appl. Phys. Lett. 76 (2000) 262

Classical Semiconductors:
Multi-crystalline Silicon

Head   Dr. Frank M. Kießling
Team   Dr. N. Dropka, Dr. T. Ervik, D. Linke, Dr. R. Menzel

Überblick

Siliziumbasierte Solarzellenprodukte dominieren weiterhin den Markt für photovoltaische Anwendungen. Dabei übersteigt der Anteil der durch gerichtete Erstarrung des Siliciums hergestellten Wafer immer noch den des mit dem Czochralski-Verfahren hergestellten einkristallinen Siliciums. Die Erhöhung der Solarzelleneffizienz steht im Mittelpunkt, um mittels des Preis/Wp-Verhältnisses die Kosten weiter zu verringern. Das Standardverfahren für die großtechnische Herstellung von multikristallinen (mc) Blöcken für Si-Solarzellen ist die gerichtete Erstarrung (DS) einer Siliciumschmelze. Die Hersteller suchen ständig nach verbesserten Züchtungstechnologien, um Lebensdauer-begrenzende Defekte weiter zu reduzieren und somit höhere Effizienzen zu erreichen. In den letzten Jahren sind mehrere neue Züchtungskonzepte mit dem Ziel entwickelt worden, die Defektdichten in DS-Si zu senken. Da die meisten Defekte ursächlich während des Erstarrungsprozesses entstehen, sind verschiedene Konzepte vorgeschlagen worden. Im Wesentlichen werden drei Haupttypen von Wachstumsansätzen verfolgt, um verschiedene Blockqualitäten zu erhalten: Multikristallin (mc)-Si, quasi-mono (QM)-Si und das sogenannte high-performance mc-Si (HPmc-Si).

Die Methode zur gerichteten Erstarrung mit dendritischem Kornwachstum ist eine Spielart des mc-Si Verfahrens, bei der große Körner über die Tiegelbodenfläche erzeugt werden. Von den dendritisch gewachsenen Körnern ist bekannt, dass diese einige vorteilhafte Orientierungen in Tiegelbodennähe ausbilden und dadurch niedrigere Versetzungsdichten verursachen. Allerdings erhöht sich die Versetzungsdichte mit zunehmender Blockhöhe und führt zur Bildung von unerwünschten Versetzungsbündelungen, welche rekombinationsaktiv sind. Ein weiterer Ansatz, welcher bei Erstveröffentlichung große Aufmerksamkeit erhielt, ist das Wachstum von quasi-mono Blöcken. Dabei werden einkristalline Keime auf dem Boden des Tiegels geschickt platziert und nach dem Aufschmelzen des darüber geschichteten Ausgangsmaterials sorgfältig angeschmolzen. Die Erstarrung erfolgt von den Keimen ausgehend und die vorgegebene Orientierung überträgt sich auf den wachsenden Block. Der QM-Wachstumsprozess beinhaltet jedoch zu viele Herausforderungen und folglich wurde nach neuen Lösungen gesucht.

Die Photovoltaik-Industrie wandte sich von dieser Technik ab und hin zu einem entgegengesetzten Technologieansatz, bei dem möglichst viele Körner von einer polykristallinen Keimschicht ausgehend kristallisiert werden. Charakteristisch für dieses HPmc-Si Material sind kleine Körner mit einer homogenen Größen- und zufälligen Orientierungsverteilung. Dieses Material weist einen hohen Anteil zufälliger Winkelkorngrenzen auf, während Zwillings- und Koinzidenzgitterkorngrenzen (CSL) charakteristisch für standardmultikristalline Si-Blöcke sind. Diese Kornstruktur in HPmc-Si Material führt zu einer Situation, in der die Ausbreitung und Bildung von Versetzungsbündelungen innerhalb der Körner durch zufällige Winkelkorngrenzen eingeschränkt werden. Es wurde gefunden, dass die Kornstruktur in HPmc-Si-Blöcken eine niedrigere Versetzungsdichte [1, 2] bis zu dem oberen Ende des Blocks bewirkt.

Die Gruppe multikristallines Silicium hat ihre Forschungsaufgaben und F&E-Aktivitäten erweitert und praktiziert alle oben erwähnte Variationen des Vertical Gradient Freeze (VGF) Verfahrens zur Erstarrung von Silicium. Bei all diesen Verfahrensentwicklungen wurden Wandermagnetfelder (TMFs) angewendet, um die Bedingungen an der fest-flüssigen Grenzfläche durch kontrollierte Schmelzenströme zu verbessern. Die Prozessentwicklungen wurden in G1- und G2-Tiegelbemaßten Öfen durchgeführt, welche mit KRISTMAG® Heizer-Magnet-Modulen (HMMs) ausgestattet sind. Diese Heizelemente erzeugen neben der üblichen Wärme für den Aufschmelz- und Kristallisationsprozess gleichzeitig magnetische Felder. Jedes Heizelement kann entweder nur mit Gleichstrom (DC), nur mit Wechselstrom (AC) oder in einem Mischbetrieb mit jedem beliebigen AC/DC-Verhältnis betrieben werden. Die entsprechenden Lorentzkräfte (F_L) können in ihrer Stärke und Richtung durch Änderung der AC-Amplitude ($F_L \propto I_0^2$), der Frequenz ($F_L \propto f$) und der Phasenverschiebung ($\Delta\phi$) variiert werden. Diese Kräfte sind ausreichend, um die Schmelzenkonvektion gezielt zu steuern, was bereits in mehreren Publikationen [3, 4] beschrieben wurde. Die mit HMMs ausgestatteten VGF-Öfen sind Prototypen und bieten einzigartige Möglichkeiten, um die Wachstumsbedingungen zu beeinflussen.

Classical Semiconductors: **Multi-crystalline Silicon**

Und in der Tat sind wir die ersten, die G2-große quasi-monokristallinen Si-Blöcke unter dem Einfluss von Magnetfeldern züchten. Umfangreiche Untersuchungen wurden durchgeführt, u.a. zusammen mit unseren Partnern aus der Industrie, Solarworld Innovations GmbH, Elkem Technology und Elkem Solar. 2014 war wieder ein Jahr, in dem viele interessante Ergebnisse durch die Prozessentwicklungen erzeugt wurden, von denen einige im Folgenden vorgestellt werden. Die Aktivitäten in der deutschen Forschungsnetzwerk „SolarWinS" wurden im Jahr 2014 beendet. Alle Prozessentwicklungen wurden durch Simulationen begleitet, insbesondere unter dem Aspekt des Einflusses der angewendeten magnetischen Kräfte auf die Temperaturprofile und der Form der fest-flüssigen Phasengrenze.

Overview

Silicon-based solar cell production dominates the PV market and the share of directionally solidified silicon is still higher than the one of Czochralski grown single crystals. The motivation for improving the performance of solar cells is high, as this leads to a significant cost reduction in terms of price/Wp. Directional solidification (DS) is the standard process for large-scale production of multi-crystalline (mc) ingots for Si-based solar cells. A strong focus towards higher efficiencies by reducing lifetime limiting defects forces manufactures to develop new growth technologies. The last few years have seen several new approaches which aim to eliminate or mitigate the defect density in DS-Si. Since the solidification process is responsible for introducing most of the defects, various solidification techniques have been suggested. Three main types of growth concept are known in order to obtain different ingot qualities: multi-crystalline (mc)-Si, quasi-mono (QM)-Si, and the so-called high performance mc-Si (HPmc-Si).

The dendritic casting method is a type of mc-Si growth, which aims at nucleating large grains spreading laterally across the crucible bottom. The dendritically shaped grains are reported to favour some advantageous orientations in the bottom of the crucible, which are associated with lower dislocation densities. However, the dislocation density increases with ingot height resulting in unfavourable dislocation clusters known to be recombination active. Another approach that received massive attention when first reported is the growth of quasi-mono ingots. Prearranged seeds are placed at the bottom of the crucible. During the melting process the top part of the seeds is carefully melted together with the feedstock material. The crystallization starts at the seeds and the solidifying material obtains the same orientations as the seeds.

There are many challenges in quasi-mono growth, and hence the photovoltaic industry was moving away from this technique and into the very opposite, which is the nucleation of small grains from an incubation layer. For HPmc-Si material, chip seeding leads to small grains with a homogenous size and random orientation distribution. A high proportion of random angle grains boundaries are characteristic for HPmc-Si, whereas the grain boundary character in standard multi-crystalline Si ingots are dominated by twins and other Coincidence Site Lattice (CSL) boundaries. The grain structure in HPmc-Si material leads to a situation where dislocation clusters are terminated by random angle grains boundaries and are therefore not allowed forming and filling entire grains. Hence, the grain structure in HPmc-Si ingots has been found to result in lower dislocation densities [1, 2] also to the very top of the ingot.

The group multi-crystalline silicon has expanded its research tasks and R&D activities, and has been involved in all the variations of vertical gradient freeze (VGF) type solidification of silicon mentioned above. For all these process developments travelling magnetic fields (TMFs) have always been applied to improve the conditions at the solid-liquid interface by controlled melt flows. Process developments have been carried out in G1- and G2-sized furnaces equipped with KRIST*MAG*® heater magnet modules (HMMs). These heaters are capable of producing magnetic fields while maintaining the common function as a heat source during the solidification process. Each heater can operate either only with direct current (DC), only with accelerating current (AC) or in a mixed mode with any AC/DC ratio. The corresponding Lorentz forces (F_L) can be varied in strength and direction by setting AC amplitude ($F_L \propto I_0^2$), frequency ($F_L \propto f$) and phase shift ($\Delta\phi$). These forces are able to control the melt convection in a way already well described in several publications [3, 4]. The VGF-type furnaces equipped with HMMs are prototypes and offer unique possibilities to influence the growth conditions.

And indeed, we were the first to grow G2-sized quasi-mono crystalline Si-ingots under the influence of TMFs. Extensive experiments have been carried out, and with our industry partners, e.g. SolarWorld Innovations GmbH, Elkem Technology and Elkem Solar. 2014 was a year where process developments again accumulated lots of interesting results, some of which will be presented below. The activities in the German research network "SolarWinS" were terminated in 2014. All the process developments have been seen through simulations, especially the influences of the applied magnetic forces on temperature profiles and the shapes of the solid-liquid interface.

Classical Semiconductors: **Multi-crystalline Silicon**

Results

Extended red-zone in seeded growth

One of the challenges in seeded ingot growth, both quasi-mono and HPmc-Si, is that there exists an extended red zone at the bottom. In general the red zone is found to be approximately 1.5 to 2 times larger than for standard mc-Si. In Figure 1, μ-PCD images and lifetime line scans from a standard mc-Si and a quasi-mono ingot are compared. The extended red-zone is clearly seen in Fig. 1b. It is also seen that a multi-crystalline structure is only found at the very right side in the quasi-mono ingot due to nucleation processes beside the seed area. In addition, grains can nucleate at the crucible sidewall. It is important that grains, which are formed here are restricted to a thin edge area. Travelling magnetic fields can assist in shaping the interface, so that the grain boundaries at the side are not allowed to grow into the mono-crystalline part. In the standard mc-Si material, boundaries can be seen starting at the bottom of the ingot as well.

The large red zone is related to the concentration of iron, which shows a high-low-high concentration distribution resulting in low-high-low lifetimes. The first low lifetime peak is due to iron in-diffusion from the crucible and reaches a small plateau after the first ~ 5 mm, reflected in the lifetime line scans in Fig. 1 b. The second low lifetime peak is explained by the formation of an iron-rich layer at the initial stage of the crystallization process. In the beginning of solidification, the crystallization rate is accelerated from zero to a higher value. When the crystallization rate reaches a certain value and the transient layer at the solid–liquid interface becomes solid in this region, most iron atoms will be captured in this layer. As a consequence, the newly formed thin solid layer is iron-rich and iron can diffuse from there in both directions, towards the seed and in the growth direction.

Compared to mc-Si material this thicker red-zone region is also found for HPmc-Si ingots. The HPmc-typical material structure is mostly obtained with a seeding layer, which consists of small silicon chips or granules. Regarding the yield, it would be beneficial to induce small grains by other nucleation spots such as rough coating. Therefore, different coating morphologies have been studied and G1-sized ingots were grown using ESS™ silicon feedstock. The crucibles were manually coated with slurries based on various Si_3N_4 powders. The process parameters and cooling curves were kept identically and suitable TMFs were applied for sufficient melt mixing. When these ingots were compared, however, a very different ingot bottom structure was evident by visual inspection. Ingot 1 had a rough structure with clearly detectable indents on the bottom surface. In contrast, ingot 2 had a smooth bottom surface and large grains resembling dendrites were visible on the bottom, see Figure 1. The ingots were cut into wafers, and the bottommost wafers for the two ingots confirmed the differences; the bottom wafer of ingot 1 displayed many small grains with uniform size, whereas the bottom wafer of ingot 2 had large planar grains. There are still some differences between the grain structure of wafer 1 and what is found in HPmc-Si type wafers. However, this study proves that the morphology of the coating is important for the grain nucleation, and that further development may lead to yet smaller grains.


a) standard mc-Si   b) quasi-mono ingot
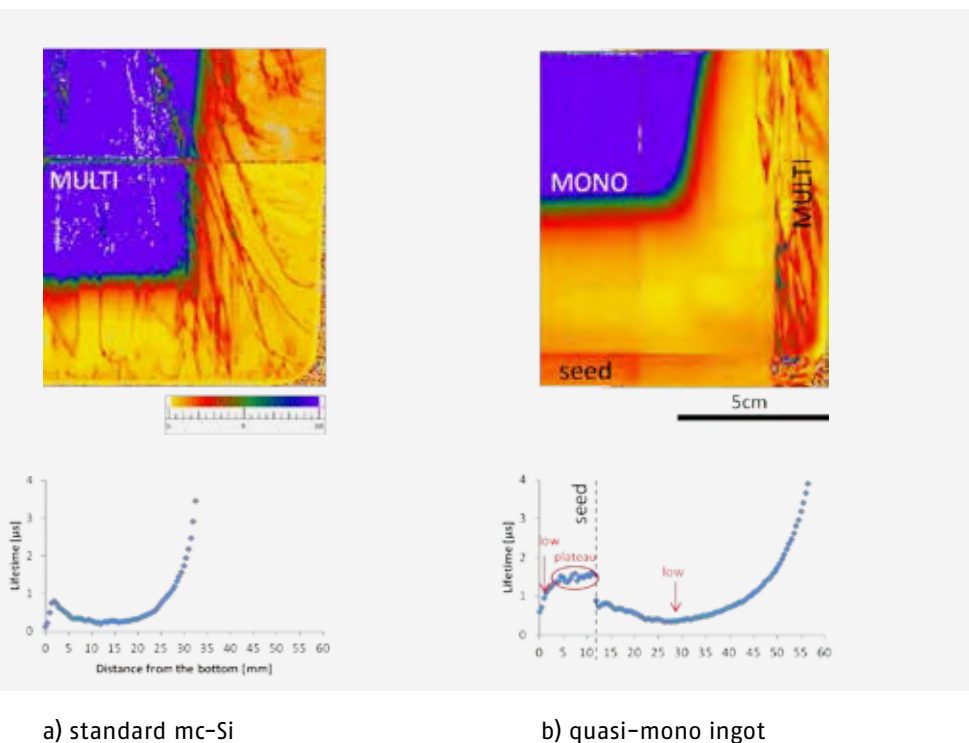
Fig. 1
μ-PCD images and line scans from a selected line in the bottom corner region of
a) a standard grown G2 mc-Si ingot and
b) a G2 quasi-mono ingot.

In the line scan, the seed is marked by a stapled line. The thicker red-zone is clearly identified in the quasi-mono ingot.

## Classical Semiconductors: Multi-crystalline Silicon
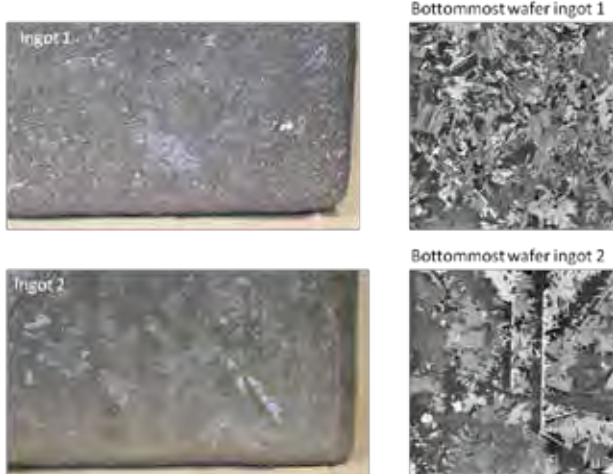
Fig. 2

The impact of coating made a significant difference on the grain structure as seen from the bottom surfaces and bottommost wafers of ingot 1 and 2.

Stirring and interface shaping by pulsed TMF

A novel electro-magnetic stirring and solid-liquid interface shaping method was proposed for directionally solidified silicon at large scale [5, 6]. The method is based on pulsed TMFs generated by either side or top KRIST*MAG*® heater-magnet-moduls in a furnace of G5 size (Figure 3). The pulsed Lorentz forces were obtained by a sinusoidal AC magnitude modulation. 3D numerical simulations were performed using the commercial code ANSYS Workbench™ 2.0.

Results showed superiority of pulsed to unmodified TMF for pulsing frequency of f_p = 0.3 Hz. The homogenization of the distribution of a pointwise released tracer in the melt was more than 2 times faster in pulsed TMF then in buoyancy mode. Concerning interface shaping, TMF generated from side-heaters was more beneficial at the beginning of solidification while top TMF showed advantages for large melts towards the end of the process. With respect to the melt homogenization, the initial distribution of impurities or dopants determined, which position of HMM was more favorable for the process. Top TMF generated the high flow velocities in the melt volume away from the crucible walls that was beneficial for the stability of the crucible coating.

The proposed pulsed technique enabled quick and inexpensive process improvement in already provided setups. For a commercial application, optimization of the process parameters is necessary.

Fig. 3

Snapshots of temperature, magnetic flux and Lorentz force density distributions in silicon melt exposed to TMF that originated from top and side HMMs.

References

[1]   F.-M. Kiessling, F. Büllesfeld, N. Dropka, Ch. Frank-Rotsch, M. Müller, P. Rudolph; J. Crystal Growth 360 (2012) 81–86

[2]   C.W. Lan, W.C. Lan, T.F. Lee, A. Yu, Y.M. Yang, W.C. Hsu, B. Hsu, A. Yang; J. Crystal Growth 360 (2012) 68–75

[3]   Y.M. Yang, A. Yu, B. Hsu, W.C. Hsu, A. Yang, C.W. Lan; Progress in Photovoltaics: Res. Appl. 23 (2015) 340–351

[4]   D. Linke, N. Dropka, F. Kiessling, R.-P. Lange, M. König, J. Krause, D. Sontag; Solar Energy Materials and Solar Cells 130 (2014) 652–660

[5]   N. Dropka, Ch. Frank-Rotsch, P. Lange, P. Krause; "The crystallization system and crystallization method for crystallization from electrically conductive melts, and ingots that can be obtained by means of the method", patent application, DE 10 2013 211 769 A1, WO 2014/202284 A1

[6]   N. Dropka, Ch. Frank-Rotsch; Proceedings of the International Scientific Colloquium "Modelling for Electromagnetic Processing" (MEP 14), Hannover, September 16–19 (2014) 79–85
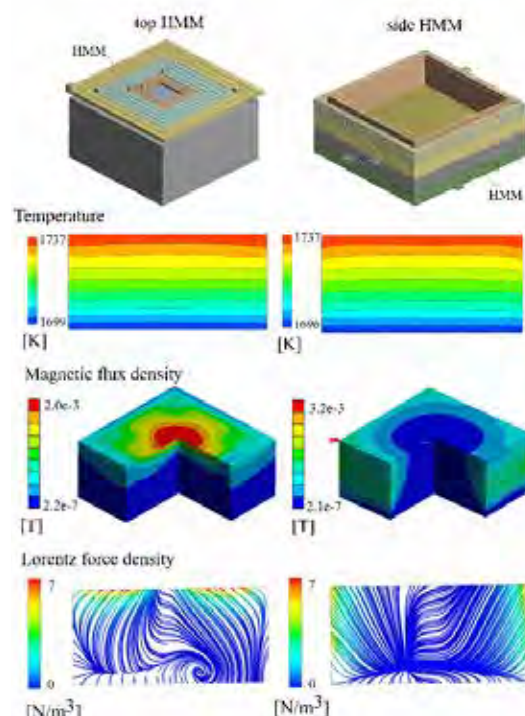
Classical Semiconductors:
Gallium Arsenide

Head   Dr. Christiane Frank-Rotsch
Team   Dr. N. Dropka Dr. A. Glacki, O. Root, Dr. R. Bertram

Überblick

Das III-V-Halbleitermaterial Galliumarsenid (GaAs) ist nach Silicium das häufigsten eingesetzte Halbleitermaterial. Besonders in der WLAN-Kommunikation, in der Mikrowellen- und in der Hochfrequenztechnologie spielt GaAs eine bedeutende Rolle. In den letzten Jahren ist der GaAs-Markt durch den rasanten Anstieg der mobilen Kommunikation stark gestiegen. Neben der stetigen Verbesserung der Kristallqualität stehen die Steigerung der Ausbeute der Kristallisationsprozesse sowie die Senkung der Prozesskosten im Fokus der Forschungsaktivitäten. Diese Zielstellungen sind nur durch eine gezielte Beeinflussung der Schmelzkonvektion während der Kristallisation erreichbar. Der Einsatz von externen Feldern, insbesondere von Wandermagnetfeldern zeigt hierbei ein großes Potenzial.

Die am IKZ entwickelte KRISTMAG®-Technologie ist ein leistungsstarkes Werkzeug zur Erzeugung von Wandermagnetfeldern in der Kristallzüchtung und ermöglicht dabei eine große Parametervielfalt. Sie wurde bereits erfolgreich für verschiedene kristalline Materialien, beispielsweise Halbleiter wie GaAs und Silicium, eingesetzt. Gegenwärtig sind zwei VGF-Anlagen mit KRISTMAG® Heizer-Magnet-Modulen (HMM) zur simultanen Erzeugung von Wärme und Wandermagnetfeld (TMF) ausgerüstet. Die Forschungsaktivitäten des Themas „Galliumarsenid" konzentrierten sich auch in diesem Berichtszeitraum auf die Effizienzsteigerung des VGF-GaAs-Züchtungsprozesses. Zur Lösung dieser technologischen und wissenschaftlichen Herausforderung wurden unterschiedliche Strategien verfolgt, z.B. die simultane Kristallisation in mehreren Tiegel und die Vergrößerung der Kristalllänge (siehe hierzu auch den Jahresbericht 2013) sowie die Erhöhung der Kristallisationsgeschwindigkeit. Weiterhin werden auch grundlagenrelevante Aspekte zu GaAs-Wachstumsprozessen untersucht. Dazu gehört insbesondere auch die Zusammenarbeit mit der Hochschule für Angewandte Wissenschaften in München zur Klärung von Sauerstoffrelevanten Defekten in Einkristallen.

*Weiterhin wurden die Forschungsaktivitäten im Rahmen des BMBF-Verbundprojektes „TEMPO" zum Lösungsverhalten von festen GaAs unter definierten Bedingungen (z.B. Temperatur, Korngröße, Lösungsmittel und pH-Wert) fortgeführt. Die Projektergebnisse sollen in toxikologischen Bewertungsprozess von GaAs im Zusammenhang mit den REACh-(**R**egistration, **E**valuation, **A**uthorisation and Restriction of **Ch**emicals) und CLP-Bestimmungen (zur Einstufung, Kennzeichnung und Verpackung von Stoffen und Gemischen) der EU einfließen.*

Overview

The III-V compound semiconductor gallium arsenide (GaAs) is, apart from silicon, the most deployed semiconductor material. Gallium arsenide is commonly used for wireless communication in microwave or high frequency technology. In the last years, strong growth of the GaAs market took place, mainly because of the rapid growth of the mobile telecommunication market. Besides the continual improvement of the GaAs single crystal quality, research focuses on the enhancement of the yield of the growth process and a reduction of the process costs. To succeed with these objectives the exact and permanent control of the melt flow is of crucial importance. The use of external fields, especially traveling magnetic fields (TMF), shows great potential to meet this requirement.

The KRIST*MAG*® technology developed at IKZ provides a simple yet powerful tool to generate such traveling magnetic fields within a broad parameter range. It has been successfully applied to the growth of different crystalline materials, among them semiconductors like gallium arsenide or silicon. Currently two of our VGF furnaces are equipped with a KRIST*MAG*® heater magnet module (HMM) allowing simultaneous generation of heat and traveling magnetic field. The research activities in the gallium arsenide group were continued to further improve the efficiency of vertical gradient freeze (VGF) crystallization process. To meet this technological and scientific challenge, different strategies have been applied, e.g. simultaneous crystallization in multiple crucibles and enhanced crystal lengths (see annual report 2013) as well as an increase of crystal growth velocity. Further, fundamental aspects of the GaAs crystal growth process have been investigated. This includes in particular the cooperation with the University of Applied Sciences in Munich to study oxygen related defects in the grown single crystals.

In addition, the research activities in the BMBF funded framework "TEMPO" on the solubility of solid GaAs as a function of specified parameters (e.g. temperature, grain size, solvent, pH-value) have been continued. Project results will be considered in the toxicological evaluation process of GaAs in connection with REACh (**R**egistration, **E**valuation, **A**uthorisation and Restriction of **Ch**emicals) and CLP (**C**lassification, **L**abelling and **P**ackaging of substances and mixtures) regulations of the EU.

Classical Semiconductors: **Gallium Arsenide**

Results

Our previous work has shown that we can improve the VGF growth of 4''-GaAs crystals by application of traveling magnetic fields [1]. We were able to stabilize the growth process, to markedly reduce the solid-liquid interface concavity , and to enhance melt stirring as well as the dopant incorporation [2]. Within the last year crystal growth in the KRIST*MAG*®-HMM focused on further process optimization and intensification [3]. After the successful increase of the crystal length and the simultaneous growth of two single crystals in the multi-crucible HMM, the enhancement of the growth velocity with the help of traveling magnetic fields has been realized.

While the application of optimized TMF parameters with a typical standard growth velocity of 2.0-2.5 mm/h resulted in the growth of single crystals with good quality, unaltered induced Lorentz forces were unable to counteract the buoyancy force when the growth velocity was enhanced up to 5 mm/h. The resulting crystal showed a strong concave deflection of the solid-liquid interface (Figure 1a), which led to polycrystalline growth and strong microsegregation. The growth of a single crystal with a 2.5-fold increase of the growth velocity to up to 6.0 mm/h was possible when the TMF parameters were adjusted to the modified conventional growth conditions (Figure 1b). The alternating current was constantly matched to the progressing process and the magnitude of the Lorentz force density was increased to 150% compared to the standard process with around 2 mm/h. The resulting crystal showed average deflections and dislocation densities, comparable to crystals grown with standard growth rate and without the application of a traveling magnetic field. Therefore, we could demonstrate that the application of traveling magnetic fields helps to improve process efficiency and with this to increase the yield.

The development of the usability of the KRIST*MAG*® technology and their easy implementation in commercial growth setups is crucial for its commercial exploitation. Therefore, efforts were made to upgrade, according our specifications, the control software of the single-crucible growth setup for an automatic adjustment of heater and magnetic field parameters during the different process phases. As major result from process optimization approaches we found that for achieving continuously flat interface shapes of the growing GaAs crystal a continuously adjustment of the Lorentz forces is necessary.

Further, fundamental growth experiments were conducted in cooperation with Prof. Hans-Christian Alt from the University of Applied Sciences Munich Department – Engineering Physics. Principles of the interactions between typical impurities in GaAs crystals such as oxygen, nitrogen, and carbon were of particular interest in order to understand their impact on the material properties. Various doping experiments were conducted with carbon ^{12}C, and oxygen isotopes ^{16}O and ^{18}O. The aim was to identify the origin of the sharp absorption band at 2060 cm^{-1} in annealed GaAs crystals, which was hitherto attributed to the local vibrational mode of a complex containing both C and O [4]. Six 4''-GaAs crystals with masses 1.0-1.3 kg were grown under the influence of traveling magnetic fields with optimized conventional parameters and conventional growth conditions. High carbon concentrations were achieved by adding roughened graphite plates to the melt (see Figure 2). Oxygen was introduced either by adding various quantities of boron oxide or/and gallium oxide hydroxide GaOOH (containing either ^{16}OH or ^{18}OH) to the crucible. The GaOOH was synthesized at IKZ. The boron oxide was either dry with 200 ppm ^{16}O-water content or wetted by $H_2^{16}O$ or $H_2^{18}O$ in different volume ratios.
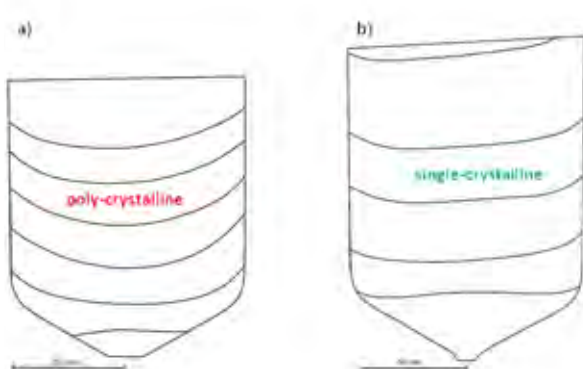
Fig.1

Interface shapes of two GaAs crystals grown with enhanced growth velocity in the KRISTMAG®-HMM. The interface shapes were made visible with the TMF marking technique and ex-situ DSL etching of axial longitu-dinal cross sections: a) poly-crystal grown with up to 5 mm/h and constant TMF parameters, Lorentz forces were not enhanced compared to the standard process, b) Lorentz forces were constantly matched to the growth pro-cess by adjusting the TMF parameters, their magnitude was additionally increased compared to the standard growth rate to 150%, which led to a severe reduction of the interface concavity and resulted in single-crystalline growth with a growth velocity of up to 6 mm/h.

Classical Semiconductors: **Gallium Arsenide**

Low-temperature Fourier transform infrared (FTIR) absorption measurements of a GaAs sample with a total oxygen concentration of 3.4×10^{15} cm^{-3} and an enrichment of the ^{18}O isotope (^{16}O:^{18}O=30:1, the natural abundance is 487:1, Figure 2b) revealed that the satellite band of 2060 cm^{-1} at 2050 cm^{-1}, which was previously attributed to the ^{18}O isotope, was not enhanced in comparison with spectra containing the natural oxygen isotope ratio [5]. This ruled out any defect model involving oxygen atoms. The origin of the 2060 cm^{-1} mode was subsequently identified as a complex of the composition CN_2 by implantation of the isotopes ^{14}N and ^{15}N into standard semi-insulating GaAs wafers. These FTIR-investigations were carried out by H.E. Wagner at the University of Applied Sciences Munich and the ion implantation by V. Häublein at Fraunhofer IISB in Erlangen.

In the frame of the project TEMPO, first results on the solubility of solid GaAs in simulated lung fluid (Gamble solution) have been achieved during the reporting period. In figure 3a the comparison of dissolved amounts of arsenic from GaAs wafer pieces and GaAs powder in Gamble solution at body temperature of 37 °C is shown as a function of time. In both cases GaAs mass of 400 mg was used. The surface of the powder was two magnitudes larger as the wafer surface with the dimension of 10 mm x 1 mm x 0.7 mm. According to the current results it can be assumed that the enhanced surface is the main reason of the higher solubility of GaAs powder compared to wafer material. The investigations will be further continued.


Fig. 2
Crucible equipment for two growth experiments for an aimed doping of GaAs crystal with ^{12}C, ^{16}O or ^{18}O:
a) ^{18}O was introduced to the crystal by adding specially synthesized GaOOH (with ^{18}O or ^{16}O) to the feed-stock, resulting in a grown crystal with increased abundance ^{16}O:^{18}O=200:1 (natural 487:1),
b) ^{18}O was introduced to the crystal by wetting the B_2O_3 with H_2^{18}O before growth, resulting in a markedly enhanced abundance ^{16}O:^{18}O=30:1 in the grown single crystal

Fig. 3

Comparison of the amount of dissolved arsenic from GaAs powder (red line) and a piece of a GaAs wafer (blue line) in Gamble solution at T=37 °C as a function of time. The initial GaAs weight in each case was 400 mg.

Finally, we are pleased to report that Dr. Alexander Glacki graduated very successfully at Humboldt University Berlin with his thesis "VGF growth of 4" GaAs single crystals with travelling magnetic fields".

References

[1] Ch. Frank-Rotsch, N. Dropka, A. Glacki, U. Juda;
    J. Crystal Growth 401 (2014) 702–707

[2] A. Glacki, N. Dropka, Ch. Frank-Rotsch,
    U. Juda, M. Naumann;
    J. Crystal Growth 397 (2014) 6–12

[3] N. Dropka, A. Glacki, Ch. Frank-Rotsch;
    Cryst. Growth & Design 14 (2014) 5122–5130

[4] W. Ulrici, M. Jurisch;
    Phys. Status Solidi B 242 (2005) 2433 – 2439

[5] H. Ch. Alt, H. E. Wagner, A. Glacki,
     Ch. Frank-Rotsch, V. Häublein;
    Phys. Status Solidi B (2015), DOI: 10.1002/
    pssb.201552028

Dielectric & Wide Bandgap Materials
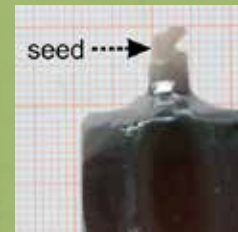
Dielectric & Wide Bandgap Materials

Head of department: Prof. Dr. Matthias Bickermann

Die Abteilung „Dielektrika und Wide-Bandgap-Materialien" hat ihren Schwerpunkt in der Volumenkristallzüchtung von Nitriden, Oxiden und Fluoriden. Die Kristalle finden Anwendung als Epitaxiesubstrate sowie in der Optik und Sensorik. Schwerpunkt der Forschung am IKZ ist die Herstellung einkristalliner Materialien mit bisher unerreichter struktureller Qualität für neuartiger und energieeffiziente elektronische, optoelektronische und piezoelektrische Anwendungen und Bauelemente. In den Themengruppen „Aluminiumnitrid (AlN)", „Galliumnitrid (GaN)" und „Oxide/Fluoride" arbeiten insgesamt 10 Wissenschaftler, 4 Doktoranden und 7 Techniker (Stand Dezember 2014).

AlN-Substrate bilden die Grundlage der Herstellung von effizienten Leuchtdioden und Festkörperlasern im tiefen Ultraviolett (200–300 nm) mit zukunftsträchtigen Anwendungsgebieten in der Wasserdesinfektion und der Sensorik. Im BMBF-geförderten Konsortium „Advanced UV for Life" wurde mit den Vorarbeiten begonnen, um unsere Technologie der AlN-Kristallzüchtung aus der Gasphase zu einer industrietauglichen Methode weiter zu entwickeln, und um den Partnern hochwertige Substrate für die Bauelemententwicklung zur Verfügung stellen. In diesem Rahmen wurde auch eine neue AlN-Kristallzüchtungsanlage am IKZ konzipiert und aufgebaut sowie Dotierung und Versetzungsdynamik bei der AlN-Kristallzüchtung untersucht. Zur Herstellung von GaN wird im Rahmen eines DFG-Projekts die von uns entwickelte pseudo-halide Gasphasenepitaxie (PHVPE) mit dem Ziel einer gezielten Kohlenstoffdotierung untersucht.

Die Expertise der Gruppe „Oxide/Fluoride" liegt in der Schmelzzüchtung bei hohen Temperaturen im Czochralski-Verfahren. Unsere Perowskitkristalle und -substrate (z.B. Seltenerdscandate) werden am IKZ sowie weltweit bei der Erforschung verspannter ferroelektrischer Schichten verwendet. Versetzungsarme Einkristalle aus Strontiumtitanat ($SrTiO_3$) mit 25 mm Durchmesser und bis zu 30 mm Länge konnten aus der TiO_2-reichen Schmelze gezüchtet werden. Im aufkommenden Feld der transparenten halbleitenden Oxide (TSO) stellen Galliumoxid-Kristalle das perfekte Substratmaterial für eine verlustarme Oxid-Leistungselektronik mit hoher Durchbruchspannung dar, die seit kurzem sehr intensiv erforscht wird. Im Gegensatz zu anderen Materialien mit hoher Bandlücke wie SiC, GaN oder Diamant werden sie am IKZ mittels Czochralski-Verfahren mit einem Durchmesser von bis zu 2 Zoll gezüchtet. Die Palette der am IKZ hergestellten TSO-Materialien β-Ga_2O_3, In_2O_3 und SnO_2 wurde 2014 ergänzt durch $MgGaO_3$, das aus der Schmelze gezüchtet und bezüglich seiner halbleitenden Eigenschaften erstmalig untersucht wurde. Gemeinsam mit der Firma Kistler Instumente AG (Schweiz) wurde die Züchtung von Kristallen aus der Langasit-Familie ($La_3Ga_5SiO_{14}$ u.a.) für Hochtemperatur-Drucksensoren weiter vorangetrieben. Schließlich hat die Gruppe, dem Servicecharakter des IKZ folgend, eine Vielzahl maßgeschneiderter Oxid- und Fluorid-Kristalle Forschungsinstituten und Universitäten zur Verfügung gestellt.

The department „Dielectric and Wide Bandgap Materials" focuses on the bulk crystal growth of nitrides, oxides, and fluorides. The crystals are used as substrates for epitaxy as well as in optical and sensor devices. Our research is focused on single crystal materials of unprecedented structural quality to enable novel and energy-efficient electronic, optoelectronic, and piezoelectric devices and applications. As of December 2014, the thematic groups of "Aluminium nitride (AlN)", "Gallium nitride (GaN)", and "Oxides/Fluorides" hosts in total 10 senior scientists, 4 PhD students, and 7 technicians/engineers.

AlN substrates form the basis for the preparation of efficient deep-UV (200–300 nm) LEDs and solid state lasers with seminal fields of application in water disinfection and sensor technology. Within the "Advanced UV for Life" consortium, promoted by the Federal Ministry of Education and Research (BMBF), we have started preliminary work to develop our AlN bulk growth by physical vapor transport into a technology suited for industrial application and to provide high quality AlN substrates to our partners for device development. Within this activity, the IKZ designed and built a new AlN bulk crystal growth facility and investigated doping and dislocation dynamics during AlN growth. Regarding preparation of GaN crystals, DFG-funded research aims at controlled carbon doping with the pseudo-halide vapour phase epitaxy (PHVPE) developed at the IKZ.

The "Oxides/Fluorides" group's activities focus on high temperature Czochralski melt growth techniques. Our perovskite crystals and substrates (e.g. rare earth scandates) are used at the IKZ and worldwide for research on strained ferroelectric layers. Single crystals of strontium titanate ($SrTiO_3$) with low dislocation density, up to 25 mm in diameter and up to 30 mm in length, have been prepared from the Ti-rich melt. In the emerging field of novel transparent semiconducting oxides (TSO), gallium oxide (β-Ga_2O_3) single crystals provide the perfect substrate material for high-breakdown and low-loss oxide semiconductor electronics which gained a high interest recently. In contrast to other wide bandgap materials such as SiC, GaN, and diamond, they are grown at the IKZ by the Czochralski method with a diameter of up to 2 inch. The TSO materials palette at the IKZ spanning from β-Ga_2O_3 to In_2O_3 and SnO_2 was extended in 2014 to include $MgGaO_3$ which was grown as bulk crystal from the melt and investigated in regard to its semiconductor properties for the first time. In collaboration with the company Kistler Instrumente AG (Switzerland), the growth of langasite-type crystals (e.g. $La_3Ga_5SiO_{14}$) for high-temperature pressure sensors was further developed. Finally, following the service function of our institute, the group again prepared several tailored oxide and fluoride crystals for research institutes and universities.

Dielectric & Wide Bandgap Materials:
Oxides/Fluorides

Head   Dr. Reinhard Uecker
Team   M. Bernhagen, M. Brützam, Dr. Z. Galazka, S. Ganschow, Dr. C. Guguschev, D. Kok, M. Rabe,
        I. Schulze-Jonack, Dr. D. Schulz, A. Tauchert, E. Thiede

Überblick

Seit der Institutsgründung im Jahr 1992 beschäftigt sich die Themengruppe mit der Züchtung von oxidischen und fluoridischen Einkristallen, wobei die Oxide im Fokus stehen. Als Standardzüchtungsmethode für die Volumenkristalle dient dabei die Czochralski-Methode, die am weitesten entwickelten Technik zur Herstellung von Kristallen mit hoher struktureller Qualität. Die in unserer Gruppe hergestellten Kristalle haben einen Durchmesser von bis zu 50 mm und eine Länge von bis zu 150 mm. Aber auch andere Schmelzzüchtungsmethoden wie die EFG-Methode (edge-defined film fed growth), die Bridgman- und die Kyropoulos-Methode kommen zum Einsatz. Inkongruent schmelzende Verbindungen werden aus der Schmelzlösung nach dem TSSG-Verfahren hergestellt, bei hoher Flüchtigkeit erfolgt die Züchtung über die Gasphase. Immer häufiger erfordern jedoch neue Materialien auch aufwendig angepasste neue Züchtungsbedingungen. Hierzu zählt die in der Gruppe entwickelte „Levitation-Assisted Self-Seeding Crystal Growth Method" (LASSCGM), die eigens für die Züchtung von In_2O_3-Volumenkristallen entwickelt und zum Patent angemeldet wurde.

Neben der Volumenkristallzüchtung werden in der Themengruppe auch Kristallfasern mittels Laser Heated Pedestal Growth (LHPG) und Micro-Pulling Down-Methoden (MPD) hergestellt.

Die Wahl der Züchtungsmethode des jeweiligen Kristalls hängt entscheidend vom thermodynamischen Verhalten des jeweiligen Kristalls ab, das in enger Kooperation mit der Gruppe Chemische & Thermodynamische Analyse untersucht wird. Nach der Züchtung werden die Kristalle in der eigenen Gruppe einer Vorcharakterisierung unterzogen, die weitere Charakterisierung erfolgt in den Gruppen Physikalische Charakterisierung und Elektronenmikroskopie.

Die Züchtung neuer Materialien als Volumenkristall ist ein Schwerpunkt der Gruppe. Zu ihnen gehören u.a. Oxidkristalle mit Perowskitstruktur. Sie dienen als Substrate für die Herstellung verspannter Schichten mit ferroelektrischen und/oder ferromagnetischen Eigenschaften, mit denen sich neue Anwendungsgebiete z.B. in der Oxidelektronik erschließen lassen. Ein wichtiges Beispiel ist Strontiumtitanat ($SrTiO_3$), das bislang einzige Material, bei dem die Bildung eines zweidimensionalen Elektronengases an der Grenzfläche zu einer anderen Oxidschicht nachgewiesen werden konnte. Das IKZ hat 2013 mit der Züchtung von $SrTiO_3$-Kristallen im Rahmen einer Förderung aus dem Pakt für Forschung

begonnen und große Fortschritte bei der Verringerung der Versetzungsdichte und der Durchmesservergrößerung erzielt. Bislang ist das IKZ auch die einzige Institution weltweit, die Seltenerd-Scandate als Einkristalle herstellen kann. Diese kristallisieren in der Perowskitstruktur, und die Gitterkonstante lässt sich durch Mischkristallbildung beliebig zwischen 3.95 Å und 4.02 Å einstellen. Mit $LaLuO_3$ (pseudokubische Gitterkonstante: 4,18 Å) hat das IKZ seit kurzem nun auch eines der wenigen Materialien mit noch größerer Gitterkonstante als Volumenkristall herstellen können [1].

Neben den Perowskiten stellen transparente halbleitende Oxide (TSOs) einen weiteren Forschungsschwerpunkt dar. Verbindungen wie ZnO [2], β-Ga_2O_3 [3], In_2O_3 [4] und SnO_2 [5] verfügen über vielversprechende Eigenschaften. Insbesondere bei der Volumenkristallzüchtung von β-Ga_2O_3, In_2O_3 und SnO_2, die bereits weit unterhalb ihrer Schmelztemperatur zur Zersetzung neigen, hat das IKZ eine weltweit führende Rolle übernommen. Über die erfolgreiche Züchtung dieser Volumenkristalle am IKZ unter speziellen Züchtungsbedingungen und teilweise mittels völlig neuer Techniken ist bereits berichtet worden. Die Verfügbarkeit dieser Kristalle, die als Substrate oder Komponenten von elektronischen Devices eingesetzt werden können, ist die Grundlage für Kooperationen mit der Abteilung „Schichten und Nanostrukturen" des IKZ und zahlreicher anderer Kooperationen, u.a. mit der Humboldt-Universität zu Berlin, dem Paul-Drude-Institut, der Universität Leipzig, der Gruppe von Prof. J. Speck an der University of California Santa Barbara, von Prof. D. Schlom an der Cornell University und von Prof. D. Jena an der Notre Dame University, USA. Mit $MgGa_2O_4$ wird weiter unten ein neues TSO-Material vorgestellt, das als Substrat für ferromagnetische sowie für halbleitende Anwendungen genutzt werden könnte.

Zuletzt sind noch die Aktivitäten der Gruppe zur Züchtung von Langasit-Kristallen zu nennen. Die Langasite, repräsentiert durch die Verbindung $La_3Ga_5SiO_{14}$, sind bedeutsam als Hochtemperatur-Piezoelektrika, z.B. für Drucksensoren und Aktoren. Im Gegensatz zu Quarz, der seine piezoelektrischen Eigenschaften bei 573 °C aufgrund des Phasenübergangs verliert, können Langasite bis 1470 °C eingesetzt werden.

Sie können nach dem Czochralski-Verfahren aus der Schmelze gezogen werden. Diese Forschung wird in einer langjährigen, engen Zusammenarbeit mit der

Dielectric & Wide Bandgap Materials: Oxides/Fluorides

Firma Kistler Insturmente AG (Winterthur/Schweiz) durchgeführt. Während das ursprüngliche Ziel, die Technologie der Züchtung von 50mm-Kristallen zu entwickeln, bereits 1998 erreicht wurde, konzentriert sich die Entwicklungsarbeit am IKZ seitdem auf die Erkundung der Züchtung neuer Verbindungen mit noch höherer Empfindlichkeit und Temperaturstabilität. Die vertragliche Zusammenarbeit wurde vor kurzem bis 2019 verlängert.

Overview

Since the institute was formed in 1992, the group is engaged in the growth of oxide and fluoride bulk single crystals, with a clear focus on oxides. Typically, such crystals are prepared by the Czochralski method, as it is the most developed technique for growing crystals of high structural quality. In our group, the crystals grown have diameters up to 50 mm and lengths of up to 150 mm. But also other melt growth techniques such as EFG (edge-defined film-fed growth), Bridgman and Kyropoulos are pursued. Incongruently melting compounds are grown from flux or by top seeded solution growth (TSSG); if the volatility is high, growth from the gas phase (physical vapor transport, PVT) is employed. More and more, though, novel materials require adapted or specially tailored growth conditions. One good example is the „Levitation-Assisted Self-Seeding Crystal Growth Method" (LASSCGM), which was designed in particular for preparation of In_2O_3 bulk single crystals in our group, and for which a patent was applied for. See the report below for further details.

Apart from bulk crystal growth, crystal fibers are prepared in the group using the Laser heated pedestal growth (LHPG) und micro-pulling down (MPD) methods.

The diversity of the prepared materials is driven by the demand of external and internal cooperation, by industrial collaborations, and by knowledge gained in the frame of own basic research which often triggers the exploration of new materials. The choice of the growth method decisively depends on the thermodynamic behavior, which is investigated prior to growth experiments in close collaboration with the IKZ group "chemical and thermodynamic analysis". After growth, the crystals are investigated within the group, whereas in-depth characterization is performed by the IKZ groups "physical characterization" and "electron microscopy".

From this materials demand, the group's main research topics as have evolved partly over more than a decade, while their topical relevance has continued or even increased. Crystals with perovskite structure are used as substrates for the preparation of strain-induced ferroelectric and/or ferromagnetic layers which open up new fields of applications, e.g. in the oxide electronics domain. One prominent example is strontium titanate ($SrTiO_3$), which is the only oxide material known as of today which can host a two-dimensional electron gas at the interface to another oxide crystal layer. Commercially available $SrTiO_3$ grown by the Verneuil method has dislocation densities $>10^6$ cm^{-2} and small angle grain boundaries which limits its application. The IKZ has started research on Czochralski and flux growth of $SrTiO_3$ supported by "Pakt für Forschung" funds in 2013, and made great progress towards preparation of bulk crystals with lower defect density and appreciable crystal sizes (see report below). Also, up to now the IKZ is the only institution worldwide to prepare bulk rare-earth scandate crystals which provide perovskite substrates with tailored lattice constants in the 3.95–4.02 Å range. With $LaLuO_3$ (pseudo-cubic lattice constant 4.18 Å), the IKZ has also recently grown bulk crystals of one of the rare materials with an even higher lattice constant [1].

Apart from perovskites, transparent semiconducting oxides (TSOs) are a further main topic. Compounds like ZnO [2], β-Ga_2O_3 [3], In_2O_3 [4] and SnO_2 [5] exhibit outstanding properties. Especially, in the field of bulk crystal growth of β-Ga_2O_3, In_2O_3 and SnO_2 which share the tendency to start decomposing far below their melting temperatures, IKZ has become a world-wide leading role.

The successful bulk growth of these compounds at the IKZ using unique growth conditions and in part also novel growth approaches has been reported already. The availability of these crystals, which can be used as substrates or components for electronic devices, is the basis for cooperations with IKZ department "Layers and Nanostructures" and numerous other cooperations, e.g., with the Solid State Physics Section at the Humboldt-University of Berlin, the Paul Drude Institute, the Institute of Physics at Leipzig University, the groups of Prof. J. Speck at the University of California Santa Barbara, of Prof. D. Schlom at Cornell University, and of Prof. D. Jena at Notre Dame University, USA. A new TSO material $MgGa_2O_4$ that can be used for ferromagnetic as well as semiconducting purposes is presented in the results section.

Finally, the group's activities on Langasite crystals growth should also be mentioned. The family of Langasite-type crystals (represented by the general type $La_3Ga_5SiO_{14}$) is very important for high-temperature piezoelectric applications, such as pressure sensors and actors. In contrast to Quartz which loses its piezoelectricity due to a phase transition at 573 °C, Langasites can be used up to 1470 °C. They can be grown from the melt by the Czochralski method. This research is done in a close, long-lasting collaboration with the company Kistler Instrumente AG in Winterthur/Switzerland. While the original goal, a technology transfer of 2-inch crystal growth, was already completed in 1998, the IKZ has

Dielectric & Wide Bandgap Materials: **Oxides/Fluorides**

continued its research with the focus shifted to explore and investigate growth of new compounds with even higher sensitivity and temperature stability. Recently, the research contract has been extended until 2019.

Results

In the following, the report focuses on the recent achievements of high temperature melt growth and characterization of flux-grown strontium titanate ($SrTiO_3$) as well as of a novel semiconducting oxide, $MgGa_2O_4$, and on the elaboration of the levitation-assisted self-seeding crystal growth method (LASSCGM), which was invented at the IKZ for growing In_2O_3 bulk single crystals.

Strontium titanate ($SrTiO_3$) is a well-known substrate material and has been used for different applications and research purposes (including strained perovskite layers as mentioned above). It is prepared at industrial scale by the Verneuil method, but the structural quality is insufficient for epitaxial film growth with high perfection needed for novel oxide electronic devices. Alas, the melt growth of $SrTiO_3$ by the Czochralski method suffers from growth instabilities, which are closely related to the low thermal conductivity of the crystals in conjunction with their very high near-infrared absorption at growth temperatures. As a consequence, the crystals form spirals. However, bulk single crystals of $SrTiO_3$ have been successfully grown at the IKZ from TiO_2-rich melts using the TSSG method at significantly decreased temperatures of about 1740 °C [6]; note that the melting point of $SrTiO_3$ is about 2080 °C, while the $SrTiO_3$–TiO_2 eutectic solidifies at 1449 °C [7]. The lower temperature leads not only to a significant decrease and infrared shift of the thermal radiation, but also the $SrTiO_3$ band-gap increases, thus mitigating self-absorption of near-infrared radiation. Despite the large crystal size obtained (1-inch diameter, 30 mm length), the quality has been improved compared to Verneuil grown crystals: typical etch pit density (EPD) values in the range of $2 \cdot 10^4$–$2 \cdot 10^5$ cm^{-2} for bulk crystals pulled in the <100> direction have been achieved [6]. Employment of a shaper (EFG technique) also allowed for better crystal diameter control.

Apart from the growth temperature, the oxygen partial pressure, which can be controlled by the growth atmosphere, was found to have a decisive impact on crystal coloration, self-absorption of heat and subsequent spiral formation during growth. If the crystal was grown with sufficient oxygen in the carrier gas (e.g. addition of 0.16 vol. % O_2 to 5N purity argon), the spiral formation could be suppressed even in long crystals, see Fig. 1. As it stands, oxygen vacancies lead to free charge carriers in the crystals at growth temperature, which absorb infrared light. At the same time, the formation of Ti^{3+} leads to a grayish-bluish coloration of such crystals.

As a consequence, the coloration of the crystals also gives valuable hints to the electrical conductivity of the crystals, e.g., blue crystals are conductive while the brownish or colorless ones are insulating. The growth at a sufficiently high oxygen partial pressure leads to a decrease in oxygen vacancies and thus to a decrease in free charge carriers and an increase in the optical transparency of the crystals. Our current research focuses on further improving the structural quality and providing a higher growth rate (currently at 0.15–0.33 mm/h due to flux growth) by adjusting the growth method and conditions.

Fig. 1

$SrTiO_3$ crystals grown by TSSG (starting temperature 1740 °C) in an oxygen enriched argon atmosphere (left crystal) and in pure argon (right crystal). All other growth conditions were kept identical. Note the spiral formation and bluish coloration of the right crystal. From Ref. [6] reproduced by permission of The Royal Society of Chemistry (RSC).

The initial motivation to grow $MgGa_2O_4$ was to obtain some test wafers to be used as substrates for magnetic spinel materials (ferrites) by Prof. Arun Gupta at Alabama University. Several melt growth runs were carried out using the Czochralski technique (the melting temperature is about 1930 °C) with oxidizing (CO_2-containing) atmospheres. Colourless, semi-insulating single crystals of up to 20 mm in diameter and 40 mm in length were obtained. Wafers were provided to Prof. Gupta's group, and first homoepitaxial growth test runs of $MgGa_2O_4$ by pulsed laser deposition were performed at the IKZ (group "Ferroelectric Oxide Layers"). Growth of smaller single crystals has been reported before in literature, e.g., from MgO-rich Pb O–PbF_2 solutions, by the Czochralski (CZ) method, and by the optical floating zone (OFZ) method. In all reported cases, the $MgGa_2O_4$ crystals were electrically insulating.

However, when growth was performed under very low oxygen partial pressure (e.g., Ar or N_2 atmospheres) the $MgGa_2O_4$ crystals with bluish coloration and semi-

Dielectric & Wide Bandgap Materials: **Oxides/Fluorides**

conducting properties were obtained for the first time. Note that growth at low oxygen partial pressures is only possible because $MgGa_2O_4$ is much more thermally stable than Ga_2O_3 (which would decompose quite rapidly under these conditions) despite of a melting point just about 110 K higher. The bluish coloration is typical for free carrier absorption in the near infrared range, as evidenced earlier for Ga_2O_3 [6], and results in foot formation and spiral growth due to crystal self–absorption of the radiated heat. Thus, Czochralski growth of longer crystals was not possible under such conditions, even if they appeared colourless at room temperature. In contrast, successful experiments under oxygen partial pressures of about 10^{-5} bar were performed by using the Kyropoulos, Bridgman, and our novel levitation–assisted self–seeding crystal (see below) growth methods.

To compensate for GaO losses during growth, the starting material composition contained 0.7 wt. % Ga excess (in respect to the Ga/Mg content). The resulting crystals showed a Ga execess ranging from zero (i.e., stoichiometric composition) to 0.6 wt. % [8]. However, we did not find any correlation with the appearance of the semiconducting state. In further experiments, we evidenced that the blue coloration becomes darker in the case of a high overheating of the melt (e.g., by 150 K), and that doping with Si previeled the semiconducting behaviour even for growth in oxidizing atmospheres (> 1 vol. %). Examples of our $MgGa_2O_4$ single crystals are shown in Fig. 2.

The obtained crystals were of single $MgGa_2O_4$ phase according to X-ray diffraction of powdered crystals. The full width at half maximum of the rocking curve was around 50 arcsec for both (222) and (400) reflections of a (110) oriented sample. $MgGa_2O_4$ has an inverse spinel structure (cubic system). A reversible change from inverse spinel ordering (which can be described as $Ga^{[4]}[MgGa]^{[6]}O_4$) to a random ordering of the cations was evidenced by differential scanning calorimetry to happen during annealing at temperatures above 1000 °C for several hours (for details see the report of the IKZ group "Chemical and Thermodynamic Analysis"). The room temperature lattice constant of a = 8.286 Å provides a low lattice mismatch to different cubic ferrite spinels. In contrast to β–Ga_2O_3, $MgGa_2O_4$ has no distinguished cleavage planes, and its medium hardness provides good preconditions for wafering.

Continuing our extensive research on bulk single crystals of transparent semiconducting oxides (TSOs) such as β–Ga_2O_3, In_2O_3, and SnO_2 which have been detailed in our previous reports, the structural, electrical, and optical properties of melt grown $MgGa_2O_4$ single crystals have been studied in detail [8].


Fig. 2

Single crystals of $MgGa_2O_4$ obtained by the Kyropoulos method (a) and LASSCGM (b). From Ref. [15]. Copyright (C) 2015 WILEY–VCH Verlag GmbH & Co. KGaA, Weinheim.

$MgGa_2O_4$	Electron concentration [cm^{-3}]	Electron mobility [cm^2/Vs]	Resistivity [Ω cm]
As–grown bluish crystals	3.1×10^{17}– 1.8×10^{18}	1.9–7.1	0.1–3.7
Annealed in H_2: 600–900 °C, 10h	1×10^{18}–2×10^{18}	4.5–6.5	0.6–1.5
Annealed in O_2/air: > 600 °C, 10–40h	Insulator (Resistivity > 10^8 Ω cm)		

Table 1

Electrical properties of as–grown and annealed $MgGa_2O_4$ single crystals [8].

Results from Hall effect measurements performed at room temperature are summarized in Table 1. The free electron concentrations of the as–grown and undoped crystals (when semiconducting) are similar to other bulk TSO single crystals [9]. However, the electron mobility is much smaller, between 1.9 and 7.1 cm^2/Vs only. We suggest that the different site occupancy of Mg in the inverse spinel structure leads to significant lowering of the free electron mobility due to scattering. While no clear correlation could be found between incomplete cation ordering or deviation from the ideal Ga/Mg ratio and the electrical and optical properties of the material, the influence of oxygen vacancies is significant, which is typical TSO behaviour: When the semiconducting crystals were annealed in oxygen–containing atmospheres (e.g., O_2 or air) at temperatures above 600 °C for 10–40 h, they became electrically insulating. On the other hand, the free electron concentration is hardly affected by annealing the crystals in the presence of hydrogen at temperatures between 600–900 °C for 10 h.

Fig. 3 shows transmittance spectra of semiconducting (as–grown) and electrically insulating (after annealing) $MgGa_2O_4$ crystal samples, which were measured at room temperature in the wavelength range from 200 to 2500 nm. As expected, the free carrier absorption leads to a significant drop in transmission in the near infrared

Dielectric & Wide Bandgap Materials: **Oxides/Fluorides**

(NIR) part of the spectrum of the semiconducting sample, which is lacking in the electrically insulating sample. The drop in NIR transmission also causes the bluish coloration. In both cases, the UV absorption edge is very steep and originates at about 250 nm corresponding to a direct optical bandgap of approx. 4.9 eV, close to that of β-Ga_2O_3 (4.8 eV). The electrical properties of Si-doped $MgGa_2O_4$ were very similar to those of the nominally undoped semiconducting crystals. Further studies are necessary to clarify whether the semiconducting behaviour of $MgGa_2O_4$ crystals could actually be utilized in novel oxide semiconductor applications.
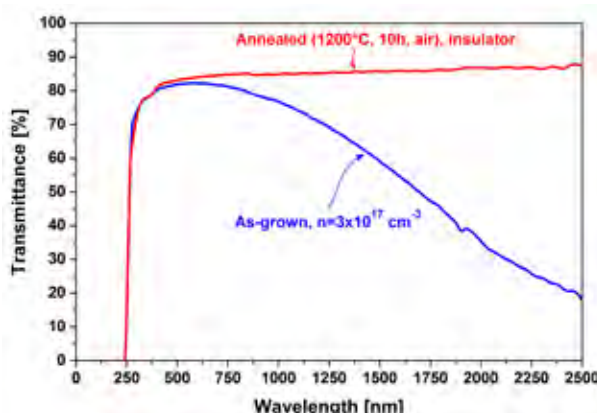
Fig. 3

Transmittance spectra of semiconducting and insulating $MgGa_2O_4$ single crystals. The sample thickness was 0.5 mm. The spectra were not corrected for reflectance. From Ref. [8]. Copyright (C) 2015 WILEY-VCH Verlag GmbH & Co. KGaA, Weinheim.

In_2O_3 is another material belonging to the group of transparent nanocrystalline, polycrystalline or amorphous semiconducting oxides. In contrast to nanocrystalline indium tin oxide (ITO) thin films, which are widely used as electrodes in solar cells, displays, touch panels, and coatings, bulk In_2O_3 is semiconducting with an optical bandgap of 2.8 eV [10]. Very high thermal instability (much higher than that of ZnO) of that compound at the melting temperature of about 1950°C makes it impossible to grow In_2O_3 single crystals from the melt by standard growth techniques [11]. For that reason we defined and developed a novel crystal growth technique based on electromagnetic levitation of the melt and self-creation of a seed, which both formulate the name of that growth technique: Levitation-Assisted Self-Seeding Crystal Growth Method (LASSCGM) [12,13].

The main components are an iridium crucible containing In_2O_3 starting material, an iridium lid with evacuation openings and an RF coil as a source of the electromagnetic field. The fundamental idea is to convert an initially insulating In_2O_3 starting material within the Ir crucible into highly conducting state in the liquid phase and levitate a portion of the melt through the crucible wall (which must be thinner than the penetration depth of the electromagnetic field) with a liquid neck being created between two liquid regions. Once the neck is formed, the system must be cooled down very quickly, at least up to the solidification, since decomposition rate is very high and the corresponding mass loss of In_2O_3 is about 20 wt. % per hour. The total time between melting and solidification is typically around or below 1 hour only. During solidification, two crystals are formed on opposite sides of the seed-neck. When the neck breaks before crystallization starts, only polycrystalline boules will form.

With the LASSCGM method, In_2O_3 single crystals of about 35 mm in diameter and 6-15 mm thick can be obtained (Fig. 4a). The as-grown crystals are dark brown or almost black in colour due to the presence of indium nanoparticles responsible for light extinction [14]. After annealing in the presence of oxygen at temperatures above 700°C for at least several hours, the Indium nanoparticles are oxidized and the crystal lattice is reconstructed in the affected areas. As the result, annealed samples cut from the crystals become yellow and transparent in the visible spectrum and the near infrared (Fig. 4b).
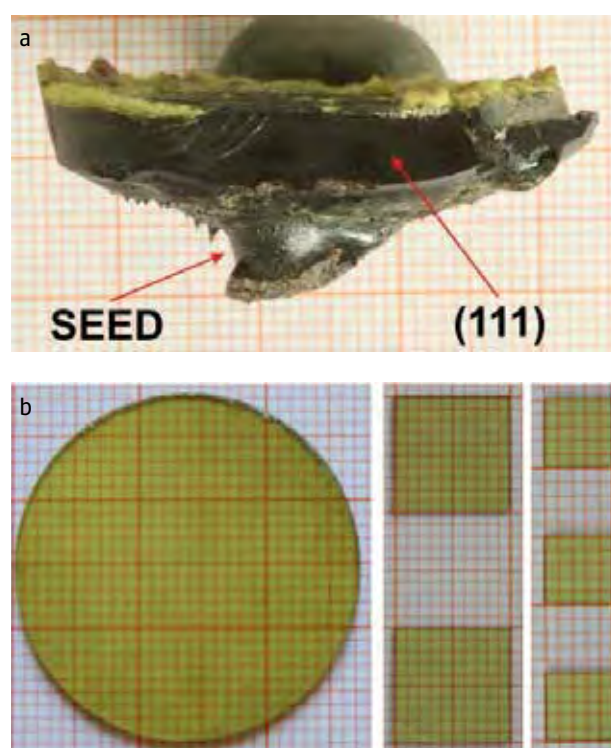

Fig. 4

As-grown bulk In_2O_3 crystal (a) and oxygen-annealed In_2O_3 wafers (b). From Ref. [8]. Reproduced with permission of ELSEVIER BV.

The as-grown In_2O_3 crystals were always semiconductors with free electron concentrations of 1-4x10^{18} cm^{-3} and electron mobilities of 130-213 cm²/Vs. The electron concentration decreases and increases by about 1 order of magnitude after annealing in the presence of oxygen and hydrogen, respectively [15].

Dielectric & Wide Bandgap Materials: **Oxides/Fluorides**

Since the LASSCGM method was established at the IKZ, we have provided bulk crystalline samples to numerous researchers worldwide, for determining the band structure and electronic bulk and surface properties as well as to provide substrates for growth of In_2O_3, $(In,Ga)_2O_3$, and even wurtzite InN layers. In turn, the LASSGCM can be considered a useful method to prepare also other semiconducting oxide crystals with strong decomposition which cannot be grown by conventional melt techniques, e.g. $MgGa_2O_4$ as shown above.

References

[1] D.G. Schlom, L.Q. Chen, C.J. Fennie, V. Gopalan, D.A. Muller, X. Pan, R. Ramesh, R. Uecker; MRS Bulletin 39 (2014) 118–130

[2] D. Klimm, D. Schulz, S. Ganschow; Growth of Bulk ZnO in: Comprehensive Semiconductor Science and Technology, P. Bhattacharya, R. Fornari, H. Kamimura (eds.), Elsevier Science, Amsterdam (2011) 302–338

[3] Y. Tomm, P. Reiche, D. Klimm, T. Fukuda; J. Crystal Growth 220 (2000) 510–514

[4] Z. Galazka, R. Uecker, K. Irmscher, D. Schulz, D. Klimm, M. Albrecht, M. Pietsch, S. Ganschow, A. Kwasniewski, R. Fornari; J. Crystal Growth 362 (2013) 349–352

[5] Z. Galazka, R. Uecker, D. Klimm, K. Irmscher, M. Pietsch, R. Schewski, M. Albrecht, A. Kwasniewski, S. Ganschow, D. Schulz, C. Guguschev, R. Bertram, M. Bickermann, R. Fornari; Phys. Status Solidi A 211 (2014) 66–73

[6] C. Guguschev, D. J. Kok, Z. Galazka, D. Klimm, R. Uecker, R. Bertram, M. Naumann, U. Juda, A. Kwasniewski, M. Bickermann; CrystEngComm 17 (2015) 3224–3234

[7] C. Guguschev, D. Klimm, F. Langhans, Z. Galazka, D. Kok, U. Juda, R. Uecker; CrystEngComm 16 (2014) 1735–1740

[8] Z. Galazka, D. Klimm, K. Irmscher, R. Uecker, M. Pietsch, R. Bertram, M. Naumann, M. Albrecht, A. Kwasniewski, R. Schewski, M. Bickermann; Phys. Status Solidi A 212 (2015) 1455–1460

[9] Z. Galazka, K. Irmscher, R. Uecker, R. Bertram, M. Pietsch, A. Kwasniewski, M. Naumann, wT. Schulz, R. Schewski, D. Klimm, M. Bickermann; J. Crystal Growth 404 (2014) 184–191

[10] K. Irmscher, M. Naumann, M. Pietsch, Z. Galazka, R. Uecker, T. Schulz, R. Schewski, M. Albrecht, R. Fornari; Phys. Status Solidi A 211 (2014) 54

[11] Z. Galazka, R. Uecker, K. Irmscher, D. Schulz, D. Klimm, M. Albrecht, M. Pietsch, S. Ganschow, A. Kwasniewski, R. Fornari; J. Cryst. Growth 362 (2013) 349

[12] Z. Galazka, R. Uecker, R. Fornari; J. Crystal Growth 388 (2014) 61

[13] Z. Galazka, R. Uecker, R. Fornari; PCT patent application, 2012, publication No. WO 2013/159808

[14] M. Albrecht, R. Schewski, K. Irmscher, Z. Galazka, T. Markurt, M. Naumann, T. Schulz, R. Uecker, R. Fornari, S. Meuret, M. Kociak; J. Appl. Phys. 115 (2014) 053504

[15] Z. Galazka, K. Irmscher, M. Pietsch, T. Schulz, R. Uecker, D. Klimm, R. Fornari; CrystEngComm 15 (2013) 2220

Dielectric & Wide Bandgap Materials:
Gallium Nitride

Head apl. Prof. Dr. Dietmar Siche
Team Dr. S. Golka, K. Kachel, R. Nitschke, Dr. R. Zwierz

Übersicht

Galliumnitrid (GaN) ist ein Basismaterial für die Opto-elektronik und die hochfrequente Leistungselektronik. Die halide Gasphasenepitaxie (HVPE) auf Saphir wurde etabliert, um das vorübergehende Fehlen von Eigen-substraten zu überbrücken. Diese sind Voraussetzung, um die Versetzungsdichte und die thermischen Span-nungen in den gewachsenen Schichten um Größenord-nungen zu reduzieren. Trotz einiger Nachteile, wie hohe Defektdichte, niedrige Umwandlungseffizienz der Ausgangsstoffe und Bildung von Ammoniumchlorid als Nebenprodukt, bleibt das GaN-Wachstum aus der Gas-phase ein vielversprechender Ansatz für die Abschei-dung von Schichten. Unsere Aktivitäten zur plasma-gestützten Gasphasenzüchtung von GaN wurden im letzten Frühjahr mit der erfolgreichen Promotion von Dr. Radoslaw Zwierz abgeschlossen [1].

Wie im letzten Jahr berichtet, wurde ein kleiner, neuer Reaktor für die gesteuerte pseudo-halide Gasphasen-epitaxie (PHVPE) [2] in Betrieb genommen. Dabei wirkt das CN^-- Ion als chemisches Transportmittel. In diesem Zusammenhang wurde das DFG-Projekt QuarzGaN zum Studium der kontrollierten C-Dotierung bei der Reakti-on von GaCN mit Ammoniak zu GaN in Zusammenarbeit mit dem Institut für Festkörperphysik der Technischen Universität Berlin, Prof. A. Hofmann, begonnen. Nach-dem sich herausstellte, dass die Wachstumsraten auf-grund der ungenügenden HCN-Bildung aus Methan und Ammoniak im Einlassrohr begrenzt sind, wurde der Aufbau durch einen neu konstruierten HCN-Reaktor ergänzt. Die bisherigen Ergebnisse wurden in einer Dissertation von Herrn Kachel [3] zusammengefasst und im November 2014 an der Humboldt-Universität eingereicht.

Das ZIM-Projekt zur Lösungszüchtung aus einer Metall-schmelze wurde mit einer geänderten Ausrichtung fort-gesetzt. Die erforderliche Reaktortechnologie wurde in Zusammenarbeit mit zwei kleinen Firmen entwickelt, der Plasmetrex GmbH, Berlin und der DTF Technology GmbH, Dresden. Im Juli 2014 wurden die praktischen Arbeiten zur Firma DTF verlegt. Dabei wurde ein Kopp-lungsprinzip für Radiofrequenz – Induktion mit einer sehr hohen Ausbeute von aktiviertem Stickstoff entwi-ckelt. Dieses Konzept wurde sowohl für die Abscheidung aus der Lösung (Metallschmelze) als auch für reaktive Plasmen untersucht. Im Fall reaktiver Plasmen können teilkristalline Nitridschichten bei Temperaturen über 1000 °C mit Raten von über 100 nm/min auf verschie-denen Substraten abgeschieden werden.

Overview

Gallium nitride (GaN) is a basic semiconductor for opto- and high frequency power electronics. The Halide Vapour Phase Epitaxy (HVPE) on sapphire substrate was estab-lished to bridge temporarily the lack of native subst-rates, which are essential to reduce dislocation density and thermal stresses in grown layers by orders of mag-nitude. Despite of some disadvantages, like high defect density, low source material conversion and ammonium chloride by-product formation, GaN growth from gase-ous phase stays highly promising for layer deposition.

Our activities to plasma enhanced vapour growth of GaN were completed in last spring with the successful gra-duation of Dr. Radoslaw Zwierz [1].

As reported in the previous year, a small new reactor was put into operation for the controlled Pseudo-Ha-lide Vapor Phase Epitaxy (PHVPE) [2], where the CN^- ion acts as chemical Ga transport agent. In this context the DFG project QuartzGaN was started to study controlled C doping at the reaction of GaCN with ammonia to GaN in collaboration with the Institute of Solid State Physics at the Technical University Berlin, Prof. A. Hofmann. As we evidenced that growth rates were limited by insufficient HCN formation using the inline conversion of methane and ammonia, the setup was extended by a newly con-structed HCN reactor. The previous results have been summarized in a thesis submitted by K. Kachel [3] to Humboldt-University in November 2014. The ZIM proj-ect on solution growth from a metal melt was carried on with modified topic. The required reactor technolo-gy was developed in cooperation with two small com-panies, Plasmetrex GmbH, Berlin and DTF Technology GmbH, Dresden. In July 2014, the practical work was moved to DTF. Within this activity a coupling concept for radio frequency induction has been developed, that produces a large amount of active nitrogen with high yield. This concept has been tested for both deposition from solution (metal melt) as well as from reactive plas-ma. In the case of reactive plasma partially crystalline nitride layers can be grown at 1000 °C exceeding depo-sition rates of 100 nm/min on various substrates.

Fig. 1
QuartzGaN equipment with
reactor scheme (1), HCN reactor (2),
gas cell for FTIR (3) and MCT detector (4)
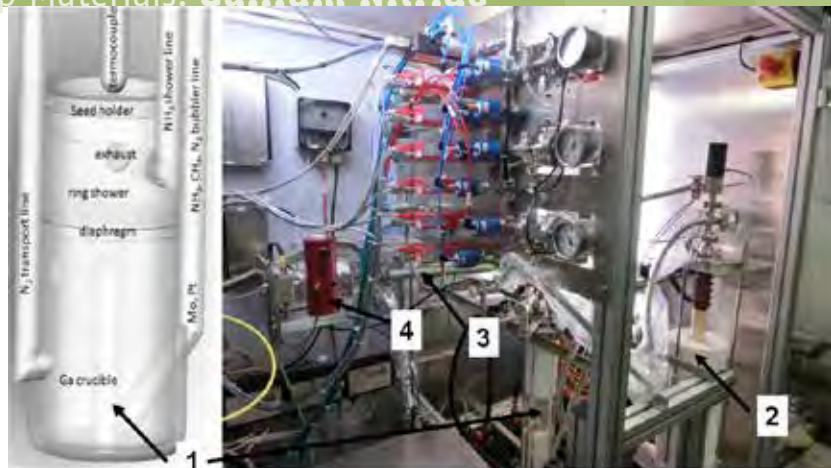
Results

Pseudo-Halide Vapour Phase Epitaxy (PHVPE) of GaN:C layers

In a PHVPE system cyano ions act as transport agent for Ga instead of chloride ions as in conventional HVPE. Carbon doping is of special interest to prepare semi-insulating (SI) GaN, but its effect on the electronic properties is not fully understood yet. This holds true in particular for higher carbon concentrations, which could be achieved with PHVPE but have the drawback that the growth rate depends on the carbon concentration. Quantum chemical ab initio calculations [4] as well as waste gas analysis by in-situ FTIR confirmed the postulated thermodynamic reactions [2]. As previously described, a carbon free setup with controlled carbon precursor (methane) supply forms the basis of our new PHVPE approach.

In the last year the newly designed graphite-free reactor (Fig. 1) was set into operation. Main efforts were put into stable production of HCN, the transport agent for Ga, formed by the Degussa process:

$$CH_4(g) + NH_3(g) \rightarrow HCN(g) + 3H_2(g) \text{ (on Pt catalyst).} \quad (1)$$
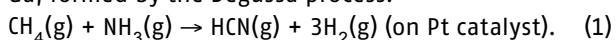
Using this approach, the GaN growth rate did not exceed 5 µm/h and the layers did not coalesce, but up to 30 µm thick islands could be grown with sizes up to 50 µm. Using in-situ exhaust gas analysis by FTIR spectroscopy to quantify the reaction products (see Fig. 2), it was found that the HCN volume was limited by the surface of the metallic Pt mesh in the supply line for the methane-ammonia mixture.
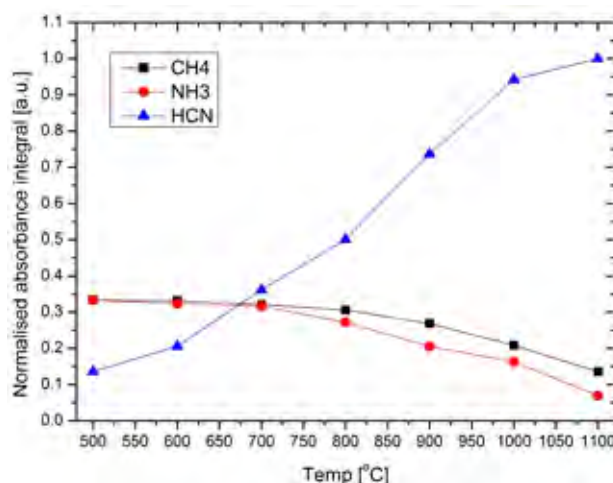

Therefore, it was necessary to increase the surface of the catalyst. First, a new HCN reactor was constructed to provide the HCN synthesis in a larger volume and separate from the growth reactor, i.e. independent of the growth reactor temperature. The Pt mesh, with a surface of approx. 1 m^2/g, was replaced by 3.2 mm sized Al$_2$O$_3$ ceramic spheres, covered by Pt with a surface of 150-250 m^2/g. The HCN containing gas is then guided through a Mo mesh to decompose remaining ammonia and into the reactor. A methane to ammonia ratio of 1 : (7–10) was found favorable to prevent remaining methane and carbon containing intermediates from getting into the reactor, as this can lead to carbon coating of the quartz tube. With the new HCN furnace the production of HCN and subsequent Ga transport by GaCN formation due to the reaction:

$$HCN(g) + Ga(l/g) \rightarrow GaCN(g) + \tfrac{1}{2} H_2(g) \quad (2)$$
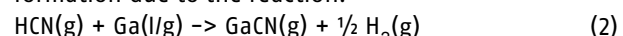
could be significantly increased. Due to the toxicity of hydrogen cyanide we had to modify the set-up to meet the required high safety standards.

Finally, first experiments have been conducted to deposit GaN on the seed under NH$_3$ excess using the reactor and HCN source as detailed above:

$$GaCN(g) + NH_3(g) \rightarrow GaN(s) + HCN(g) + H_2(g) \quad (3)$$
$$GaCN(g) + 2NH_3(g) \rightarrow GaN(s) + C(s) + N_2(g) + 3H_2(g) \quad (4).$$
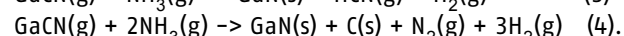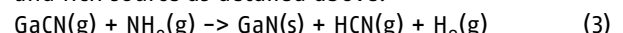
Free energy changes of reactions (3) and (4) at Ptot = 600 mbar in thermodynamic equilibrium were calculated as a function of temperature with ''FactSage'' software using thermochemical standard data [2]. Considering the thermodynamic driving forces at typical growth conditions (ca. 1300 K at Ptot = 600–800 mbar) reaction (4) was found dominant, but reaction (3) is also possible. However, kinetic effects cannot be neglected and the influence of GaCN transport on carbon doping has to be studied experimentally in future experiments.

Fig. 2
HCN formation (normalized integrated intensity of FTIR spectra) when supplying a proper methane/ammonia ratio to the bubbler line with in-line conversion at a Pt catalyst.

Low pressure, high density plasma based solution growth

Low pressure (atmospheric) solution growth of GaN has already been performed by Liquid Phase Epitaxy (LPE) at Fraunhofer IISB in Erlangen, using ammonia as nitrogen source at growth temperatures between 900–1020 °C. The average growth rate R for conditions described in [5] was R = 0.1 µm/h.

However, for InN, having the highest nitrogen partial pressure of nitrides and therefore is much more challenging to grow, this method could be suitable, especially if nitrogen plasma is used instead of ammonia. Therefore, we attempted to use dense nitrogen plasma to dissolve nitrogen in a solution, followed by layer growth caused by super-saturation inside the solution. Hence our approach features a two stage process that we expected to be advantageous for realizing high growth rates. The layer should grow near thermal equilibrium on the seed at the crucible bottom, while the plasma itself, far away from equilibrium, hits the liquid surface. The energetic, dense plasma would not create layer damage, because the growing interface is covered by the solution. This technique was expected to produce dissociated nitrogen solved in the liquid surface by temperature independent bombardment with nitrogen plasma, which can be controlled to keep the surface free of a blocking crust. At the same time the temperature gradient should be increased between plasma heated solution surface and seed, thus enhancing nitrogen diffusion to the seed.

At IKZ an Inductively Coupled Plasma (ICP) reactor has been constructed within a project funded in the frame of the central innovation program for small and medium-sized businesses (ZIM) in cooperation with Plasmetrex GmbH, Berlin and DTF GmbH, Dresden. Thick polycrystalline InN layers could be grown on the molten indium surface only. Due to the low nitrogen solubility in gallium or indium, the plasma density had to be decreased to prevent N_2-bubbles formation in the beginning and then, at lower density, crust formation. Unfortunately, it proved that the remaining temperature difference between hotter solution surface and cooler seed at the bottom was too low to enhance the diffusion in the thin, convection unaffected boundary layer. Due to the low pressure required for sustaining the plasma, it proved very difficult to control the temperature gradients necessary to provide high growth rates. As a consequence the project topic was extended to cold reactive plasmas that include the usage of acetylene to grow layers from a reactive atmosphere. In the case of reactive plasma, partially crystalline nitride layers can be grown at 1000 °C exceeding deposition rates of 100 nm/min on various substrates and on the indium solvent (see Fig. 3).
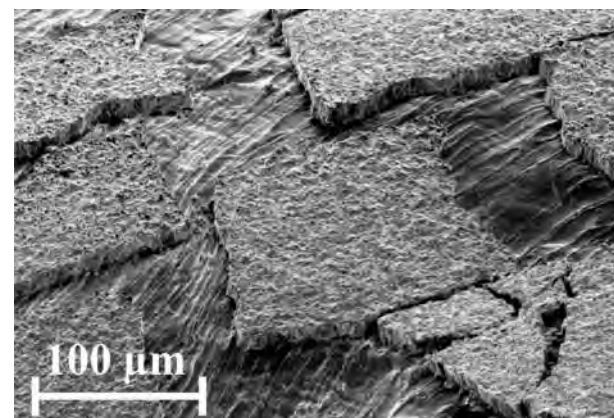

Fig. 3
InN crust of about 10 µm thickness formed on In, unintentionally oxygen doped.

References

[1] R. Zwierz; Plasma Enhanced Growth of
 GaN Single Crystalline Layers from Vapour Phase;
 PhD thesis, Brandenburg University of Technology
 Cottbus–Senftenberg (2014)

[2] K. Jacobs, D. Siche, D. Klimm, H.-J. Rost, D. Gogova;
 J. Crystal Growth 312 (2010) 750–755

[3] K. Kachel; Pseudo Halide Vapour Phase Epitaxy
 Growth of GaN Crystals;
 PhD thesis, Humboldt-Universität zu Berlin (2015)

[4] O.B. Gadzhiev, P.G. Sennikov, A.I. Petrov, D. Gogova,
 K. Kachel, S. Golka, D. Gogova, D. Siche;
 J. Mol. Model. 20 (2014) 2473;
 DOI 10.1007/s00894-014-2473-4

[5] S. Hussy, E. Meissner, P. Berwian,
 J. Friedrich, G. Müller;
 J. Crystal Growth 310 (2008) 738–747

Dielectric & Wide Bandgap Materials:
Aluminium Nitride

Head   Dr. Jürgen Wollweber

Team   Prof. Dr. M. Bickermann, Dr. A. Dittmar, Dr. C. Hartmann, S. Kollowa, F. Langhans

Überblick

AlGaN–Schichten sind dank ihrer einstellbaren physikalischen Eigenschaften extrem vielseitig einsetzbar. Mit Blick auf eine Kommerzialisierung ist vor allem die im Bereich von 3,4 eV bis 6,1 eV (GaN–AlN) einstellbare Bandlücke relevant. Diese Eigenschaft gestattet die Herstellung von Leuchtdioden und sogar Lasern für den UV-Bereich, die spezifische Anwendungen bei der Wasser- und Nahrungsmitteldesinfektion, in Härteprozessen, in der Medizin für Diagnostik und Behandlung aber auch für die Kurzstreckenkommunikation ermöglichen, um nur einige Beispiele zu nennen. Hinzu kommen interessante Anwendungen dieses Materials in schnellen Leistungstransistoren und, wegen des ausgeprägten Piezoeffekts bei hohen Temperaturen, in Drucksensoren. Momentan werden wegen des Mangels an AlN-Wafern, die man als Quasi-Eigensubstrate ansehen kann, aber auch aus Kostengründen Fremdsubstrate wie SiC, Saphir oder sogar Silicium in der AlGaN–Schichtabscheidung eingesetzt. Die damit verbundenen großen Gitterfehlpassungen und die unterschiedlichen chemischen Bindungen führen jedoch zu hohen Defektdichten in den AlGaN–Schichten mit Werten von maximal $10^6 cm^{-2}$. Daher ist allgemein akzeptiert, dass sich das volle Potential von AlGaN nur bei Verfügbarkeit von qualitativ hochwertigen AlN-Wafern ausschöpfen lässt. Auf dem Weg zu diesen AlN-Wafern hat sich in den letzten Jahren die Sublimation-Rekondensation (PVT) als geeignetste Züchtungsmethode erwiesen. Deren Implementierung ist wegen der Prozesstemperaturen von über 2000 °C und der aggressiven Al-0-Gasspezies, die nahezu alle Tiegelmaterialien angreifen, eine große Herausforderung.

Im IKZ wurde deshalb eine Gruppe aufgebaut, die sich während der letzten 10 Jahre sowohl mit der benötigten Infrastruktur (Sinter-TaC-Tiegel, Reinigung des Quellmaterials und chemo-mechanische Politur) als auch mit der Entwicklung einer Basistechnologie für die AlN–Sublimationszüchtung befasst hat. Das dabei erreichte Niveau ist im Bereich der Forschungsinstitute einzigartig und entspricht dem Stand der wenigen kommerziellen Anbieter.

Epitaxie-geeignete AlN-Wafer (max. 10 x 10 mm², Rocking Curve FWHM ~ 20 arcsec, epd 10^2–10^4 cm⁻²) aus diesem Prozess sind von Partnern im BMBF-Projekt WideBase (Abschluss 2014) für die Prozessierung von MOCVD-Homoepitaxieschichten und für optisch gepumpte Laserstrukturen verwendet worden. Trotz des frühen Entwicklungsstadiums konnte die Wettbewerbsfähigkeit von AlN-Substraten im Vergleich zum Saphir deutlich demonstriert werden.

Im Berichtszeitraum lag der Fokus der Gruppenarbeit auf den Themen Durchmesservergrößerung, Si-Doping, Versetzungsdynamik und optisch/elektrische Eigenschaften mit dem generellen Ziel die Substrateigenschaften den gewünschten Anwendungen anzupassen.

Auf Grundlage dieses prä-kommerziellen Stadiums werden die Forschungsaktivitäten jetzt im Konsortium „Advanced UV for Life" (BMBF Initiative Unternehmen Region: „Zwanzig20 – Partnerschaft für Innovation") mit verstärkter Orientierung auf Industrieanforderungen weitergeführt. Dabei finden nicht mehr nur strukturelle und elektrische Parameter, sondern verstärkt auch Epitaxiefähigkeit und Technologietransfer im industriellen Kontext Berücksichtigung.

Overview

AlGaN layers have an enormous versatility owing to their adjustable physical properties. In view of commercialization, it is the direct bandgap which can be chosen from 3.4 eV up to 6.1 eV (GaN to AlN). This feature allows the fabrication of UV light emitting diodes and even lasers for very specific applications in water/food disinfection, curing processes, medical diagnostics, medical treatment and short distance communication, just to name a few examples. Additionally, there are many interesting applications such as fast high-performance transistors and pressure sensors based on piezo elements.

Today, in the absence of AlN wafers as quasi-native substrates as well as for cost reasons, foreign substrates like SiC, sapphire, or even silicon are used for AlGaN layer deposition. However, the large lattice mismatch and different chemical binding properties lead to high defect densities in the AlGaN layers with values of orders above the desired 10^6 cm⁻² as maximum. Therefore, it is generally accepted that the full potential of AlGaN is strictly bound on the availability of high-quality AlN wafers. The implementation of a commonly accepted suitable growth technology, sublimation-recondensation (PVT), is a real challenge because of process temperatures above 2000 °C and aggressive Al and 0 gas species that attack nearly all crucible materials during crystal growth.

The IKZ has therefore established a group which has developed during the last decade not only the needed infrastructure (sintered TaC crucible, purified source material, and chemo-mechanical planarization) but also a basic technology for AlN single crystal growth by sublimation-recondensation. The level of development corresponds generally to the one found at the few commercial providers and is unique for research institutes. Epi-ready AlN wafers (max. 10 x 10 mm^2, rocking curve FWHM ~ 20 arcsec, epd 10^2-10^4 cm^{-2}) from this process have been used by partners in the Berlin WideBase framework to process homoepitaxial layers by MOCVD as well as optical pumped laser structures. This project had been funded by BMBF and was concluded in 2014. The competitiveness of AlN substrates in comparison to sapphire could be clearly demonstrated already in this early stage. During the report period, the focus of our group was on geometry enlargement, Si doping, dislocation dynamics, and optical/electrical properties, in order to provide substrates with tailored properties for the desired applications.

On the basis of this pre-commercial stage, the research activities will be continued now as partner in the project "Advanced UV for Life" (BMBF Innovation Initiative "Entrepreneurial Regions") with a view on industrial demands, including not only structural and electrical parameters, but also epitaxial usability and technology transfer into an industrial context.

Results

Initially based on spontaneously grown crystals, subsequent homo-epitaxial growth runs on seeds cut from such crystals with limited diameter enlargement have demonstrated to maintain the crystalline quality [1]. The current work focuses on the two remaining major challenges: (i) to enlarge the diameter in a reproducible manner, and (ii) to provide and control the electrical and optical properties of the bulk AlN crystals as demanded for the envisaged application (e.g. deep-UV optical transparency or electrical semi-insulating behavior) by influencing the impurity concentrations inside the growth room during growth and thus in the growing crystals.

The main problem impeding a straightforward diameter enlargement is the strong tendency of AlN to form slow-growing prismatic m-plane facets. By means of a proprietary, specifically shaped seed holder, a convex thermal field in front of the seed combined with a controlled species flow around the growth interface, a gradual and smooth crystal enlargement can be achieved (Fig. 1) [2]. The special kind of seed holder design leads to a variation of the thermal gradient along the seed surface with low values in the center (~10 K/cm), which are almost doubled at the outer rim. Currently,

crystals of up to 15 mm diameter with average rocking curve FWHM values between 13 and 21 arcsec and dislocation densities < 10^4 cm^{-2} across the whole surface area are obtained by using this technique. However, reproducibility is still an issue as structural defects from the seed, even ones that are hardly visible under crossed polarizers, penetrate into the crystal. Such defects form strained areas where dislocations easily multiplicate and finally form low-angle grain boundaries, which render these areas useless for epitaxy and applications.


Fig. 1

Homoepitaxially grown AlN single crystal; seed diameter 10 mm, end diameter 12 mm

The achievements and issues stated above trigger an interest for a deeper understanding of the evolution of structural defects in the AlN crystals grown in our topical setup, especially concerning interaction, multiplication and propagation processes of dislocations. This interest was fueled by the observation that dislocations can be decorated during growth when using dedicated growth parameters. While an influence of growth temperature and the presence of tungsten or silicon are noticed, the origin of the decoration is still under investigation. Such decoration is not visible in the crystals with state-of-the-art structural quality, and also not visible in the crystal border areas grown on the prismatic facets.

Monitoring the decoration in the crystal volume has been performed by laser scattering tomography (LST), a technique developed at the IKZ originally for dislocation analysis in bulk GaAs crystals. In this technique, two optical polished sides which are perpendicular to each other are subjected to a laser beam with line focus, whose scattered light fraction is recorded on the other polished face by a photomultiplier. CCD camera and bulk crystal can be moved in all three dimensions in space, allowing a layer by layer imagining of scattering centers within the whole crystal volume with micrometer resolution. The technique exploits the fact that even small centers (down to 50 nm) can be reliably detected. The crystals investigated show a variety of dislocation patterns, such as areas dominated by dislocations propagating on the {0001}, {1-100} and {11-22} planes, areas

with cellular dislocation networks, low-angle grain boundaries, and border areas with clear polygonization patterns. Through the analysis of cross-slip processes it was possible to identify the absolute Burgers vector of dislocations. Exclusively dislocations with 1/3<11-20> Burgers vector gliding on planes {1100} and {1122} were observed which allowed us to conclude on glide and interaction processes of dislocations in AlN bulk crystals as dependent on the thermal gradient acting during growth. Fig. 2 features an insight into a cross slip process from m-plane {1-100} to the basal plane {000-1} and vice versa.
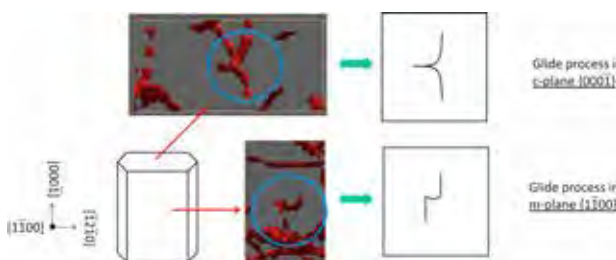
Fig. 2
Cross slip process from {1-100} to {000-1} and back,
3D-reconstructed LST image

Fig. 3 shows a typical LST 2D image taken in the vicinity to the enlargement area of an AlN bulk crystal with view through the as-grown {000-1} facet in the deep layer 0.95 mm below the surface. Besides a number of single dislocations propagating roughly in [0001] direction, the area denoting the transition to the expansion region (lower end of the figure) features strain-induced lateral dislocation bunching originating from the crystal edge. While the investigations give important insights into what kind of dislocation processes can be observed, a systematic study on dislocation behavior in AlN crystal with high structural perfection is still outstanding. As such crystals typically do not have their dislocations decorated, further work on the topic will include extensive studies by wet chemical etching and X-ray topography. For the latter, we have filed an application for synchrotron beamtime at the ANKA, operated by the Karlsruhe Institute of Technology.
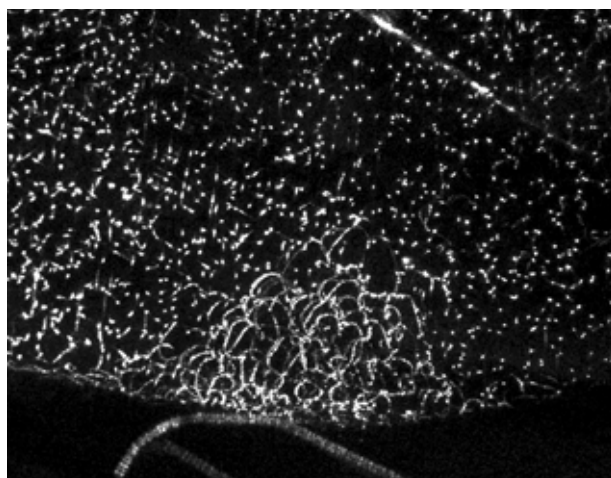
Besides structural issues, impurities are the second inherent problem. Due to the strong oxygen affinity of AlN and the high porosity of some setup materials, background impurities are unavoidable in PVT growth. Unfortunately, the main impurities oxygen, carbon, and silicon affect the optical and electrical characteristics of AlN. Understanding these effects and the interplay of the impurities is indispensible for providing AlN substrates with well defined properties. This is important because preconditions for a commercial exploitation of AlN embrace not only structural requirements but also defined optical and electrical characteristics which are determined by the concentrations of the electrically active impurities and intrinsic defects.

The impurity incorporation in the growing AlN crystal depends on the impurity release of the setup materials (source material, crucible, ...), the ambient (quartz recipient, streaming gas N_2), the growth facet [3], and the growth temperature. Typical concentrations found in the crystals are $3 \cdot 10^{18} - 3 \cdot 10^{19}$ cm^{-3} for oxygen and $3 - 6 \cdot 10^{18}$ cm^{-3} for carbon, while the values for silicon are significantly lower ($1 - 5 \cdot 10^{16}$ cm^{-3}).

By shifting the growth temperature in the range of 2000–2100 °C the oxygen concentration in the grown AlN crystal can be varied by a factor of about 2–3. The higher oxygen concentrations can be achieved at lower temperatures. In contrast, carbon and silicon concentrations are almost unaffected by the growth temperature. In our current set-up and conditions, growth temperatures T < 2040 ° lead to 3[C] < ([O] + [Si]) which result in deep UV transparent AlN crystals accompanied by weak n-type conductivity at elevated temperatures (> 600 °C). In contrast, high temperature semi-insulating (SI) AlN can be generated at T > 2050 °C. In this case the impurity concentrations are ([O] + [Si]) < 3[C] (Fig. 4).

Fig. 3
LST 2D image taken through
the {000-1} facet
close to the, via m-plane
facet grown, enlargement
area of an AlN bulk crystal,
width of the image 1.43 mm,
z = 0.95 mm below the
as-grown surface

# Dielectric & Wide Bandgap Materials: *Aluminium Nitride*
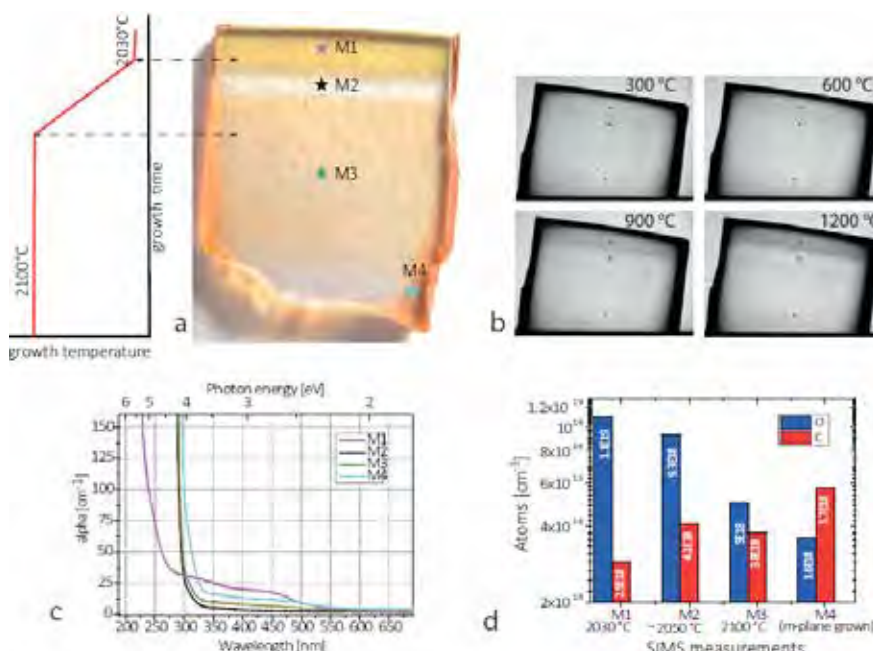
Fig. 4:

a) m-plane longitudinal cut of a homoepitaxially grown AlN crystal with decreasing growth temperature (2100 °C → 2030 °C) during the growth time;

b) images of optical transmission at 940 nm, which is correlated to the free carrier absorption, at different temperatures;

c) UV-VIS absorption spectra and

d) SIMS measurements of the sampling points M1 through M4 as indicated in a).

The transition from deep UV transparent AlN to high temperature SI-AlN with the change of the impurity concentrations ratio is due to a Fermi level shift which results in a change of the charge state of the carbon defects [4].

A better control of the impurity concentrations is intentional doping which may be achieved by adding certain doping elements into the growth cell. In the case of AlN, Si which is reported to act as a shallow donor is particularly interesting [5]. A simple gas phase doping (SiHCl3, SiH4) does not work because the dissociation temperatures of the compounds are much too low and hydrogen introduces additional problems such as crystal etching, passivation, etc. On the other hand, controlled doping via addition of solids is challenging as the respective compounds either decompose, melt, or react already during the heating-up stage (and evade from the crucible) or do not provide sufficient Si partial pressure even at growth temperature.

To realise a constant Si supply to the growing crystal we added Si containing sintered bodies to the AlN source material. These compacts consist of TaC with a small amount of WSi2 (1 to 3 mol-%). The relatively high melting point (~2160 °C) of WSi2 and its sufficient high Si partial pressure at growth temperatures (estimated by equilibrium calculations with FactSage™) makes it suitable as solid dopant source during PVT growth. Embedding it in dense sintered TaC ceramics prevents damage of the growth setup from liquid Si formation, suppresses fast dopant depletion, and promotes a smooth and constant Si release during the whole growth time. Thus, the solution found by the AlN group shows major progress in intentional doping with silicon towards a technology that needs only minor changes to standard growth setups.

Using this approach, AlN crystals were grown with Si concentrations in the range of 1-5·10^{19} cm^{-3}, three orders of magnitude higher than in nominally undoped crystals (Fig. 5).
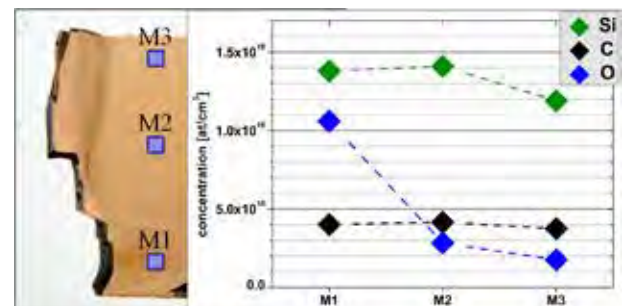

Fig. 5

Distribution of impurities in intentional Si doped AlN crystal; a) longitudinal cut of the crystal with sampling spots indicated, b) SIMS measurements

With the exception of the initial layer, in which a high oxygen concentration originating from residual humidity insight the setup is observed, all impurity concentrations are fairly constant in the whole crystal volume. The concentrations of the background impurities carbon and oxygen remained at their usual levels in the range of mid 10^{18} cm^{-3}. Other measurements have shown that the Si concentration in crystal parts grown on the prismatic {10-10} side facets of the crystal is about three times lower, while the carbon concentration is increased, compared to the respective concentrations in the main crystal body which was grown on the (000-1) facet.

Dielectric & Wide Bandgap Materials: *Aluminium Nitride*

The n-type conductivity of our Si doped AlN samples were determined by capacitance-voltage measurements on Ni Schottky contacts. The net donor concentration was about $2 \cdot 10^{18}$ cm^{-3} (Fig. 6).
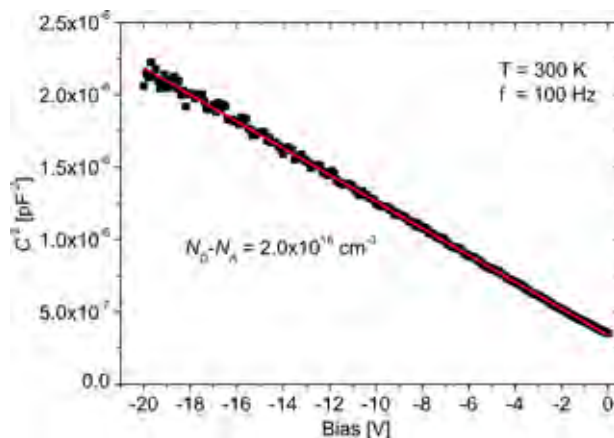
Fig. 6

Capacitance-voltage measurements on a Si-doped bulk AlN sample

Compared to the SIMS measurements with Si concentrations of a few 10^{19} cm^{-3}, most of the Si is electrical inactive. This is caused by compensation of the donors by deep levels. To determine possible charge carrier traps we used frequency and temperature dependant admittance spectroscopy. The measurements were conducted in the temperature range between 140 K and 580 K; giving the possibility to determine trap levels up to 1 eV below the conduction band. Trap activation energies could be identified at about 250 meV and at about 620 meV with respect to the conduction band (Fig. 7). The 250 meV trap may be attributed to silicon, as similar values are reported in literature. The deeper trap may act as a compensation center and might well be correlated to oxygen. The compensation mechanism is still under investigation; further knowledge is considered essential to reach a technically useable conductivity.
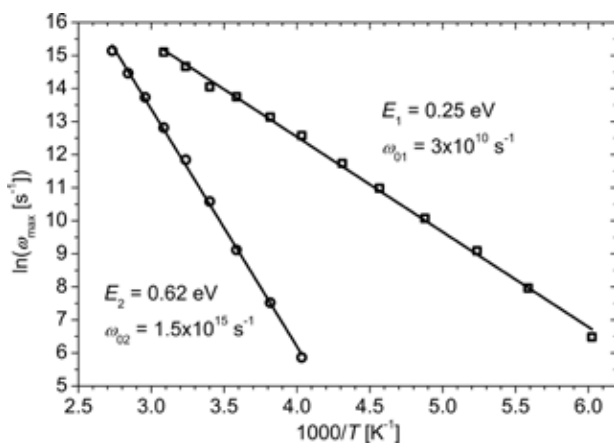
We succeeded to provide quasi-ohmic contacts to Si-doped AlN samples and to perform electrical measurements. A carrier concentration of $1.2 \cdot 10^{15}$ cm^{-3}, an electron mobility of 37 cm^2/Vs, and a conductivity of about $7 \cdot 10^{-3}$ Ω^{-1}cm^{-1} was obtained using resistivity and Hall effect measurements at room temperature on a sample with $2 \cdot 10^{19}$ cm^{-3} silicon concentration. This is a very reasonable and encouraging result (e.g. compared to AlN layers grown by MOCVD [6]) if compensation effects and the activation energy of silicon of 250 meV is taken into account.

As a side note, it was also evidenced by optical characterization of our Si doped crystals that silicon doping can also lead to deep UV transparent AlN crystals, as 3[C] < ([O] + [Si]) is provided by the high silicon content. However, the general optical absorption (both in the UV and the visible wavelength range) in such crystals is somewhat higher due to the higher concentration of compensating impurities (Fig. 8).

In conclusion, the group has made significant progress towards understanding and control of impurities for tailoring the electrical and optical properties of the AlN crystals. While deep UV optical transparency is key for use as substrates for UV optoelectronics as envisaged in the "Advanced UV for Life" consortium, high temperature semi-insulating crystals would enable the use of AlN as high-temperature piezoelectric material or as substrate for power electronics. On the other hand, a deeper understanding of structural defect generation evolution is required to provide strategies for further diameter increase while perpetuating the high structural quality of the crystals. The acquired results provide a solid basis enabling the transition from basic research to a more technology oriented approach.

Fig. 7

Estimation of charge carrier trap activation energies and electron capture/emission frequencies of a Si-doped AlN sample, measured by frequency and temperature dependent admittance spectroscopy (140-580 K)
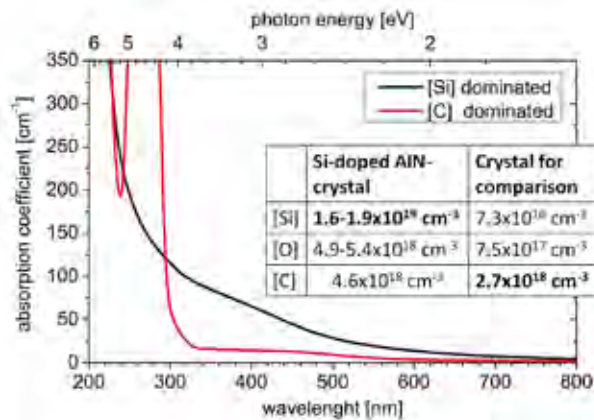
Fig. 8

UV/VIS absorption absorption in Si-doped and nominally undoped (carbon dominated) AlN bulk crystals. The absorption around 4.7 eV is correlated to carbon; the generally higher optical absorption of the Si-doped sample is caused by compensation effects, i.e., its higher impurity content.

References

[1] C. Hartmann, A. Dittmar, J. Wollweber,
     M. Bickermann;
     Semicond. Sci. Technol. 29 (2014) 084002 (10pp)

[2] C. Hartmann;
     Aluminiumnitrid-Volumenkristallzüchtung
     mittels physikalischen Gasphasen-transports,
     PhD thesis, Brandenburg University of Technology
     Cottbus-Senftenberg (2013)

[3] C. Hartmann, J. Wollweber, A. Dittmar,
     K. Irmscher, A. Kwasniewski, F. Langhans,
     T. Neugut, Bickermann;
     Jpn. J. Appl. Phys. 52 (2013) 08JA06

[4] K. Irmscher, C. Hartmann, C. Guguschev,
     M. Pietsch, J. Wollweber, M. Bickermann;
     J. Appl. Phys. 114 (2013) 123505

[5] N. T. Son, M. Bickermann, E. Janzén;
     Appl. Phys. Lett. 98 (2011) 092104

[6] R. Collazo, S. Mita, J. Xie, A. Rice,
     J. Tweedie, R. Dalmau, Z. Sitar;
   Phys. Status Solidi C 8 (2011) 2031

Layers & Nanostructures
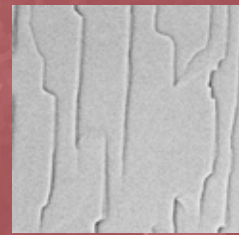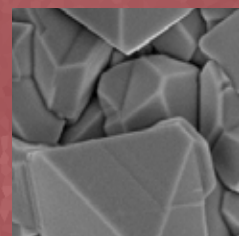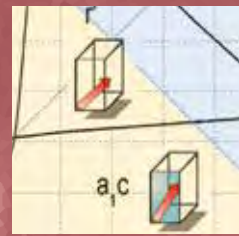
Layers & Nanostructures

Acting head of department: Dr. Günter Wagner

In der Abteilung "Schichten und Nanostrukturen" werden folgende Themen bearbeitet:
- *Grundlegende Untersuchung der Keimbildung und Wachstumsmechanismen*
- *Weiterentwicklung von Abscheidungstechnologien*
- *Herstellung und Charakterisierung von Schichten und Nanostrukturen für die Sensorik, Mikroelektronik, Photovoltaik, Speicher und thermoelektrische Anwendungen*

Eine Hauptaufgabe dieser Abteilung besteht darin, die physikalischen Eigenschaften verschiedener kristalliner Substanzen durch maßgeschneiderte Größe, Form, chemische Zusammensetzung und Verspannungszustand gezielt einzustellen, um neue Anwendungsgebiete zu erschließen.

Folgende Forschungsaktivitäten wurden 2013 in den drei Gruppen der Abteilung bearbeitet:

Epitaktisches Wachstum von transparenten halbleitenden Oxidschichten:
Dies umfasst die Abscheidung von β-Ga_2O_3–Schichten auf einkristallinen Al_2O_3– und β-Ga_2O_3 Substraten und die Substitution von Ga durch In bei der Abscheidung von $Ga_{(2x-1)}In_xO_3$–Schichten. Ein weiteres Ziel ist die Erzeugung und Einstellung einer n–Leitfähigkeit in den Schichten durch Dotierung mit Si und Sn.

Abscheidung von ferro-/piezoelektrischen bleifreien Oxidschichten:
Hierzu zählen ferro-/piezoelektrische $Na_xK_{1-x}NbO_3$ Schichten und Übergitterstrukturen mit variabler Zusammensetzung (x = 0 – 1), $SrTiO_3$ Schichten, sowie leitfähiges $SrRuO_3$ und $La_{0.7}Sr_{0.3}MnO_3$ als Elektrodenschichten. Zudem erfolgt die Abscheidung auf gitterfehlangepassten Oxidsubstraten (Heteroepitaxie) zum gezielten Einbau von Gitterverspannungen und der Untersuchung ihres Einflusses auf die funktionellen Eigenschaften.

Si– und Ge–Nanodrähte; Abscheidung von polykristallinem Si auf Glas:
Die Gruppe befasst sich mit den Themen: (1) Züchtung von polykristallinen Siliciumschichten auf kostengünstigen Glassubstraten, (2) Erzeugung von Indiumtröpfchen als Vorstufe für die Entwicklung von $Cu(In_xGa_{1-x})Se_2$ (CIGSe) Mikrokonzentrator-Solarzellen und (3) Züchtung von Si, Ge und $Si_{1-x}Ge_x$ Nanodrähten mit Molekularstrahlepitaxie (MBE). Diese Forschungsthemen werden seit Beginn des Jahres 2014 auch im Rahmen des EU–Projekts CHEETAH – Cost-reduction through material optimisation and Higher EnErgy outpuT of solAr pHotovoltaic modules – joining Europe's Research and Development efforts in support of its PV industry – bearbeitet. Ziel des Projekts ist die Erforschung und Entwicklung von modernen Technologien im Bereich der Photovoltaik entlang der Wertschöpfungskette und vereint dabei die Expertise von insgesamt 33 Institutionen der European Energy Research Alliance EERA.

Die Abteilung verfügt über eine sehr moderne, hochwertige Ausstattung: Molekularstrahlepitaxie, sowohl flüssigkeits- als auch gasbasierte MOCVD, Physikalische Gasphasenabscheidung, gepulste Laserabscheidung, Flüssigphasenepitaxie mit Schiebekassette und eine selbst entworfene Epitaxieapparatur für die Temperatur-Differenz-Methode. Zur Charakterisierung der Proben stehen eine Reihe von Methoden zur Verfügung: Atomkraftmikroskopie mit diversen Messoptionen an zwei modernen Geräten (u.a. Piezo-Response AFM), taktile Profilometrie und Ellipsometrie.

The activity carried out within the department „Layers and Nanostructures" is focused on:

- fundamental investigation of nucleation and growth mechanisms
- development of deposition technologies
- growth and characterization of layers and nanostructures or sensors, microelectronics, photovoltaics, memories and thermoelectric applications.

By controlling chemical composition and strain of epitaxial layers as well as size, shape and position of nanostructures it is possible to tailor the physical characteristics and make them suitable for novel applications.

The department includes three groups, which performed the following research activities in 2013:

Epitaxy of transparent semiconducting oxides:
This includes deposition of β-Ga_2O_3-layers on Al_2O_3- and β-Ga_2O_3 single crystalline substrates, substitution of Ga by In during epitaxy in order to grow $Ga_{2(1-x)}In_{2x}O_3$-layers, as well as realizing and tuning the n-type conductivity by doping with group IV elements (Si, Sn).

Deposition of ferro-/piezoelectric lead-free oxide layers:
The research tasks focus on ferro-/piezoelectric $Na_xK_{1-x}NbO_3$ layers and superlattice structures with variable composition (x = 0 − 1), deposition of $SrTiO_3$ layers and conductive $SrRuO_3$ and $La_{0.7}Sr_{0.3}MnO_3$ as electrode layers. Another topic is the deposition on lattice mismatched oxide substrates (heteroepitaxy) for targeted adjustment of lattice strain and investigation of the influence of the layers' functional properties.

Si and Ge nanowires; deposition of polycrystalline Si on glass:
Mainly three topics are investigated in this group: (1) the growth of polycrystalline silicon layers on low cost substrates, (2) the deposition of indium droplets as precursors for the development of $Cu(In_xGa_{1-x})Se_2$ (CIGSe) micro-concentrator solar cells, and (3) the MBE growth of Si, Ge and $Si_{1-x}Ge_x$ compound nanowires. There topics are also addressed in the frame of EU-project CHEETAH – Cost-reduction through material optimisation and Higher EnErgy outpuT of solAr pHotovoltaic modules – joining Europe's Research and Development efforts in support of its PV industry, funded in the frame of the 7th European Framework Programme. The project aims at the development of advanced photovoltaic technologies in all parts of the value-added chain and brings together the expertise of 33 institutions of the European Energy Research Alliance (EERA).

The department has an excellent infrastructure for the deposition and characterization of epilayers and nanostructures:
Molecular Beam Epitaxy, both liquid-delivery and conventional MOCVD, Physical Vapor Deposition, Pulsed Laser Deposition, sliding-boat Liquid Phase Epitaxy, and in-house designed Temperature Difference Method Epitaxy. A variety of characterization methods are available: Atomic Force Microscopy at two state-of-the-art AFM devices enabling a variety of measuring options (e.g. piezo-response AFM), Stylus Profilometry, and Ellipsometry.

Layers & Nanostructures:
Semiconducting Oxide Layers

Head   Dr. Günter Wagner
Team   Dr. M. Baldini, Dr. D. Gogova, R. Grüneberg, R. Schewski

Überblick

Die Erforschung der Verbindungen der transparenten Metalloxide als eine neue Klasse von Halbleitern ist ein sich enorm schnell entwickelndes Forschungsfeld, welche zur Entwicklung von neuen innovativen elektronischen Bauelementen und zum Verständnis spannender physikalischer Prozesse beitragen kann. $\beta-Ga_2O_3$, als ein der interessantesten Verbindungen in dieser Klasse, wurde in den letzten Jahren sehr intensiv studiert. $\beta-Ga_2O_3$ zeichnet sich durch einen großen Bandabstand von 4.8 eV und eine vorhergesagte elektrische Durchbruchsspannung von ca. 8 MV/cm aus. Diese exzellenten Materialeigenschaften können die Grundlage für eine Anwendung in Photodetektoren für den tiefen UV–Bereich und für Leistungsbauelemente bilden. Die homoepitaktische Abscheidung von dünnen Ga_2O_3-Filmen wurde in den letzten Jahren im Wesentlichen durch die Molekular–Strahl–Epitaxie (MBE) realisiert und ihre hervorragende Eignung zur Herstellung von Schottky–Dioden und Feldeffekt–Transistoren demonstriert (MESFETs) [1]. Bis zum jetzigen Zeitpunkt wurde die Homoepitaxie von Ga_2O_3 durch das Verfahren der metallorganischen Gasphasenabscheidung (MOVPE), welche ein Standardverfahren bei der Massenproduktion von mikroelektronischen Baudelementen darstellt, fast ausschließlich durch unser Team im IKZ durchgeführt.

Die Arbeiten im IKZ finden im Rahmen des Projektes: „Homo- und Heteroepitaxie von transparenten halbleitenden Oxiden des ternären Materialsystems Ga–In–Al auf $\beta-Ga_2O_3$ und In_2O_3-Substraten", gefördert durch die Leibniz Gemeinschaft, statt. Das Projekt wurde im Jahr 2012 begonnen und wird bis Februar 2015 bearbeitet.

Im Bearbeitungsjahr 2013 konnte die Abscheidung von kohärent gewachsenen einkristallinen Schichten demonstriert werden. Als metallorganische Verbindungen wurden dazu Trimetylgallium (TMGa) und Wasser als Gallium- und Sauerstoffquelle eingesetzt. Die Präsenz von Wasserstoff im Reaktor während der Abscheidung zeigte einen positiven Effekt hinsichtlich der kinetischen Bedingungen auf der Substratoberfläche. Dadurch wird das Wachstum von glatten, spiegelnden Schichtoberflächen gefördert. Die kristalline Perfektion der Schichten ist jedoch durch das Auftreten von Stapelfehlern und Zwillingen gestört, was zu einer erhöhten vertikalen Gitterfehlordnung führt [2].

Im dritten Bearbeitungsjahr des Projektes konzentrierten sich die Forschungsarbeiten auf zwei Schwerpunkte:

1. Die Verbesserung der strukturellen Perfektion in den Ga_2O_3-Schichten durch den Einsatz von Indium als Oberflächenkatalysator während der Schichtabscheidung.
2. Die Einstellung einer n–Typ Leitfähigkeit in den Ga_2O_3-Schichten.

Overview

The study and development of transparent metal oxides as a new class of semiconductors is a rapidly expanding research field that could lead up to the realization of innovative devices and the understanding of new exciting physics. $\beta-Ga_2O_3$ has been widely studied in the last years, emerging as one of the most interesting example in this class of materials. $\beta-Ga_2O_3$ has a large band gap of 4.8 eV and an expected breakdown electric field in the range of 8 MV/cm. These excellent material properties can be the basic for application in deep–UV photodetectors and power-devices. Homoepitaxy of Ga_2O_3 thin film have been performed in the very last year's mainly by molecular beam epitaxy (MBE), leading to the fabrication of Schottky barrier diodes and field–effect transistors (MESFETs) [1]. Up to now, the homoepitaxy of Ga_2O_3 by metal organic vapour phase epitaxy (MOVPE), which is more suitable for large scale production and faster commercialization of the prototype devices, has been performed mainly by our group at IKZ.

Our research is carried out in the frame of the project "Homo- and heteroepitaxy of transparent semiconducting oxide layers of the Ga–In–Al ternary system on $\beta-Ga_2O_3$ and In_2O_3 substrates" funded by the Leibniz association. The project was started in 2012 and will continue until spring 2015.

In 2013 we have demonstrated the growth of coherent monocrystalline layers by using trimethylgallium (TMGa) and H_2O as precursors for gallium and oxygen. The presence of hydrogen in the reactor showed a positive effect on kinetic conditions of the substrate surface, supporting the growth of smooth layers. However, the crystalline quality of the layers was disturbed by the presence of stacking faults and twins, which induced strong vertical stacking disorder [2].

Layers & Nanostructures: **Semiconducting Oxide Layers**

In the third year of the project, the research activities were focused on two topics:

1. The improvement of the structural perfection of Ga_2O_3-layers by using indium as surfactant during the layer growth.
2. The development of n-type conductive Ga_2O_3-layers.

I. Effect of Indium as a surfactant in $(Ga_{1-x}In_x)_2O_3$ epitaxial growth on Ga_2O_3

It is known that β-Ga_2O_3 can be alloyed with In_2O_3 (Eg=2.9 eV), in order to modulate its bandgap. However, the focus of our work has not been the development of $(Ga_{1-x}In_x)_2O_3$, but rather on studying the effect of In on the growth dynamic of Ga_2O_3. In order to prevent a high incorporation of In in the layers, the experimental conditions were adjusted according to the experience gained in growth of $(Ga_{1-x}In_x)_2O_3$ on α-Al_2O_3 (0001) as reported in the annual report 2013. The employment of In during the growth turned out as essential to limit the concentration of structural defects in the homoepitaxial layers. This result has been explained, in analogy to the growth of GaN [3], by the tendency of In to float on the surface of Ga_2O_3, delivering a surfactant effect that promotes a step-flow growth mode. The dependence of the beneficial effect of In on different growth parameters has been carefully studied.

$(Ga_{1-x}In_x)_2O_3$ layers were grown on (100) Ga_2O_3 substrates, providing an Ar flow through TMIn-bubbler that was varied between 0 and 200 sccm. In order not to grow an In-rich $(Ga_{1-x}In_x)_2O_3$ alloy but to limit the In incorporation below 3% the reactor pressure has been set at 50 mbar. The results obtained with these growth parameters can be classified in two main groups, depending on different TMIn amount injected in the reactor.

The samples grown with Ar/TMIn in the range 75–200 sccm present a particular surface morphology, as shown in Figure 1. The layers exhibit the presence of 1–5 µm wide and 1–2 nm high terraces, with an elongated and quite irregular shape, whose long axis is perpendicular to the [001] step down direction of the substrate. On the surface of the terraces it can be observed that the growth of the layers took place with a step-flow mechanism, shown in the AFM picture of figure 2. The steps are ~600 pm high and 50–100 nm wide, mimicking the morphology of the Ga_2O_3 substrate surface prior to the growth. The morphological properties of the layers did not change significantly at different Ar/TMIn flows, in the range 75–200 sccm.
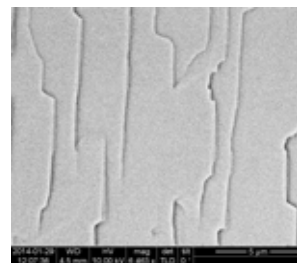

Fig. 1
Typical SEM image of a $(Ga_{1-x}In_x)_2O_3$ layer grown on β-Ga_2O_3 with an Ar/TMIn flow in the range 75-200 sccm.
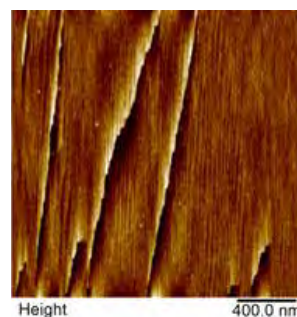

Fig. 2
AFM image of the same sample of Figure 1.

On the contrary, if the Ar/TMIn flow is lower than 75 sccm, the morphology of the layers is completely different. Terraces and steps are not visible anymore, while a high amount of small defects appears, as shown in Figures 3 and 4, respectively. The number of these defects increases with the reactor pressure.
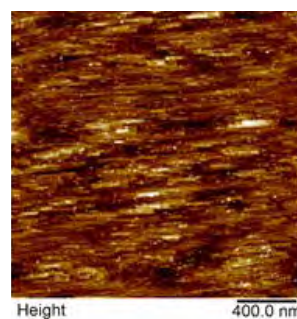

Fig. 3
AFM image of a $(Ga_{1-x}In_x)_2O_3$ layer grown on β-Ga_2O_3 with an Ar/TMIn flow < 75 sccm.
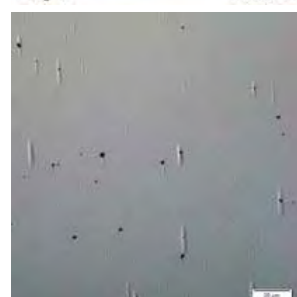
*Fig. 4*
Optical microscope image of the same sample of figure 3.

Layers & Nanostructures: **Semiconducting Oxide Layers**

$(Ga_{1-x}In_x)_2O_3$ epitaxial layers grown with different In-flux TMIn were characterized by TEM and high resolution high-angle annular dark-field (HAADF) STEM. Figure 5a shows a typical cross sectional TEM micrograph of a (100)-oriented layer grown with Ar/TMIn flow in the effective 75-200 sccm range. The layer has a very high crystalline perfection.

In contrast, layers grown with Ar/TMIn flow below 75 sccm have a very different crystal structure, exhibiting a high density of stacking faults and twins, see Figure 5b.


a   *b*
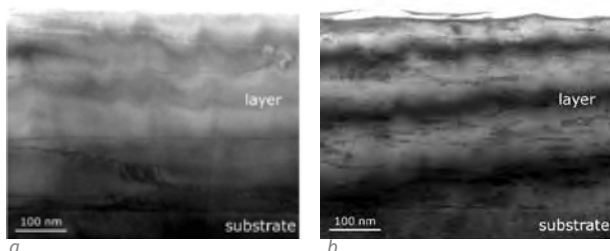
Fig. 5

TEM images of (a) $(Ga_{1-x}In_x)_2O_3$ and (b) Ga_2O_3 layers grown on β-Ga_2O_3. The concentration of stacking faults decreases dramatically thanks to the surfactant effect provided by In.

In conclusion, we can assert that we are able to deposit high quality epitaxial layer of the mixed $(Ga_{1-x}In_x)_2O_3$ phase by metal organic vapour phase epitaxy on (100) β-Ga_2O_3 substrates, by applying TMGa, TMIn and water as precursors. The incorporation of In was limited below 3% by suitable tuning of the experimental parameters, in particular of the growth pressure. It was observed that by injecting into the reactor a sufficiently high amount of TMIn, Indium has an essential role in limiting the concentration of crystallographic defects, promoting the step-flow growth of the layers [4].

2. n-type doping of Ga_2O_3

Prerequisites for applying of Ga_2O_3 layers in power electronic and sensor devices are a high crystalline structure with low density of lattice defects and a net donor concentration in the range of 10^{17} up to 10^{19} cm^{-3}. For a long time the unintentional n-type conductivity of β-Ga_2O_3 has been attributed to an oxygen deficiency which leads to oxygen-vacancies (V_o) or Ga-interstitials (Ga_i). Recently, theoretical studies showed that (V_o) act as deep donors and does not contribute to the conductivity [5]. Therefore, doping with elements acting as shallow donors is necessary to enable growth of β-Ga_2O_3 with the electrical conductivity demanded by applications. In 2014 we have continued with our doping experiments and now we are able to show that homoepitaxial n-type Ga_2O_3 layers can be grown by MOVPE. In the recent two years [6], we used TMGa and water as Ga and oxygen source and TESn as Sn-precursor. Nevertheless, we were not able to achieve conductive layers. Independently from oxygen/TMGa ratio and additional thermal annealing steps the growth experiments did not provide

reproducible conductive Ga_2O_3 layers. We assumed that the high carbon content in the growth atmosphere, deriving from the MO-precursors, contribute to the high resistivity in the layers. Theoretical studies [5, 7] have shown that also the formation of Ga-vacancies at oxygen rich conditions may have even negative formation energy and can compensate the incorporated donors.

From the MOVPE growth of III-nitrides it is known that the decomposition of TEGa-precursor in comparison to TMGa delivers much less free carbon and C_2H_5-groups, which does not effectively interact with the growth surface in comparison to TMGa and CH_3 groups. With respect to this knowledge, we have replaced TMGa by TEGa to reduce the carbon content in the grown layers. In addition, we performed the layer deposition at a reduced oxygen/TEGa-ratio of about 100 and to support the activation of the incorporated donor atoms we increased the deposition temperature to 850 °C. As result of these changes in growth parameters, we were able to incorporate Sn from 10^{18} cm^{-3} up to beginning of 10^{20} cm^{-3}. Figure 6 shows the Sn-SIMS depth profiles of five Ga_2O_3 layers grown with a TESn flux between 4.6×10^{-12} and 6.6×10^{-10} mol/min. The layer thickness is about 160 nm.

By increasing the TESn-flux in the growth atmosphere by two order of magnitude the chemical Sn-concentration in the layers increased nearly in the same range. In addition, the SIMS profiles demonstrate that at a TESn-flux of 4.6×10^{-12} mol/min the chemical Sn concentration in the layer is in the same range as in an unintentional doped layer. Therefore, we conclude that the background doping level in the layers is in the beginning of 10^{17} cm^{-3} as a result of Sn-pollution in the reactor and additional memory effects after long time deposition of Sn-doped layers.

All the Sn-doped layers have shown n-type conductivity. By Hall-measurements, it was found that while the mobility fluctuates around 25 cm^2/Vs, the carrier concentration increases from 5×10^{17} cm^{-3} to 3×10^{18} cm^{-3} by increasing the TESn-flux in the growth atmosphere. The highest mobility value of 41 cm^2/Vs was observed at a carrier concentration of 1×10^{18} cm^{-3}. Figure 7 shows the dependence of the free carrier concentration (left y axis) and the chemical Sn-concentration (right y axis) in dependence on the TESn-flux in the gas atmosphere. It can be observed that at TESn-fluxes lower than 5×10^{-11} mol/min the chemical Sn-concentration is below the estimated net carrier concentration. This may indicate the existence of other doping elements or point defects that can influence the electrical properties.

Layers & Nanostructures: **Semiconducting Oxide Layers**

The comparison of chemical and electrical Sn-concentration shows that up to 10% of Sn is electrical active. SIMS measurements relative to carbon in the Sn-doped layers delivered chemically concentration in the beginning of 10^{17} cm^{-3}. These results are not completely reliable because it is very difficult to distinguish between the carbon background of the SIMS-system and the real C-concentration in the layers. A more detailed investigation is necessary to understand the role of carbon and its interaction with structural defects and its influence on the electrical properties of the layers.

Summarizing, in the reported period we have shown that Sn is an effective n-type dopant for Ga_2O_3 and that the free-carrier concentration can be controlled over one order of magnitude by varying the TESn-flux in the gas phase during layer deposition.
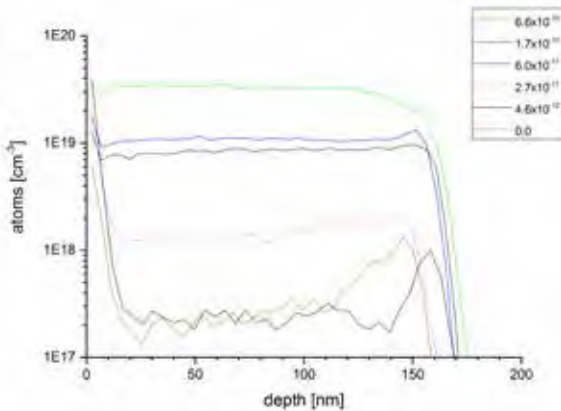

Fig. 6
SIMS Sn depth profiles of β-Ga$_2$O$_3$ layers grown at 850° C with different TESn-flux in the growth atmosphere.
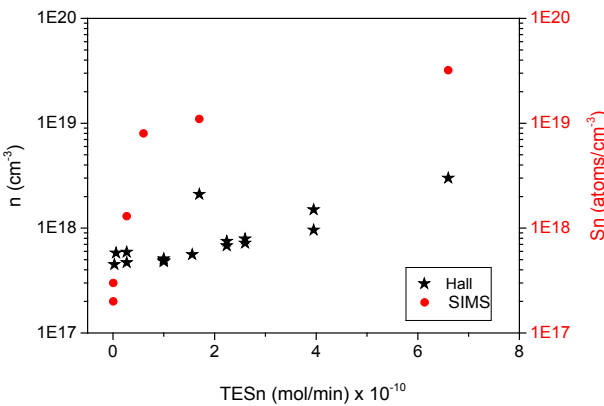

Fig. 7
Free carrier concentration, n, (Hall) and chemical indium concentration (SIMS) in dependence on the TESn-flux in the growth atmosphere.

References

[1] K. Sasaki, M. Higashiwaki , A. Kuramata, T. Masui, S. Yamakoshi; J. Crystal Growth 378 (2013) 591

[2] G. Wagner, M. Baldini, D. Gogova, M. Schmidbauer, R. Schewski, M. Albrecht, Z. Galazka, D. Klimm, R. Fornari; Phys. Status Solidi A 211 (2014) 27 – 33

[3] D. Won, X.Weng, J.M. Redwing; App. Phys. Lett.100 (2012) 021913

[4] M. Baldini, M. Albrecht, D. Gogova, R. Schewski, G. Wagner; Semicond. Sci. Technol. 30 (2015) 024013

[5] J.B. Varley, H. Peelaers, A. Janotti, C.G. Van de Walle; J. Phys.: Condens. Matter 23 (2011) 334212

[6] D. Gogova, G. Wagner, M. Baldini, M. Schmidbauer, K. Irmscher, R. Schewski, Z. Galazka, M. Albrecht, R. Fornari; J. Crystal Growth 401 (2014) 665

[7] J.B. Varley, J.R.Weber, A. Janotti, C.G. Van de Walle; Appl. Phys. Lett. 97 (2010) 142106

Layers & Nanostructures:
Si/Ge Nanocrystals

Head   Dr. Torsten Boeck
Team   R. Bansen, Dr. K. Böttcher, C. Ehlers, Dr. F. Ringleb, Dr. J. Schmidtbauer, H.-P. Schramm, F. Schütte, Dr. T. Teubner

Überblick

Die Forschung der Gruppe umfasst drei Themen: (1) Die Züchtung von polykristallinen Siliciumschichten auf kostengünstigen Glassubstraten, (2) Materialforschung zur Entwicklung von $Cu(In_xGa_{1-x})Se_2$ (CIGSe) Mikrokonzentrator-Solarzellen und (3) die Züchtung von Si, Ge und $Si_{1-x}Ge_x$ Nanodrähten mit Molekularstrahlepitaxie (MBE).

Mit den ersten zwei Themen ist die Gruppe Partner bei zwei sog. Arbeitspaketen des EU-Projekts CHEETAH. Dieses mit dem 7. Europäischen Rahmenprogramm geschaffene wissenschaftliche Verbundprojekt, welches außerdem Management- und Erfahrungsaustauschaktivitäten umfasst, wurde offiziell im Januar 2014 begonnen. CHEETAH fördert die Entwicklung von fortschrittlichen Photovoltaiktechnologien in allen Stadien der Wertschöpfungskette. Das Projekt bündelt die Kompetenz von 33 Mitgliedseinrichtungen der Europäischen Energieforschungsallianz (EERA), zu denen nun auch das IKZ zählt.

Zum einen erfolgt die Entwicklung von Herstellungsprozessen für Dünnschicht-Siliciumsolarzellen in Zusammenarbeit mit Partnern aus Deutschland, Belgien, Norwegen und den Niederlanden. Diese Thematik unserer Gruppe wird zusätzlich durch das Projekt „Lösungsmittelinduzierte Phasenumwandlung von kristallinen Siliciumschichten" der Deutschen Forschungsgemeinschaft (DFG) gefördert.

Zum anderen wurde im Rahmen von CHEETAH die Entwicklung CIGSe-Mikrokonzentrator-Solarzellen als neuer Forschungsschwerpunkt im IKZ begonnen. Partner sind hierbei das Helmholtz-Zentrum Berlin für Materialien und Energie (HZB), die Bundesanstalt für Materialforschung und -prüfung (BAM) sowie Forschungseinrichtungen in Italien, Estland und Portugal. Zusätzliche Unterstützung für diese Thematik kommt vom DFG-Projekt INSEL, ein Gemeinschaftsvorhaben zusammen mit Forschern der Freien Universität Berlin (FUB) und der BAM, das ab Januar 2015 für drei Jahre bearbeitet werden wird.

Auf dem Gebiet der Nanodrähte – dem dritten Thema – stand die MBE-Züchtung von Si, Ge- und SiGe-Nanodrähten auf Si-Substraten mit der Vapor-Liquid-Solid-Methode (VLS) im Vordergrund. Während reine Silicium- und Germanium-Nanodrähte als vielversprechende Elemente in zukünftigen elektronischen und optoelektronischen Bauelementen angesehen werden, haben Si- und SiGe-Nanodrähte auch auf dem Gebiet neuer Batterien und thermoelektrischer Generatoren Interesse ausgelöst. Thermoelektrika mit solchen Nanodrähten zeigen verbesserte Effizienz wegen der geringeren thermischen Leitfähigkeit bei gleichbleibenden elektrischen Eigenschaften [4]. Ein typisch kristallografischer Aspekt der Forschung umfasst Untersuchungen zu den unterschiedlichen Wachstumsrichtungen und zur Facettierung der Si-, Ge- und SiGe-Nanodrähte.

Die Arbeiten zum Wachstum von Si, Ge und $Si_{1-x}Ge_x$ Nanodrähten und die Charakterisierung von Halbleiter-Nanostrukturen für Thermophotovoltaik werden durch ein Verbundprojekt mit der Abteilung „Physik der Halbleiter und Mikroelektronik" der Staatlichen Universität Jerewan (YSU) und dem Paul-Drude-Institut für Festkörperelektronik (PDI) durch das Bundesministeriums für Bildung und Forschung (BMBF) gefördert.

Studenten und Hochschulabsolventen arbeiteten in allen Forschungsfeldern mit. Zwei kürzlich promovierte junge Wissenschaftler befassen sich jeweils mit der Materialforschung auf dem Gebiet der CIGSe-Solarzellen und dem Wachstum von Nanodrähten. Zwei Doktoranden (HU Berlin und TU Berlin) sind auf dem Gebiet der Si-Kristallisation auf Glas tätig. Eine vormalige Bachelorstudentin unserer Gruppe unterstützte die Arbeit weiterhin als studentische Hilfskraft.

Overview

The team has focused on three research topics: (1) the growth of polycrystalline silicon layers on low cost substrates, (2) materials research for the development of $Cu(In_xGa_{1-x})Se_2$ (CIGSe) micro-concentrator solar cells, and (3) the MBE growth of Si, Ge and $Si_{1-x}Ge_x$ compound nanowires.

With the first two of these activities, the group is an official project partner in two work packages of the EU-CHEETAH project. CHEETAH – a collaborative project as well as a coordination and support action funded under the 7th European Framework Program – has been officially launched in January 2014. It aims at the development of advanced photovoltaic technologies in all parts of the value-added chain and brings together the expertise of 33 institutions of the European Energy Research Alliance (EERA).

Layers & Nanostructures: **Si/Ge Nanocrystals**

On the one hand, the group is involved in the development of a preparation processes for thin film silicon solar cells. In this field, there is an ongoing cooperation with partners from Germany, Belgium, Norway, France, and the Netherlands. This research of our group is also supported by the DFG project "Solvent-Generated Phase Transformation for Crystalline Silicon Layers". On the other hand, within the framework of CHEETAH, the development of CIGSe micro-concentrator solar cells has been established as a new topic for our institute. Partners are the Helmholtz-Zentrum Berlin (HZB), the Federal Institute for Materials Research and Testing (BAM), as well as institutions in Italy, Estonia and Portugal. The future work on this research is additionally secured by the 3-year DFG cooperation project INSEL with Freie Universität Berlin and the Federal Institute for Materials Research and Testing, starting in January 2015. For nanowires – the third topic – the focus has been the MBE growth of Si, Ge and $Si_{1-x}Ge_x$ nanowires on Si substrates by means of the Vapor-Liquid-Solid mechanism (VLS). While silicon and germanium nanowires are widely considered as promising structures for future electronic and optoelectronic devices, Si and SiGe nanowires have also attracted high interest in the field of modern batteries thermoelectric generators. Materials based on such nanowires have been shown to increase the thermoelectric efficiency due to low thermal conductivity while a high electrical conductivity is maintained [1]. Another aspect of research has been the investigation of different growth directions of Si, Ge and SiGe nanowires. The growth of Si, Ge and $Si_{1-x}Ge_x$ compound nanowires and the characterization of semiconductor nanostructures for thermophotovoltaics is fostered by a joint project with the Department of Physics of Semiconductors and Microelectronics of the Yerevan State University (YSU), Armenia, and the Paul-Drude-Institut für Festkörperelektronik (PDI) under the auspices of the German Federal Ministry of Education and Research (BMBF).

Students and postgraduates have been involved in all topics of research. Two postdocs are concerned with materials research for CIGSe solar cells and the growth of nanowires, respectively, and two PhD students (HU Berlin and TU Berlin) work on Si crystallization on glass. A former bachelor student of our group continued supporting our work as a student research assistant.

Results

Silicon on glass

To achieve low temperature deposition of crystalline silicon on glass, as is desirable for photovoltaics, a two-step process is used. In the first step, nanocrystalline Si films are formed at low temperatures in the range of 300 to 450 °C through either metal-induced crystallization, or direct deposition on heated substrates. In the second step, the crystallized films serve as templates for further Si deposition by the temperature difference method (TDM), a steady-state solution growth technique using metals as solvent. The research has focused on Si crystallization by applying the metallic solvent tin, on the characterization of indium-grown samples by transmission electron microscopy (TEM), and on preliminary experiments for UV laser supported oxide removal from Si seed layers prior to TDM processing.

Our research activities have concentrated on further development and evaluation of the TDM growth process from a tin solution to deposit a closed polycrystalline Si layer as shown in Figure 1.

In TEM characterization of such samples, the originally nanocrystalline seed layers were found to be penetrated by twin boundaries, reaching all the way from the glass substrate interface, through the entire seed layer, deep into the large crystallites obtained by solution growth from tin. Therefore, it can be assumed that the seed layer's nanocrystallites have merged into large grains, covering several micrometers in diameter. The assumption was confirmed by means of selected area diffraction (SAD) of different areas in the seed layers, where most of the examined areas were found to be single crystalline, cf. Fig. 2. The seed layers were also found to be rich in crystal defects, especially dislocations and twin boundaries. Results for growth from both indium and tin solutions have been published and presented at international conferences [2].

A UV laser and laser scanner system have been acquired in 2014 to address the problem of surface oxidation of the seed layers during handling and heat-up prior to steady-state solution growth. To meet the specific demands of the handling and growth process, and of the limited space at the growth chamber, the laser system was developed in close cooperation with the laser manufacturer.

Layers & Nanostructures: **Si/Ge Nanocrystals**
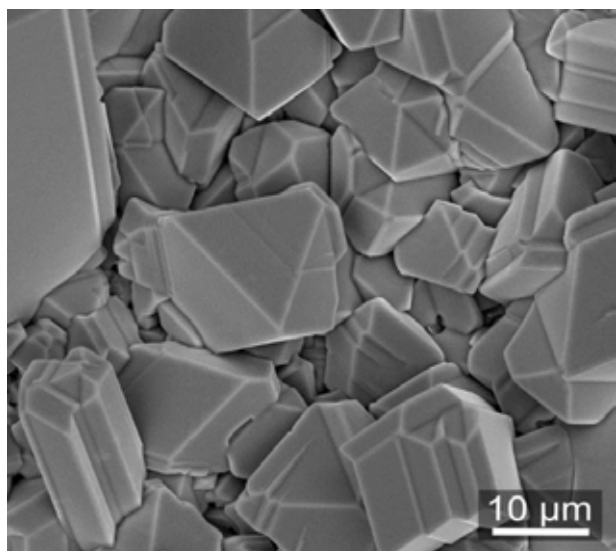
Fig. 1
Scanning electron microscopy image (SEM) of a closed polycrystalline Si layer on glass, grown by TDM from Sn solution.
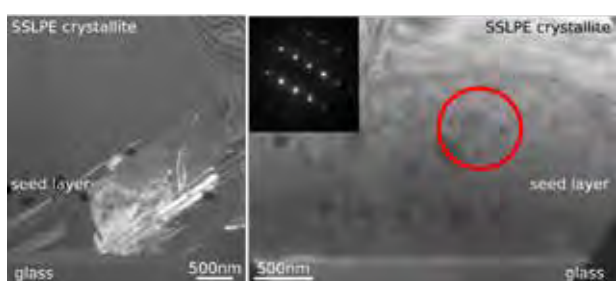

Fig. 2
Cross-sectional TEM micrograph of seed layer and bottom parts large Si crystallites grown by TDM from Sn solution. Twin boundaries penetrate the entire seed layer (left). Selected area diffraction pattern (inset) of the area marked by a circle proves single crystallinity of large areas in the seed layer (right).

CIGSe Microconcentrator Solar Cells

The preparation of CIGSe micro-concentrator CIGSe cells is motivated by the high cost for the raw materials, in particular indium, of this excellent direct absorber [3]. While macro-concentrators suffer from large heat accumulation and therefore reduced efficiency and lifetime, micro-concentrators allow for better heat dissipation and furthermore for a compact module design [4]. In contrast to well established CIGSe thin film solar cells, which currently exhibit the highest efficiency of all thin film solar cells (21.7 %) [5], the production of micro-concentrator cells requires − regarding the aim of saving material − the development of an efficient bottom up process for preparing absorber islands. The group works on an approach which is based on the use of indium islands on a molybdenum back contact as a starting point for further processing. There are several sample properties that have to be optimized for this approach to be suitable: (i) Since CIGSe is a very efficient, direct absor-

ber, indium is only saved if the islands are flat. (ii) Island diameters and inter-island distances must be suitable for optimum micro-concentrator geometries. (iii) A process has to be developed, which allows for a reliable arrangement of the islands in a well-defined pattern.

The CIGSe microconcentrator solar cells research was mainly focused on how to influence the contact angle, size and distance of the indium droplets. Furthermore, preliminary results were obtained on the further processing by deposition of copper on top of the indium islands and subsequent selenization. Indium islands were grown by Physical Vapor Deposition (PVD) on a range of molybdenum films supported on a glass substrate. The molybdenum layers were either prepared by sputtering or PVD. However, low contact angles and large island sizes (several tens of micrometers) were only obtained for the PVD-prepared molybdenum substrates, which exhibit a much lower roughness than the molybdenum films prepared by sputtering. This indicates that the island morphology is highly sensitive to the surface roughness as has also been observed for other systems [6, 7]. Furthermore, temperature and rate applied during indium deposition were shown to be influential parameters. Increasing temperatures resulted in larger islands with larger separations and lower contact angles (see Figure 3). This can be explained by the increase of diffusion length and decrease of surface tension of indium with rising temperatures. Reversely, an increased rate led to lower inter-island distances (see Figure 4). This can be understood regarding the fact that a higher density of indium atoms diffusing on the surface leads to higher collision rates and therefore nucleation events. A significant influence of the deposition rate on the contact angle was, however, not observed.

XRD spectra of indium islands, which were further processed by addition of copper by PVD and subsequent selenization by a rapid thermal processing step, were clearly dominated by peaks attributed to $CuInSe_2$ (CIS). Even though spatially resolved information demonstrating that this signal originates from the islands is still pending, chemical and morphological analysis by SEM/EDX showed that indium and selenium were accumulated mainly in the islands which had maintained their original diameter and flatness (see Figure 5). These results demonstrate that indium islands can be used as precursors for the formation of CIS absorber structures with a diameter range of several ten micrometers.

First experiments have been carried out on the incorporation of gallium into the system and the preparation of ordered arrays of the indium precursors which is a prerequisite for the later alignment between absorber islands and micro-lens arrays. In collaboration with the BAM, the creation of nucleation centers for indium could be introduced by a femtosecond laser. Furthermore, there are strong indications of an indium wetting layer

connecting the islands. Since this would have a strong impact on the dynamics of growth and interaction between the islands, this issue will be investigated in more detail by PEEM measurements at BESSY II in cooperation with a group from Fritz Haber institute. An appropriate research proposal has been positively evaluated.

Fig. 3

Influence of deposition temperature: 355 nm indium on molybdenum, deposited at 0.9 Å/s with increasing temperature from left to right: Tmin(left): ca. 300°C; Tmax(right): ca. 330°C.
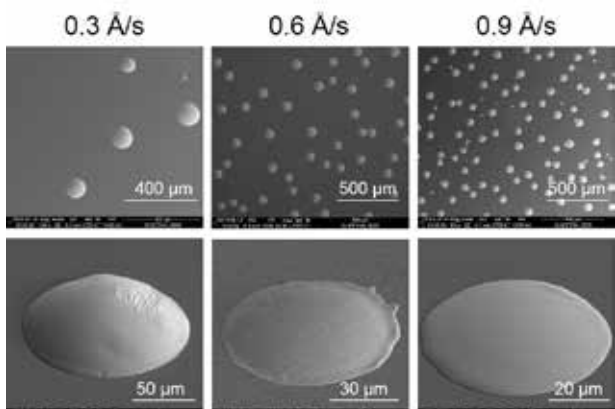

Fig. 4

*Influence of deposition rate: 350 nm indium on molybdenum deposited at 320°C.*
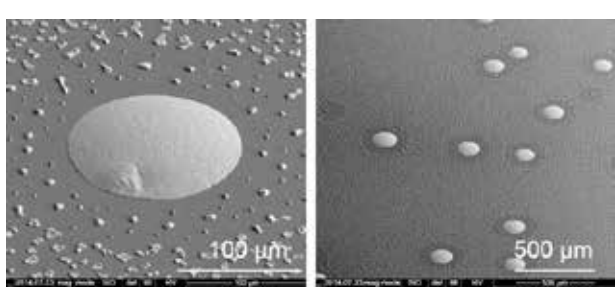
Fig. 5

Indium islands after deposition of copper and subsequent selenization: (1) 357 nm indium on molybdenum at 0.27Å/s at 330°C; 2) 123 nm copper at 0.35 Å/s at 180°C; 3) selenization at 500°C.

Germanium nanowires

The work focused on the growth of SiGe compound nanowires with intentionally tuned Ge contents. Starting with pure Si nanowires, the Ge content during deposition was raised up to 20% and SiGe nanowires were grown successfully, see Fig. 6. However, the exact Ge content in the wires needs to be confirmed by analytical TEM investigations. Future work will aim to increase the Ge content further up to 30% – 40% which gives the highest theoretical thermoelectric efficiency in SiGe [6] but is not available as bulk material [8].

Beside the growth of SiGe nanowires, the control of growth directions of Si and Ge nanowires was studied [9]. It is known that Si nanowires predominantly grow along <111> directions, whereas Ge nanowires show preferred <110> directions when grown by MBE. Consequently, the work focusses on the question how the Ge content in SiGe nanowires influences their growth direction. Furthermore, there are many hints that the different surface energies of Si and Ge play an important role when it comes to the question which direction is dominant. The MBE chamber has been equipped with a hydrogen and an oxygen injection source in order to influence the surface energies by creating H or O surface terminations and to study the directional growth in detail.

A main drawback of nanowire growth by conventional solid-source MBE is the strong influence of diffusive material transport on the substrate surface, which leads to a process-related limitation of the achievable length and aspect ratio. To solve this issue, a gas-source MBE system, using silane and germane as precursors, is going to be implemented, see Fig. 7. Due to the use of hazardous process gases a comprehensive safety control system has been installed.
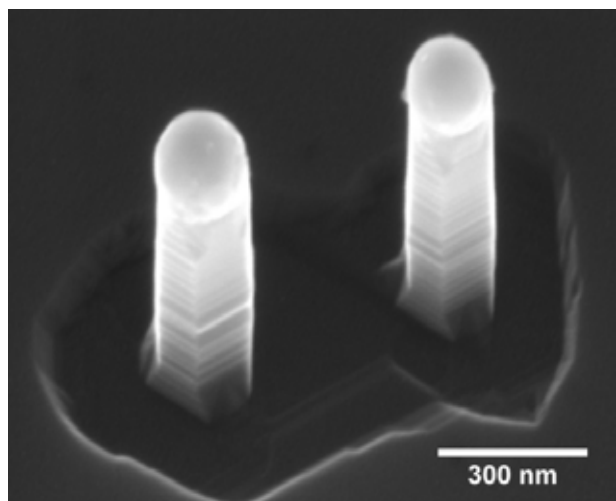

Fig. 6

SiGe nanowires on Si(111) grown by MBE. Si and Ge have been deposited at a 0.024 nm/s and 0.006 nm/s leading to $Si_{0.8}Ge_{0.2}$.

Layers & Nanostructures: Si/Ge Nanocrystals
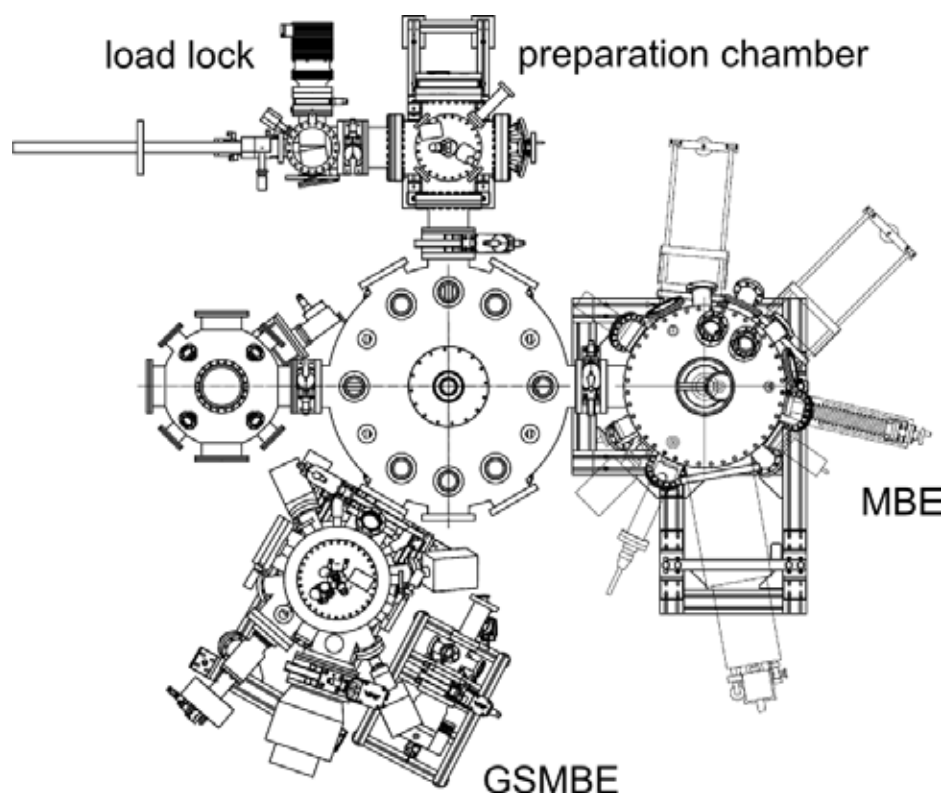
Fig. 7
Technical drawing of the UHV cluster system with MBE and
gas-source MBE process chambers attached to the central
handling unit.

Layers & Nanostructures: **Ferroelectrical Oxide Layers**

References

[1] A.I. Boukai, Y. Bunimovich, J. Tahir-Kheli,
    J.-K. Yu, W. a Goddard, J.R. Heath;
    Nature 451 (2008) 168–171

[2] R. Bansen, R. Heimburger, J. Schmidtbauer,
    T. Teubner, T. Boeck;
    29th European Photovoltaic Solar Energy Conference
    and Exhibition, Amsterdam, (2014) 1908–1911,
    DOI: 10.4229/EUPVSEC20142014-3DV.4.16

[3] G. Angerer, F. Marscheider-Weidemann,
    A. Lüllmann, L. Erdmann, M. Scharp,
    V. Handke, M. Marwede;
    Rohstoffe für Zukunftstechnologien, Studie:
    Fraunhofer-Institut für System- und
    Innovationsforschung ISI und des Institut für
    Zukunftsstudien und Technologiebewertung IZT;
    Karlsruhe, Berlin (2009).

[4] M. Paire, A. Shams, L. Lombez, N. Pere-Laperne,
    S. Colling, J.L. Pelouard, J.F. Guillemoles, D. Lincot;
    Energy & Environ. Sci. 4 (2011) 4972

[5] ZSW Press Release 12 (2014);
    http://www.zsw-bw.de/uploads/media/
    pr12-2014-ZSW-WorldrecordCIGSe.pdf

[6] Y.-Y. Chen, J.-G. Duh, B.-S. Chiou; J. Mater. Sci.:
    Mater. Electronics 11 (2000) 279-238

[7] J. Aguilar-Santillan;
    Metallurgical and Materials Transactions
    A 41A (2010) 684

[8] A.M. Chockla, K.C. Klavetter, C.B. Mullins,
    B.A. Korgel;
    ACS Appl. Mater. Interfaces 4 (2012) 4658–4664

[9] J. Schmidtbauer, R. Bansen,
    R. Heimburger, Th. Teubner, T. Boeck;
    J. Crystal Growth 406 (2014) 36–40,
    DOI: 10.1016/j.jcrysgro.2014.08.013

Layers & Nanostructures:
Ferroelectrical Oxide Layers

Head   Dr. Jutta Schwarzkopf
Team   D. Braun, M. Klann, Dr. J. Sellmann

Überblick

Von Alkaliniobatkristallen ist bekannt, dass sie viel-versprechende piezo- und ferroelektrische Eigenschaf-ten aufweisen, die vergleichbar sind mit denen des etablierten, aber toxischen Pb(Zr,Ti)O$_3$. Insbesondere an der morphotropen Phasengrenze von K$_x$Na$_{1-x}$NbO$_3$ bei x ≈ 0.5 bietet dieses Material exzellente Eigenschaften, die potentiell interessant sind für technische Anwen-dungen wie Sensoren, akustische Oberflächenwellen oder Speicherbauelemente. Aufgrund der hohen Flüch-tigkeit der Alkalimetalle stellt jedoch das Wachstum von stöchiometrischen Schichten bis heute eine Her-ausforderung dar. Daher sind Abscheidung und ferro-elektrischen Eigenschaften von dünnen K$_x$Na$_{1-x}$NbO$_3$ Schichten bisher kaum untersucht worden. Nach-dem wir uns zunächst auf reines NaNbO$_3$ fokussiert hatten, haben wir in 2014 erfolgreich voll verspannte K$_x$Na$_{1-x}$NbO$_3$ Schichten mit x zwischen 0.45 und 1 abgeschieden.

In der Gruppe „Ferroelektrische Oxidschichten" wurden drei Aspekte bezüglich Wachstum und Optimierung von ferroelektrischen Schichten detailliert untersucht. Ers-tens wurde eine epitaktische Gitterverspannung in den Schichten durch das Aufwachsen auf verschiedenen gitterfehlangepassten Oxidsubstraten erreicht. Wäh-rend des Abkühlens von Wachstums- zu Raumtempe-ratur werden elektrostatische und elastische Energien durch das Zerfallen der Schicht in Domänen mit unter-schiedlicher Orientierung der elektrischen Polarisation (ferroelektrische Domänen) und/oder des Verspan-nungsvektors (ferroelastische Domänen) reduziert. In dieser Weise kontrolliert die eingebaute Gitterverspan-nung die Orientierung des Polarisationsvektors und das Domänenmuster. An den Domänengrenzen treten star-ke Verspannungsgradienten auf, die eine Änderung in der lokalen Orientierung der Polarisation und damit einen zusätzlichen Beitrag über den flexoelektrischen Effekt verursachen. Daher ist die gezielte Beeinflussung der ferroelektrischen Domänen und der Domänen-wanddichte ein Schlüsselpunkt in unserer Forschung und ermöglicht die Kontrolle der ferro-/piezoelektri-schen Schichteigenschaften. Das könnte ein breites Spektrum von möglichen Anwendungen eröffnen, wie z.B. nicht-flüchtige ferroelektrische RAMs, akustische Oberflächenwellenbauteile, Hochfrequenz-Ultraschall-Wandler und -filter. Daher haben wir in den letzten Jahren unseren Fokus zunehmend auf das Verständnis und die Kontrolle der ferroelektrischen Domänenbil-dung und der Domäneneigenschaften gelegt.

Als zweiter Punkt ist zu erwähnen, dass voll verspannte Schichten nur für Dicken unterhalb der kritischen Schichtdicke zu erreichen sind. Die Größe der kritischen Schichtdicke hängt von der Gitterfehlanpassung zwi-schen Schicht- und Substratmaterial ab. Eine Möglich-keit, um für technische Anwendungen über diese Gren-ze hinauszugehen, besteht darin, ferroelektrische Übergitter zu wachsen. Diese Strukturen stellen eine Klasse von künstlichen Materialien dar, deren Eigen-schaften wie die Curie-Temperatur und die spontane Polarisation, oftmals die der entsprechenden Volumen-materialien übertreffen und welche das Potential für neuartige Funktionalitäten bieten. Das wird durch zu-sätzliche strukturelle Verzerrungen, elektronische Um-verteilungen und/oder komplexe Domänenstrukturen ermöglicht.

Der dritte Bereich betrifft das Verständnis von unaus-geglichenen Ladungsverteilungen am Interface von zwei isolierenden Perovskiten. Es ist bekannt, dass solche Materialsysteme eine Vielfalt von Eigenschaften aufweisen, die nicht in den entsprechenden Volumen-materialien existieren. Zum Beispiel wird im System LaAlO$_3$/SrTiO$_3$ die Bildung eines zweidimensionalen Elektronengases (2DEG) am Interface beobachtet [1]. Mit der Realisierung eines 2DEG am Interface zwischen einem ferroelektrischen, polaren Oxid und einem un-polarem Oxid könnte das Schalten des Elektronengases durch die Polarisationsumkehr in der ferroelektrischen Schicht ermöglicht werden. Allerdings erfordert die Verwertung und Einstellung solcher Interfaceeffekte eine detaillierte Interfacecharakterisierung.

Overview

Bulk alkaline niobates are known to exhibit promising piezo- and ferroelectric properties similar to those of the well-established, but toxic Pb(Zr,Ti)O$_3$. Especially at the morphotropic phase boundary at x ≈ 0.5, K$_x$Na$_{1-x}$NbO$_3$ offers excellent properties making this material poten-tially interesting for technical applications like sensor, surface acoustic waves or memory devices. However, due to the high volatility of the alkali metals growth of stoichiometric films is challenging yet. Hence, little is known about deposition and ferroelectric properties of K$_x$Na$_{1-x}$NbO$_3$ thin films. After focusing on pure NaNbO$_3$ thin films, in 2014 we have now succeeded to grow fully strained K$_x$Na$_{1-x}$NbO$_3$ thin films with x = 0.45 - 1.

Layers & Nanostructures: Ferroelectrical Oxide Layers

In the group „Ferroelectical Oxide Layers", three topics regarding growth and optimization of ferroelectric films are investigated in detail. First, epitaxial strain has been incorporated in the films imposed by epitaxial growth on different lattice-mismatched oxide substrates. In order to reduce electrostatic and elastic energy during cooling from growth to room temperature, the film splits into domains with different orientation of the electric polarization (ferroelectric domains) and/or the strain vector (ferroelastic domains). Thus, variation of the incorporated lattice strain controls the orientation of the polarization vector and determines the domain pattern. At the domain walls strong strain gradients cause a change of the local orientation of the polarization and give additional contributions via the flexoelectric effect. Therefore, tuning of ferroelectric domains and domain wall density are key points of our research and allow the control of ferro-/piezoelectric film properties. Since this may open a wide range of possible applications like non-volatile ferroelectric RAMs, thin film surface/bulk acoustic wave devices and high frequency ultrasonic transducers, in the last years research activities have been increasingly focused on the understanding and controlling of the ferroelectric domain formation and their properties.

Second, fully strained films can only be achieved below a critical thickness depending on the lattice mismatch between film and substrate material. In order to exceed this limit in regard to technical applications, one possibility is to grow ferroelectric superlattices. These structures represent a class of artificial materials whose properties, such as the Curie temperature and spontaneous polarization, often exceed those of the corresponding bulk materials or which offer the potential to produce novel functionalities. This is provided by the possibility of additional structural distortions, electronic redistributions and/or complex polarization domain structures.

The third point is the understanding of charge imbalanced interfaces between two insulating perovskites that are known to exhibit a variety of properties which do not exist in the constituent bulk materials. For example, in the $LaAlO_3/SrTiO_3$ system the formation of a two-dimensional electron gas (2DEG) at the interface is observed [1]. Realization of a 2DEG at the interface between a ferroelectric, polar oxide and a nonpolar one would allow switching of the 2DEG by polarization reversal in the ferroelectric layer sharing the interface. However, exploitation and tunability of such interface effects demand a detailed interface characterization.

Results

Thin, strained films consisting of $KNbO_3$, $NaNbO_3$ and their solid solutions have been epitaxially grown by liquid-delivery spin metal-organic chemical vapor deposition (MOCVD) and pulsed laser deposition (PLD) as a chemical and physical deposition method, respectively. Several oxides, partially provided by IKZ's "Oxides/Fluorides" group, have been used as substrates for the epitaxial growth of $K_xNa_{1-x}NbO_3$ thin films and offer the incorporation of different lattice strain states in the films. In the following the indices "o" and "c" refer to the orthorhombic symmetry of the substrate and the pseudocubic notation of the films, respectively.

Ferroelectric domains in anisotropically strained $K_xNa_{1-x}NbO_3$ thin films grown by MOCVD

By the use of oxide substrates with different lattice parameters and altering the Na/K ratio in the films the incorporated lattice strain was varied in $K_xNa_{1-x}NbO_3$ thin films from compressive to tensile. In doing so domain alignment and size critically depend on the magnitude of lattice mismatch ε between substrate and film material ($\varepsilon = (a_s - a_f)/a_s$, where a_f and a_s are the bulk lattice parameters of the film and the substrate, respectively). According to theoretical predictions [2], in this way the polarization vector can be rotated within the unit cell, as it is illustrated in Fig. 1 calculated for single-domain potassium niobate at room temperature. In addition, phase field simulations of anisotropically strained thin $PbTiO_3$ films [3] show that even several domain types can coexist, leading to a complex multi-domain structure. This can clearly been observed in our lateral piezoresponse force microscopy (LPFM) measurements on $K_xNa_{1-x}NbO_3$ thin films grown on $SrTiO_3$, $TbScO_3$, $GdScO_3$ and $NdScO_3$ substrates (Fig. 2a). Due to the orthorhombic symmetry of substrate and/or film material all films experience anisotropic in-plane lattice strain.
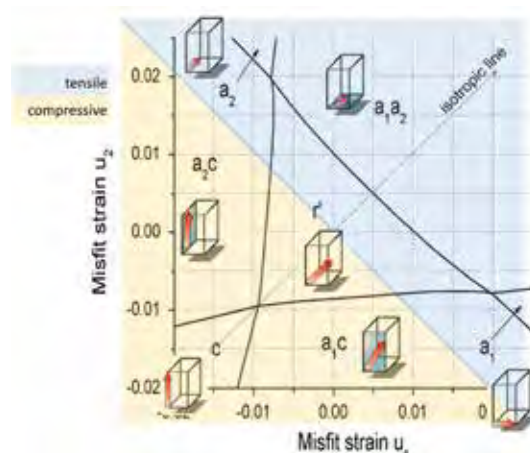

Fig. 1

Misfit strain – misfit strain phase diagram calculated for $KNbO_3$ single-domains at room temperature [1].

Layers & Nanostructures: **Ferroelectrical Oxide Layers**

For compressively strained $K_{0.75}Na_{0.25}NbO_3$ films on $SrTiO_3$ (sample 1 in Fig. 2(a), average lattice mismatch $\varepsilon_{av} = -1.84$ %) small spotty domains with large out-of-plane polarization components are visible in accordance with theoretical predictions of c domains in films under high compressive lattice strain [3]. With decreasing compressive lattice stress by depositing $K_xNa_{1-x}NbO_3$ on rare-earth scandate substrates, two-dimensional, regularly arranged stripe domain patterns appear. Domain walls run along the $[1-12]_o$ direction of the substrate. On $GdScO_3$ (sample 2, $\varepsilon_{av} = -0.69$ %) and $TbScO_3$ (sample 3, $\varepsilon_{av} = -0.47$ %) substrates they are superimposed by superdomains with significantly larger lateral dimension. However, for films under lowest compressive in-plane lattice strain (film on $NdScO_3$, sample 4, $\varepsilon_{av} = -0.10$ % in Fig. 2a) the domain walls are oriented in $[001]_o$ direction. This effect is attributed to the change of surface orientation of the films from $(001)_c$ for sample 2 and 3 to $(100)_c$ for sample 4. From the combination of vertical and lateral PFM measurements in conjunction with structural investigations by XRD (in cooperation with the group "Physical Characterization") we conclude that with the application of decreasing compressive lattice strain the electric polarization vector rotates from a strong vertical arrangement in sample 1 to an almost exclusive in-plane orientation in sample 4. This is schematically presented by the different polarization vectors and the inscribed polarization pathway in Fig. 2(b). The observed behavior fits to the theoretical prediction presented in Fig. 1 and has also been observed for strained $NaNbO_3$ films [4]. A high resolution transmission electron microscopy cross section image of sample 3 in Fig. 3 clearly shows a regular arrangement of ferroelectric domains. This has been observed for the first time for $K_xNa_{1-x}NbO_3$ films.

Ferroelectric characterization

For technical applications of ferroelectric films, e.g. in memory devices or sensors, remnant polarization, coercive field and piezoelectric coefficients have to be optimized in terms of incorporated lattice strain, defect and vacancy densities as well as domain wall contribution. For this purpose, the functional film has to be sandwiched in a capacitor structure between a bottom and top electrode, as shown in Fig. 4(a). Top contacts with a diameter between 5 and 100 μm are realized in cooperation with the Ferdinand Braun Institut, Leibniz-Institut fuer Hoechstfrequenztechnik and the group "Physical Characterization". With the upgrade of the existing FE-Tester from 5 kHz to 1 MHz hysteresis curves of ferroelectric films could be measured in series with a reference capacitor. An example is illustrated in Fig. 4(b) which points to typical ferroelectric hysteresis behavior. Based on these preliminary results it is now envisaged on the one hand to optimize electrode materials and preparation of top contacts and on the other hand to reduce leakage current which is connected with vacancies and defects in the films.
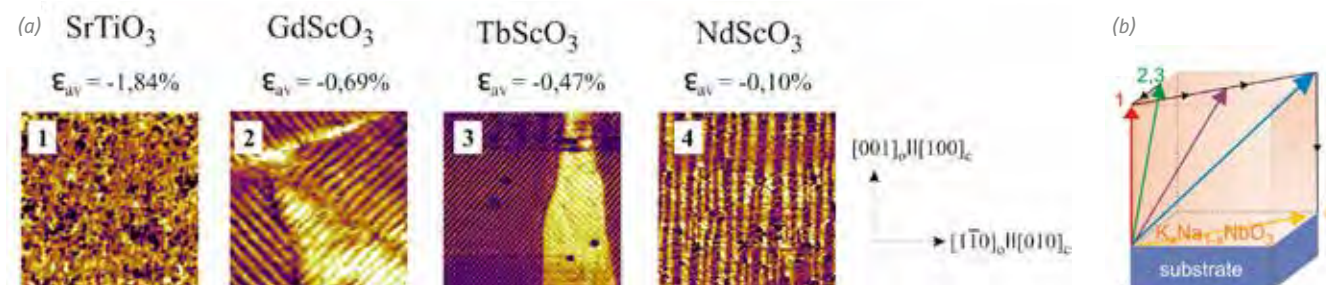

Fig. 2

a) Lateral ferroelectric domain structure of $K_xNa_{1-x}NbO_3$ films on different substrates, 1 µm x 1 µm scans,

b) possible positions and rotation pathway of the electric polarization vector within the unit cell depending on the strain state
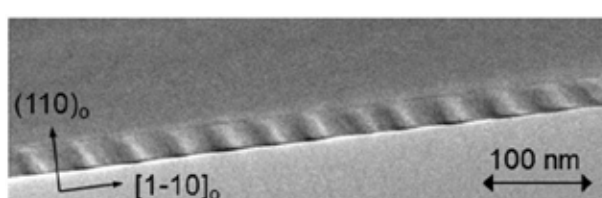


Fig. 3

HRTEM image of 30 nm $K_{0.75}Na_{0.25}NbO_3/TbScO_3$

## Layers & Nanostructures: Ferroelectrical Oxide Layers

(a)

(b)
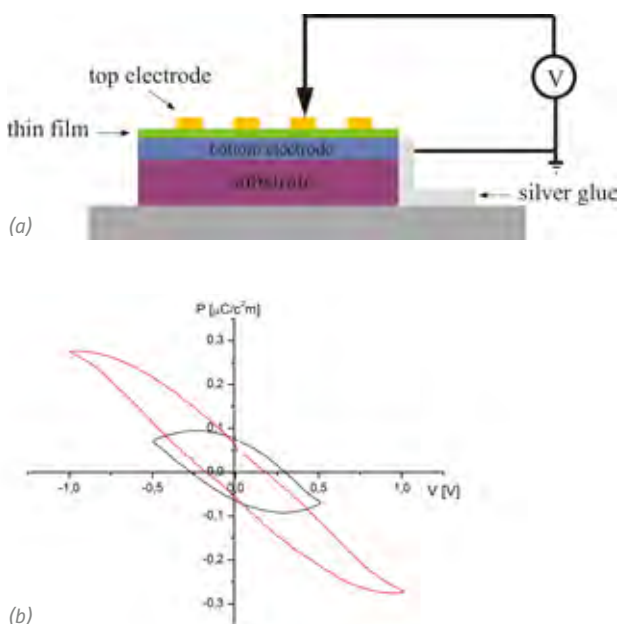
Fig. 4

a) Typical film geometry to measure macroscopic film properties like remnant polarization or coercive field, b) ferroelectric hysteresis measurement performed with the upgraded FE-Tester.

In this regard first experiments have been performed on $NaNbO_3$ films grown by PLD on conductive Nb-doped $SrTiO_3$ substrates with different Na and O content. Both Na-/O-deficient and Na-enriched $NaNO_3$ films exhibit nearly closed local hysteresis curves which we attribute to the occurrence of a high density of point defects causing leakage current and columnar arranged impurity phase precipitates consisting of edge-shared NbO_6 octahedra, respectively. Only films with nearly stoichiometric composition reveal well pronounced ferroelectric hysteresis loops like in Fig. 4(b) measured in PFM. Since density and type of defects critically depend on the incorporated lattice strain resulting from the use of different substrates, it is necessary to optimize film growth for each film/substrate combination. Subsequently, impact of lattice strain, film composition and domain wall density on remnant polarization and piezoelectric coefficient d_{zz} will be investigated in detail.

Temperature and frequency dependent in-plane C-V measurements performed at the FZ Jülich, AG Prof. Dr. Roger Wördenweber, have revealed that on $NdGaO_3$ substrates a small anisotropy of the compressive in-plane strain in a $(001)_c$ oriented $NaNbO_3$ film of −0.67% and −1.33% for the $[100]_c$ and $[010]_c$ direction, respectively, leads to a significant anisotropy of the ferroelectric properties. For instance, the permittivity in $[100]_c$ is increased by a factor of two compared to the value in $[010]_c$ direction. As a consequence, the ferroelectric properties of the film strongly depend on the orientation of the applied electric field [5].

$(K_{0.5}Na_{0.5}NbO_3)_x/(NaNbO_3)_y/DyScO_3$ superlattices

Above the critical thickness strained films grown on lattice mismatched substrates may start to plastically relax by the formation of misfit dislocations which leads to a deterioration of the ferro-/piezoelectric properties. Maintenance of a full epitaxial strain state for thicker films can be obtained by the growth of almost strain compensated superlattices with alternating tensily and compressively strained films. For this purpose five stacks of $K_{0.5}Na_{0.5}NbO_3$-$NaNbO_3$ with different individual layer thickness but constant stack thicknesses of 35 nm were grown on $DyScO_3$ substrates.

Figure 5 shows that for $((NaNbO_3)_x/(K_{0.5}Na_{0.5}NbO_3)_y)_5$ superlattices with x + y = 7 nm the effective piezoelectric coefficient d_{zz}^{eff} could significantly be increased by increasing the thickness proportion of the $K_{0.5}Na_{0.5}NbO_3$ layers up to y = 4.8 nm (x/y = 0.46). If the thickness of the $K_{0.5}Na_{0.5}NbO_3$ layers is further raised to 5.8 nm (x/y = 0.21), the superlattice partially relaxes and d_{zz}^{eff} remarkably decreases again. The increase of d_{zz}^{eff} with increasing y (i.e. decreasing x/y) in Fig. 5 is explained by two effects: (i) higher compressive strain, which is known to improve piezoelectric properties in out-of-plane direction, and (ii) more incorporated (average) K in the superlattice (for bulk $K_xNa_{1-x}NbO_3$ an increase of the piezoresponse is expected for increasing K up to x ≈ 0.5 at the morphotropic phase boundary). For comparison, d_{zz}^{eff} of a single $K_{0.5}Na_{0.5}NbO_3$ film is introduced in Fig. 5, which indeed has a composition corresponding to the MPB. But since here the compressive strain is plastically released by defects, the piezoelectric properties are significantly lower than for superlattice structures with lower K content. This emphasized the impact of strain on functional properties and demonstrates the potential for improvement of ferro-/piezoelectric properties by the deposition of adequate superlattices.
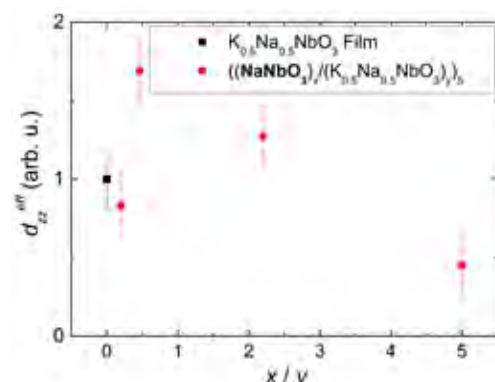
**Fig. 5**

Effective piezoelectric coefficient $d_{zz}e^{ff}$ in dependence of the ratio of the individual layer thicknesses of $NaNbO_3$ (x) and $K_{0.5}Na_{0.5}NbO_3$ (y) in $((NaNbO_3)_x/(K_{0.5}Na_{0.5}NbO_3)_y)_5$ superlattices (red squares). For comparison $d_{zz}e^{ff}$ for a $K_{0.5}Na_{0.5}NbO_3$ single layer is also shown (black square).

Interface studies by Scanning Transmission Electron Microscopy (STEM)

The realization of a 2DEG between ferroelectric perovskite (general formula: ABO_3) films and insulating oxide substrates with nominally charged interfaces is necessarily correlated with an atomically abrupt interface. For that purpose $K_xNa_{1x}NbO_3$ (x = 0 – 1) films on several substrates have been investigated by STEM in cooperation with the "Electron Microscopy" group. As an example, a STEM image of a $NaNbO_3$ film grown by MOCVD on a $DyScO_3$ substrate is shown in Fig. 6(a). On the left side the positions of the metal ions are indicated by red, yellow, green and violet, while on the right hand the z-contrast is quantitatively presented at the A (= Dy or Na) positions according to the color code to the right of the STEM image. Due to the high atomic number of Dy (Z = 66) these ions are clearly visible and cause a high z-contrast (orange squared). In contrast, Na ions (Z = 11) provoke a very low intensity (blue squares). However, at the interface the intensities at the Dy and Na positions are slightly reduced (yellow squares) and enhanced (light blue squares), respectively. This is more evident in the averaged intensity profiles presented in Fig. 6(b). Several intensity values along crystallographically equivalent positions labeled 1 and 2 (blue diamonds and red squares, respectively) are accumulated and compared showing that: (i) in both cases the intensity at the interface cannot be attributed to a pure Na column nor to a pure Dy column and (ii) the intensities at positions 1 and 2 are different. From these results we conclude that the A position at the interface is given by an intermixing of Na and Dy. Additionally, we infer to a regular arrangement of intermixed ions at the interface with twofold periodicity in $[1-10]_o$ direction. Furthermore, also on the B side (= Sc or Nb) an intermixing is visible at the interface, indicated by the intermediate point of the green intensity profile at the interface in Fig. 6(b).

The A-site ion intermixing is observed for all $K_xNa_{1x}NbO_3$ films on $ReScO_3$ substrates and tentatively explained by the formal polarities of the substrate surface (ScO_2 terminated) and the first layer of the film (NaO). These two adjacent layers have nominally the same −1 charge. The resultant "polar catastrophe" can be prevented by a partial exchange of Na^{1+} ions by Dy^{3+} ions. A similar effect is observed for $K_xNa_{1-x}NbO_3/SrTiO_3$ with a substrate surface termination of TiO_2, but not for $K_xNa_{1-x}NbO_3/NdGaO_3$ films, which might be correlated with the A0 termination of the $NdGaO_3$ substrates.
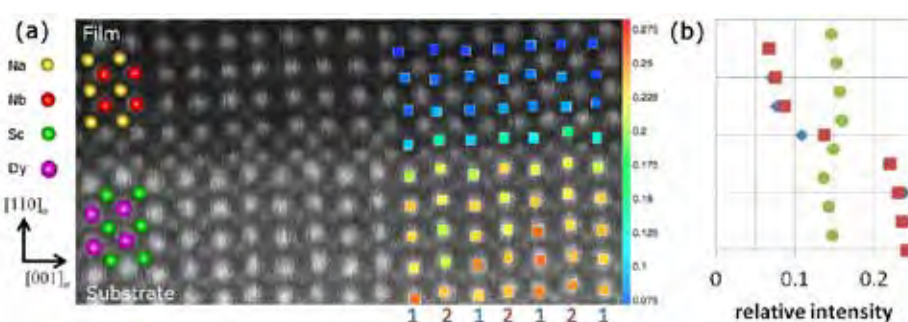
Fig. 6

a) STEM image of a $NaNbO_3$ thin film grown by MOCVD on a $DyScO_3$ substrate.

b) Intensity profiles along the positions 1 (blue diamonds) and 2 (red squares) in (a) as well as along the B side positions (green circles).

References

[1] A. Ohtomo, H. Y. Hwang;
    Nature 427 (2004) 423

[2] G. Bai, W. Ma; Physica B 405 (2010) 1901

[3] G. Sheng, J. X. Zhang, Y. L. Li,
    S. Choudhury, Q. X. Jia, Z. K. Liu, L. Q. Chen;
    J. Appl. Phys. 104 (2008) 054105

[4] J. Schwarzkopf, D. Braun, M. Schmidbauer,
    A. Duk, R. Wördenweber;
    J. Appl. Phys. 115 (2014) 204105

[5] B. Cai, J. Schwarzkopf, E. Hollmann,
    M. Schmidbauer, M. O. Abdel-Hamed,
    R. Wördenweber;
    J. Appl. Phys. 115 (2014) 224103

Simulation & Characterization
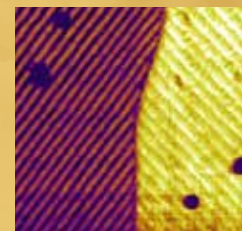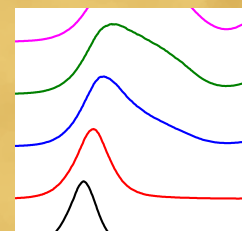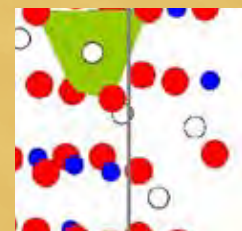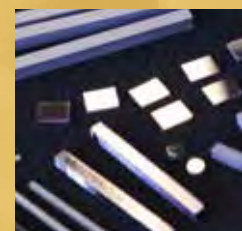
Simulation & Characterization

Head of the section: PD Dr. habil. Detlef Klimm

Wie schon in den vorigen Berichtszeiträumen besteht unsere Tätigkeit zu einen beträchtlichen Teil in der kontinuierlichen Unterstützung der Kristallzüchter-Gruppen aus den anderen Abteilungen des IKZ. Dies beinhaltet zum einen Routinearbeiten zur Kontrolle von Ausgangsmaterialien mit verschiedenen chemischen und physikalischen Verfahren. Außerdem werden Keimkristalle hergestellt, wozu in der Regel kristallographische Orientierung mit Röntgenbeugung sowie Sägen und Oberflächenbearbeitung durchzuführen sind. Das IKZ warb in den vergangenen Jahren eine Reihe großer Projekte zur Züchtung recht unterschiedlicher kristalliner Materialien ein. Dazu gehören beispielsweise Si (für einen neuen Kilogramm-Prototypen sowie zur Photovoltaik), Ge (doppel-β-Zerfall von ^{76}Ge für die Neutrinoforschung), AlN (effektive Lichterzeuger im UV-VIS-Bereich) sowie SrTiO$_3$ (wichtiges Substrat für Oxidelektronik und Spintronik). Diese breite Palette unterschiedlicher Materialien erfordert spezifische Technologien zur Handhabung und Präparation, die teilweise nicht unmittelbar zur Verfügung stehen, sondern erarbeitet werden müssen. Sicherlich wird hierfür die Kristallbearbeitung in personeller und technischer Hinsicht weiter entwickelt werden müssen.

Die Forschungsthemen aller Gruppen der Sektion ergeben sich hauptsächlich aus den verschiedenen neuen Materialklassen die teilweise bereits oben erwähnt wurden. Oft werden die Arbeiten in enger Kooperation mit den Kristallzüchtern des IKZ durchgeführt; darüber hinaus spielen aber langjährige Partner wie zum Beispiel OSRAM für die Elektronenmikroskopie eine wichtige Rolle. Gemeinsam mit Kollegen der Technischen Universität Berlin wurden für diesen Partner bahnbrechende Erkenntnisse gewonnen, die zum Verständnis verhelfen, welche mikroskopischen Prozesse zum Wirkungsgradabfall von LEDs führen. Dies wird detailliert im Beitrag der Gruppe Elektronenmikroskopie in diesem Jahresbericht beschrieben. Neue Aktivitäten sind auf die Einrichtung eines „Science Campus" an unserem Standort in Berlin-Adlershof gerichtet. Hierdurch soll den schon existierenden Kooperationsbeziehungen insbesondere zu lokalen Partnern wie Humboldt-Universität und Paul-Drude-Institut ein besserer organisatorischer Rahmen gegeben werden. Diese Aktivitäten betreffen Untersuchungen zu verschiedenen Oxiden als aktiven Elementen mit halbleitenden oder ferroelektrischen Eigenschaften. Wir erwarten, dass solche Materialien zumindest mittelfristig eine herausragende Bedeutung in der internationalen Forschungslandschaft behalten werden.

Like in the previous reporting periods a substantial share of our efforts is devoted to the continuous support of crystal growth groups from the other IKZ departments. This includes routine inspection of starting materials by different chemical and physical methods, and the preparation of seed crystals which requires typically crystallographic orientation by X-ray diffraction as well as cutting and surface preparation. IKZ acquired during the last years several large projects which are aimed on the growth of quite different crystalline materials for different applications, such as Si (for kilogram prototype and solar energy harvesting), Ge (double β decay of ^{76}Ge for neutrino research), AlN (effective light emitters in the UV-VIS region), SrTiO$_3$ (substrate for oxide electronics and spintronics). This broad palette of different materials requires specific handling and preparation technologies, which are partially not immediately available and have to be developed. Certainly the personnel and technical basis for crystal preparation has to be developed further to meet this increasing demand.

The research topics of all groups in the section reflect mainly the different new materials which were partially mentioned above. The work is very often performed in close collaboration inside IKZ, but also other long term partners like OSRAM for the Electron Microscopy play an important role. A seminal contribution on the efficiency droop of LEDs, which was reached also together with Technical University Berlin, will be presented in this report. New efforts are devoted to the establishment of a "Science Campus" collaboration network (e.g. with Humboldt University and Paul Drude Institute) on our site in Berlin Adlershof, which is expected to enhance mutual interaction with local partners in the field of oxides for semiconductor as well as ferroelectric applications. We expect that functional oxides remain in the focus of worldwide scientific activities at least on a medium timescale and will do our part, which is the supply of sophisticated materials together with expertise to handle and analyze them.

Simulation & Characterization:
Physical Characterization

Head   Dr. Klaus Irmscher
Team   K. Banse, A. Kwasniewski, M. Naumann, M. Pietsch, Dr. M. Schmidbauer

Übersicht

Die Gruppe Physikalische Charakterisierung beschäftigt sich hauptsächlich mit der Untersuchung der im IKZ gezüchteten Volumenkristalle und epitaktischen Schichten mittels Röntgenbeugung, optischer Spektroskopie und Bildgebung, elektrischer Messungen sowie verwandter Techniken. Einerseits liefern die Ergebnisse dieser Messungen die erforderliche Rückinformation an die Kristallzüchter, um die Züchtungsprozesse zu optimieren. Andererseits können interessante physikalische Effekte, die von grundlegendem oder anwendungsspezifischem Interesse sind, nachgewiesen werden. Viele wichtige Resultate werden in den Einzelberichten der entsprechenden Züchtungsgruppen beschrieben. Hier konzentrieren wir uns auf zwei ausgewählte Themen unserer Arbeit: (i) Es werden das Studium ferroelektrischer Domänen in $(K,Na)NbO_3$ Dünnschichten auf (110) $TbScO_3$ Substraten mittels Röntgenbeugung und (ii) die Untersuchung der Temperaturabhängigkeit der $SrTiO_3$ Bandlücke mittels optischer Spektroskopie dargestellt.

Overview

The group Physical Characterization is mainly concerned with investigations of bulk crystals and epitaxial layers grown at IKZ using x-ray diffraction, optical spectroscopy and imaging, electrical measurements, and related techniques. On one hand the results of these measurements provide necessary feedback to the crystal growers for optimizing the growth processes. On the other hand interesting physical effects in these crystals may be revealed being of basic as well as application specific interest. Many important results are communicated in the individual reports of the respective crystal growth groups. Here we focus on two selected topics of our work: (i) An x-ray diffraction study of ferroelectric domains in $(K,Na)NbO_3$ films on (110) $TbScO_3$ substrates and (ii) an optical spectroscopy investigation of the temperature dependence of the $SrTiO_3$ band gap are presented.

Results

Ferroelectric domains in $(K,Na)NbO_3$ films on (11̄0) $TbScO_3$ substrates studied by x-ray diffraction

Lattice strain is an important parameter to intentionally modify the piezoelectric properties of ferroelectric materials and to control size and symmetry of domains and domain walls. This is usually realized through coherent epitaxial growth of thin films on lattice-mismatched substrates. Targeted incorporation of epitaxial strain has been shown to result in a change of the film orientation and domain pattern [1], and is crucially connected with a shift of the Curie temperature, an increase of the remnant polarization and large piezoelectric coefficients [2,3]. Hence, fundamental understanding and intentional engineering of domain formation are essential for further application in nanometer sized electronic devices.

We have reported on $NaNbO_3$ thin films grown under anisotropic strain on orthorhombic (110) $TbScO_3$ [4] and (110) $DyScO_3$ [5] substrates. Recently, these investigations have been extended to $KNbO_3$ and $(K,Na)NbO_3$ ferroelectric thin films which are even more promising than $NaNbO_3$ due to very large electro-optic and electromechanical coupling coefficients [6]. These samples were grown by metal organic chemical vapor deposition (MOCVD) in the group "Ferroelectric Oxide Layers".
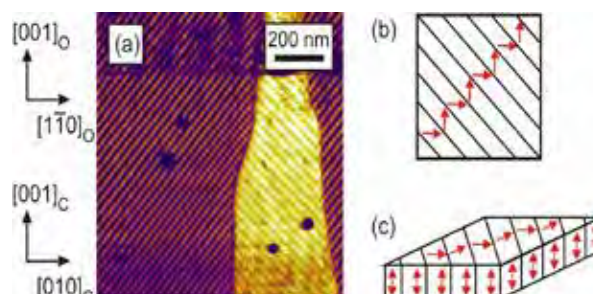
Fig. 1

*(a) Lateral piezoresponse force micrograph of a 30 nm $K0.75Na0.25NbO_3$ thin film grown on orthorhombic (110) $TbScO_3$ substrate. The pseudocubic ($[001]c$, $[010]c$) and orthorhombic ($[001]o$, $[1\text{-}10]o$) in-plane directions of the film and substrate, respectively, are shown as arrows. (b),(c) schematic view of in-plane and out-of-plane arrangement of electric polarization vector.*

Simulation & Characterization: **Physical Characterization**

In this report we focus on $K_{0.75}Na_{0.25}NbO_3$ thin films grown on (110) $TbScO_3$ substrates under slight compressive strain. Lateral and vertical piezoresponse force micrographs (PFM) of a 30 nm thin film indicate that the electric polarization vector exhibits both a lateral and vertical component. The lateral PFM (Fig.1a) shows a pronounced regular stripe pattern (with a period of about 50 nm) of ferroelectric domains with domain walls aligned along the pseudocubic <110>$_c$ directions. A more detailed analysis of the PFM data shows that the domains consist of 90° variants with the in-plane electric polarization components aligned along the pseudocubic edges of the films (Fig. 1b,c).

In order to obtain information about the thin film crystallographic orientation and the symmetry of the film unit cell out-of-plane high-resolution x-ray diffraction (HR-XRD) and in-plane grazing incidence x-ray diffraction (GIXD) experiments have been performed in our home laboratory and at the European Synchrotron Radiation Facility (ESRF) in Grenoble at station BM02 (D2AM), respectively. HR-XRD ω-2θ scans (not shown here) prove that the film has been grown under compressive strain and exhibits (001)$_c$ surface orientation which agrees with energetic considerations using linear elasticity theory. X-ray reciprocal space maps have been measured in the vicinity of different out-of-plane Bragg reflections. While for the symmetric (220)$_o$ reflection only a single film peak can be detected (Fig. 2(a)), the Bragg peak of the film nearby the asymmetric (444)$_o$ substrate peak in Fig. 2(b) shows a significant splitting (marked as P1 and P2) in vertical direction. By contrast, no vertical splitting can be observed for the (620)$_o$ Bragg reflection. These observations prove a shearing of a cubic unit cell along the [100]$_c$ axis leading to monoclinically distorted unit cells (β = ± 0.20°) as schematically shown in Fig. 2(d).

With regard to the existence of both an in-plane and an out-of-plane polarization component (Fig. 1(c)) as well as to the monoclinic distortion of the unit cell, we conclude to the occurrence of monoclinic M$_C$ domains in the $K_{0.75}Na_{0.25}NbO_3/TbScO_3$ thin films, similar to the results of Christen et al. [3] for $BiFeO_3$ films.

Beside peak splitting the intensity distribution in the proximity of the asymmetric (444)$_o$ Bragg reflection (Fig.2(b)) shows pronounced lateral satellite peaks nearby the film contribution which are caused by the periodic arrangement of domains with alternating in-plane and/or out-of-plane polarization components. Similar satellite reflections are also visible in the GIXD pattern (Fig.2(c)). From the peak spacing a lateral periodicity of the domains of about (49 ± 1) nm has been evaluated, which is in excellent agreement with the PFM data. On the other hand, no positional correlation peaks have been observed for the symmetric (220)$_o$ reflection (Fig. 2(a)), proving that only the in-plane polarization changes periodically between adjacent domains.

Additionally, the aperture angle of the two red lines in Figs. 2(b) corresponds to the angle between the domain walls and the surface normal in the cross section. From our measurements an angle a of about 40° can be derived which fits well to result obtained from the HR-TEM cross section images (see Fig. 3 in report "Ferroelectric Oxide Layers")
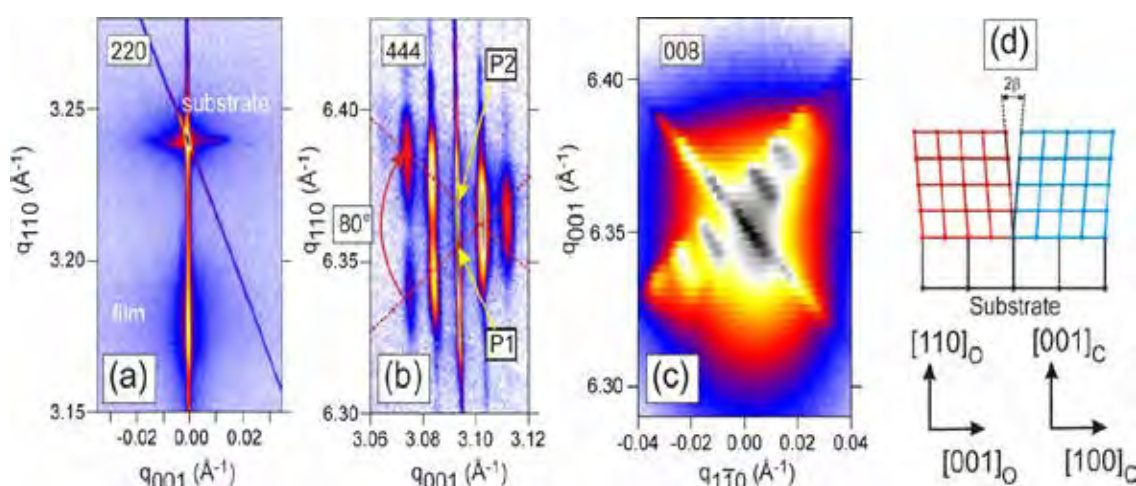
Fig. 2
X-ray intensity distribution of the sample shown in Fig.1 around the (a) 220, (b) 444, and (c) in-plane 008 reciprocal lattice points of the (110) $TbScO_3$ substrate. (d) Schematic view of the monoclinic distortion of the pseudocubic unit cells of the film (β = ± 0.20°).

Temperature dependent optical absorption of SrTiO₃

$SrTiO_3$ is presently in the focus of intensive materials research because this prototype of a complex oxide plays an important role in the emerging field of oxide electronics. It is the basic component of the oxide heterostructures for which two-dimensional electron gases (2DEG) at the heterointerfaces have been shown experimentally, including the most widely investigated interface $LaAlO_3/SrTiO_3$ [7]. However, the physical origin of the 2DEG is still not well understood. To distinguish between intrinsic and extrinsic influences on the formation of the 2DEG it is highly desirable to have bulk $SrTiO_3$ single crystals of very low defect densities available. On the one hand, heteroepitaxial growth on such $SrTiO_3$ substrates may enable defect reduced interfaces. On the other hand, the three-dimensional physical properties (in particular electrical and optical properties) of the single crystals can be investigated more reliably than before, allowing a clear assessment of their effect on the 2DEG formation.

The group Oxides/Fluorides and the characterization groups work together on a project (funded by the Leibniz Association) which aims to grow $SrTiO_3$ bulk single crystals of superior structural quality. Although the growth from the melt is the method of choice for $SrTiO_3$, it suffers from the occurrence of growth instabilities resulting from insufficient heat transport away from the liquid-solid interface of the growing crystal. The heat transport around the high melting point of $SrTiO_3$ of 2350 K is dominated by radiation. Therefore, we investigated the temperature dependent optical absorption of $SrTiO_3$ to find out which absorption processes could be responsible for reduced radiative heat transport at such high temperatures. The observation of a strong shrinkage of the $SrTiO_3$ band gap with increasing temperature is an essential result of these investigations and is briefly communicated in the following.

Samples prepared from undoped crystals grown by the Verneuil method were supplied by CrysTec GmbH. They were electrically insulating at room temperature. Optical transmission spectra were measured using a commercial spectrophotometer equipped with a liquid helium flow cryostat for temperatures from 4 K to 300 K. Above room temperature up to 1703 K we used our custom setup consisting of a high-intensity laser-driven xenon lamp, a small tube furnace allowing optical access and a grating monochromator equipped with a charge-coupled device line detector. In this setup the polychromatic radiation of the xenon lamp first traverses the sample and is then spectrally analyzed. The spectra were corrected for the thermal radiation of the sample by subtracting spectra recorded without lamp irradiation at the corresponding temperatures. The absorption coefficient *a* was calculated from the measured transmittance using the familiar expression including the reflectance correction.

The spectral dependence of the absorption coefficient as measured for the low and high temperature ranges is shown in Fig. 3. From these data the band gap energy can be determined when the dominant absorption process is known. $SrTiO_3$ has an indirect gap [8] and we assume allowed transitions. Then the proportionality $\alpha \propto (h\nu - E_{g,indir} \pm E_p)^2$ holds, where $h\nu$, $E_{g,indir}$, and E_p are the energy of the photon, of the indirect band gap, and of the momentum conserving phonon, respectively. A plot of $\alpha^{1/2}$ versus $h\nu$ should show, under ideal conditions, two linear parts around the band gap, one for phonon emission and one for phonon absorption. Here we neglect E_p which is expected to be only few 10 meV and within the experimental error of the measurements at high temperatures. Therefore, the extrapolation of the linear part of $\alpha^{1/2}$ vs. $h\nu$ to zero gives an estimation of the band gap energy at each temperature. In this way one obtains the temperature dependence of the band gap of $SrTiO_3$ shown in Fig. 4. The data can be fitted by using a single-oscillator model expressed by

$$E_g(T) = E_g(0) - S\langle\hbar\omega\rangle\left[\coth\left(\frac{\langle\hbar\omega\rangle}{2kT}\right) - 1\right],\qquad(1)$$

where $E_g(0)$ is the energy gap at zero temperature, S is a measure of the strength of the electron-phonon coupling, and $\langle\hbar\omega\rangle$ an average of effectively contributing phonon energies [9]. The best-fit parameters $E_g(0)$ = 3.268 eV, S = 5.6, and $\langle\hbar\omega\rangle$ = 60 meV are obtained. The average phonon energy is in the range of the optical phonon modes reported for $SrTiO_3$ [10]. The large S parameter indicates strong electron-phonon coupling which we assume to be the main reason for the strong shrinkage of the band gap with increasing temperature. A similarly strong temperature dependence we have observed for the band gap of In_2O_3 (S = 8.24) [11]. Such large S values, and in turn strong temperature dependences of E_g, may be characteristic for oxide semiconductors with their dominating ionic bonding. More covalently bound semiconductors have at most half as large S values [9], and consequently they show a much weaker temperature dependence of their band gap. However, the basic physical origin of this difference in optical absorption behavior is still unclear.

Extrapolation of the calculated fitting curve to the melting point of $SrTiO_3$ yields an energy gap of only 1.2 ± 0.1 eV (Fig. 4). Therefore, one expects that a large amount of the high-energy photons of the black-body radiation can be fundamentally absorbed over the gap at temperatures above 2000 K. Furthermore, intrinsic charge carriers are thermally generated in high concentrations due to the small gap and contribute substantially to the absorption of low-energy photons of the black-body radiation by free carrier absorption. Both effects effectively suppress radiative heat transport during crystal growth from the melt and cause growth instabilities. One

Simulation & Characterization: **Physical Characterization**

way to overcome this problem is flux growth at lower temperatures (around 1800 K), a method that is refined in the group Oxides/Fluorides. A detailed description and discussion of the experiments can be found in our recent publication [12].
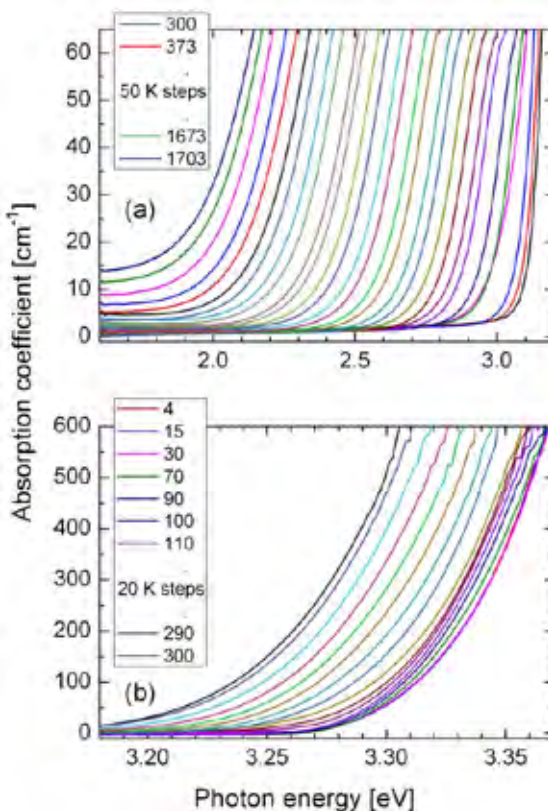
Fig. 3

Spectral dependence of the absorption coefficient of
SrTiO$_3$ for (a) high and (b) low temperatures. Parameter is the
temperature in K. The furnace for the measurements at high
temperatures was flushed by ambient air.
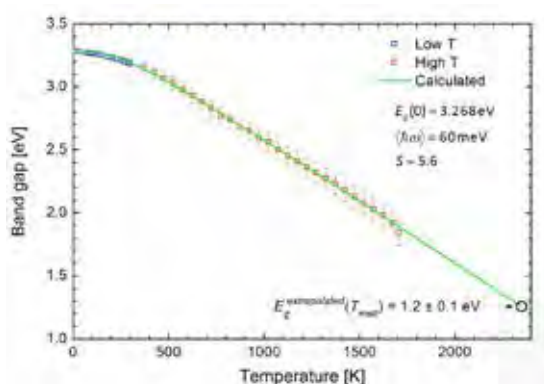
Fig. 4

Temperature dependence of the band gap of SrTiO$_3$.
Blue (red) symbols represent the measurements below (above)
room temperature. The green curve was calculated using Eq. (1),
see text, and the given best-fit parameters. By extrapolation of
this curve the energy gap near the melting point T_{melt} = 2350 K
can be estimated.

References

[1] J. Schwarzkopf, A. Duk, M. Schmidbauer, D. Braun, R. Wördenweber; J. Appl. Phys. 115 (2014) 204105

[2] K. J. Choi, M. Biegalski, Y. L. Li, A. Sharan, J. Schubert, R. Uecker, P. Reiche, Y. B. Chen, X. Q. Pan, V. Gopalan, L.-Q. Chen, D. G. Schlom, C. B. Eom; Science 306 (2004) 1005

[3] H. Christen, J. Nam, H. Kim, A. Hatt, N. Spaldin; Phys. Rev. B 83 (2011) 144107

[4] A. Duk, M. Schmidbauer, J. Schwarzkopf; Appl. Phys. Lett. 102 (2013) 091903

[5] M. Schmidbauer, J. Sellmann, D. Braun, A. Kwasniewski, A. Duk, J. Schwarzkopf; Phys. Status Solidi RRL 8 (2014) 522

[6] T. V. Murzina, S. A. Savinov, A. A. Ezkov, O. A. Aktsipetrov, I. E. Korsakov, I. A. Bolshakov, A. R. Kaul; Appl. Phys. Lett. 89 (2006) 062907

[7] A. Ohtomo, H. Y. Hwang; Nature 427 (2004) 423

[8] K. van Benthem, C. Elsässer, R. H. French; J. Appl. Phys. 90 (2001) 6156

[9] K. P. O'Donnell, X. Chen; Appl. Phys. Lett. 58 (1991) 2924; R. Pässler; J. Appl. Phys. 89 (2001) 6235

[10] U. Balachandran, N. G. Eror; J. Am. Ceram. Soc. 65 (1982) 54

[11] K. Irmscher, M. Naumann, M. Pietsch, Z. Galazka, R. Uecker, T. Schulz, R. Schewski, M. Albrecht, R. Fornari; Phys. Status Solidi A 211 (2014) 54

[12] D. J. Kok, K. Irmscher, M. Naumann, C. Guguschev, Z. Galazka, R. Uecker; Phys. Status Solidi A (2015); DOI: 10.1002/pssa.201431836

Simulation & Characterization:
Electron Microscopy

Head   Dr. Martin Albrecht
Team   K. Banse, T. Markurt, S. Mohn, M. Naumann, M. Niu, T. Remmele,
       N. Stolyarchuk, R. Schewski, Dr. T. Schulz

Übersicht

Die Arbeitsgruppe Elektronenmikroskopie charakterisiert kristalline Materialien mit elektronenmikroskopischen Methoden sowohl im Rahmen des wissenschaftlichen Service als auch im Bereich der Grundlagenforschung. Thematischer Schwerpunkt ist der Zusammenhang zwischen physikalischen Eigenschaften und Struktur von Halbleitern. Die Methoden reichen von der Rasterelektronenmikroskopie (energie- und wellenlängendispersive Röntgenspektroskopie, Elektronenrückstreubeugung (EBSD), Kathodolumineszenz) über die Ionenstrahlbearbeitung bis zur Transmissionselektronenmikroskopie (aberrationskorrigierte Transmissionselektronenmikroskopie und Rastertransmissionselektronenmikroskopie mit atomarer Auflösung). Die Gruppe arbeitet eng mit Gruppen des Kristallwachstums, der ab-initio Modellierung und der Simulation zusammen und trägt wesentlich zur Qualifizierung des wissenschaftlichen Nachwuchses bei. Innerhalb der Gruppe arbeiten drei Doktoranden und eine Doktorandin sowie ein Gastwissenschaftler. Doktoranden und Doktorandinnen, Master- und Bachelorstudierende anderer Arbeitsgruppen des Institutes werden in elektronenmikroskopische Verfahren eingewiesen oder gemeinsam betreut. Neben der Standardcharakterisierung von Oberflächen und Zusammensetzung, Phasenanalyse und Analyse von Einschlüssen werden insbesondere grundlegende Arbeiten zu Wachstums- und Relaxationsprozessen epitaktischer Schichten sowie zu Kristalldefekten durchgeführt. Um bildgebende Verfahren zu verbessern und sie auf die spezifischen Probleme und die laufenden Arbeiten am Institut anzupassen werden eigenständige methodische Arbeiten durchgeführt. Die Gruppe arbeitet in nationalen und internationalen Forschungsprojekten und Forschungsverbünden.

Da einige der Ergebnisse der Elektronenmikroskopie in den Berichten der Arbeitsgruppen der Kristallzüchtung vertreten sind, sollen im Folgenden drei ausgewählte Themen unserer derzeitigen Arbeit dargestellt werden. Dabei handelt es sich um Arbeiten (i) zur Rekombinationsdynamik in Gruppe-III Nitrid-basierten Leuchtdioden in Kooperation mit OSRAM OS und der Technischen Universität Berlin, (ii) zu grundlegenden Wachstumsmechanismen von Ga_2O_3 auf Saphir, die zusammen mit der Universität Leipzig und dem Paul-Drude-Institut durchgeführt wurden und (iii) zur Grenzfläche zwischen ferroelektrischen Schichten und deren Substraten zusammen mit der Arbeitsgruppe „Ferroelektrische Oxidschichten".

Overview

The electron microscopy group performs scientific service and basic research in the field of characterization of crystalline material by means of electron microscopy. Focus is the relation between physical properties and structure. The methods cover the whole field ranging from scanning electron microscopy, i.e. energy and wavelength dispersive spectroscopy, electron backscatter diffraction, cathodoluminescence through transmission electron microscopy, i.e. aberration corrected transmission electron microscopy and scanning transmission electron microscopy with atomic resolution. The team works in close collaboration with groups performing crystal growth and ab-initio modelling and simulation. Within the group four PhD students are working and we host one guest scientist. PhD students, master and bachelor of other groups in the institute are introduced into electron microscopy techniques and are commonly supervised. We perform standard characterization of surfaces and composition, phase analysis and analysis of inclusions as well as basic analyses of growth and relaxation mechanisms and of defects. To improve electron optical imaging techniques and to adopt them to the specific problems at the institute we perform methodological work. The group is partner in collaborative national and international research projects.

Some of our results are already contained in the individual reports of the groups working in crystal growth. We will therefore highlight three selected topics of our current work. These have been (i) performed in cooperation with OSRAM OS and Technical University of Berlin on the recombination dynamics in III-Nitride base light emitting diodes, (ii) with the group "Semiconducting Oxide Layers" at IKZ and external partners from Paul-Drude-Institut and University Leipzig on fundamental growth studies of Ga_2O_3 on sapphire and (iii) with group "Ferroelectric Oxide Layers" at IKZ on the interface between strained ferroelectric layers and their substrates.

Results

Recombination dynamics in $In_xGa_{1-x}N$ quantum wells – contribution of excited subband recombination to carrier leakage

In collaboration with OSRAM Opto Semiconductors, we have tackled one of the major issues of today's (InGa)N based optoelectronic devices, i.e. the decrease of the quantum efficiency with increasing current density [1]. This effect, which is in literature denoted as the "efficiency droop", is typically observed when the current density of blue or white LEDs exceeds approximately 10 A/cm². Recent reports have focused the discussion on the origin of this effect on non-radiative Auger transitions. Indeed, high energy charge carriers, which are a fingerprint of Auger processes, have been detected in photo- and electroluminescence experiments [2,3]. However, whether non-radiative recombination via Auger transition is the dominant effect in the efficiency droop remains a controversial point [4]. In our own studies, we have conducted time resolved photoluminescence studies on dedicated single quantum well samples to monitor the recombination dynamics of the non-equilibrium charge carriers. The emission spectra have been compared against simulations using a Schrödinger Poisson approach. Fig. 1 (left) shows experimental photoluminescence spectra for different delay times after the excitation pulse. While only one emission band is present for delay times above 17 ns, a second band emerges on the high-energy side as the delay time decreases. This implies that that two distinct recombination process occur in the quantum well, one at large delay times (when the non-equilibrium charge carrier density is small) and one at small delay times (when the non-equilibrium charge carrier density is high). A very similar change of the emission spectrum can be observed in the simulation in Fig. 1 (right) for different current densities. For small current densities below 10 A/cm², only one emission band is observed while for larger current densities, a second band emerges on the high energy side. In these simulations, the low and high energy band originate from transitions involving ground and first excited electron subband states of the quantum well, respectively. Due to the analogy with the simulations, we attribute the two experimentally observed emission bands to the same recombination mechanism. Fig. 2 displays the simulated band structure and the probability density for electrons and holes in the (In,Ga)N quantum well. Due to the smaller electronic confinement, excited electron subband states have a larger probability to tunnel out of the quantum well, which corresponds to a leakage mechanism. Since the onset of excited subband transitions occurs at current densities already above 10 A/cm², such transitions contribute to the decrease of the device efficiency. Hence, this recombination mechanism could play a crucial role in the efficiency droop.
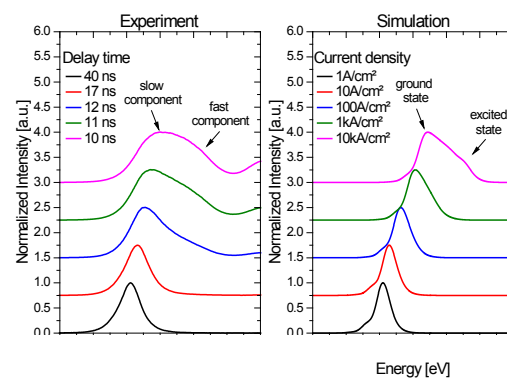
Fig. 1.

(left) Time resolved photoluminescence measurements of an $In_{0.19}Ga_{0.81}N$ single quantum well.
(right) Simulated emission spectra for a 3 nm $In_{0.19}Ga_{0.81}N$ quantum well for varying current densities.
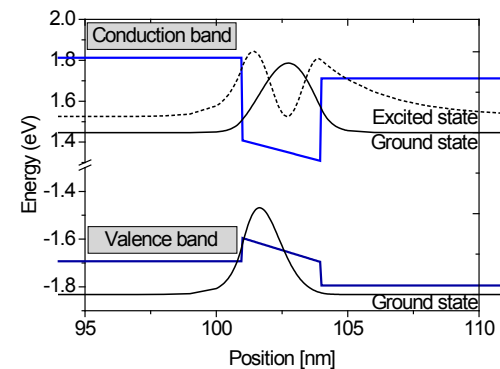
Fig. 2.

Simulated band diagram of a 3 nm $In_{0.19}Ga_{0.81}N$ quantum well showing the probability density for the hole ground state and the electron in the ground and first excited state.

Epitaxial stabilization of pseudomorphic α-Ga_2O_3 on sapphire (0001)

Coherent epitaxial growth of heterostructures formed of semiconducting β-Ga_2O_3 and insulating α-Al_2O_3 is of high interest for its potential device applications. The moderate misfit (0.047) and the huge difference in their fundamental band gap (an indirect around 5.03 eV has been reported for α-gallium oxide and of 8.8 eV for aluminum oxide) offer the opportunity to realize two-dimensional electron gases and intersubband devices operating at telecommunication wavelengths. Under ambient conditions, however, only the monoclinic β-Ga_2O_3 phase is stable [5]. Single crystals in the trigonal α-modification (space group Rc) have been grown at 1000° C at hydrostatic pressures as high as 4.4 GPa. In epitaxial growth thermodynamical equilibria can be influenced through chemistry or strain. An example for chemical stabilization is the MOCVD growth of diamond, where the presence of H stabilizes the otherwise unstable diamond phase. Stabilization through strain has

Simulation & Characterization: **Electron Microscopy**

been put forward by Bruinsma and Zangwill and Froyen and Zunger [6,7]. In case of coherent growth, the strain induced by the lattice mismatch between substrate and layer may shift the thermodynamic equilibrium towards the desired phase and revise the order of stability found in the strain free bulk. For example, early experimental reports gave evidence for epitaxial stabilization of α-Sn rather than β-Sn when grown on InSb or CdTe or of the zincblende phase of MnSe (instead of the stable rock-salt phase) when grown on ZnSe. The theoretical work by Froyen et al. showed that even phases that are not accessible by pressure experiments may be realized by epitaxial growth. A prerequisite for epitaxial stabilization by mismatch induced strain is that at the required pressure the critical thickness for plastic relaxation is sufficiently high (at least > 1 monolayer). For the compound semiconductors mentioned above (e.g. CdTe) the transition from the zincblende to the rocksalt structure occurs at pressures as low as 3 GPa. This allows coherency to be maintained up to a thickness of several monolayers. Group III sesquioxides are characterized by a high value of the bulk modulus (between 172 GPa for In_2O_3 and 253 GPa for Al_2O_3). On the other hand as shown by high pressure experiments as well as by Density Functional Theory (DFT) calculations, the phase transition from the $β-Ga_2O_3$ to the metastable $α-Ga_2O_3$ phase takes place at moderate hydrostatic pressures between 3.3 and 13.6 GPa, even at temperatures as high as 1000 °C.

In a recent contribution [8] we showed by means of transmission electron microscopy that a single crystalline $α-Ga_2O_3$ layer can be grown coherently on a sapphire (0001) substrate through metal-organic vapor phase epitaxy (MOVPE), molecular beam epitaxy (MBE) and pulsed-laser deposition (PLD). The α-phase remains stable up to a critical thickness of 3 monolayers at temperatures ranging between 650°C and 800°C, i.e. well above the experimentally determined temperature for the phase transition between the α-phase and the β-phase. Fig. 3 shows a typical STEM HAADF image of a MOVPE grown layer. In the bottom part the $α-Al_2O_3$ in the <1-100> projection is visible. The upper part of the image shows the textured $βGa_2O_3$ layer. At the interface between the layer and the substrate a bright interlayer is visible. Fig. 4 a) and b) shows this interlayer in the <11-20> and <1-100> projection, respectively. STEM simulations (shown in Fig. 5) reveal that the interlayer consists of Ga_2O_3 in the α modification. We showed further that plastically relaxed $β- Ga_2O_3$ grows on top of the pseudomorphic coherent $α-Ga_2O_3$ layer as often described by domain matching epitaxy. It causes the formation of rotational domains induced by the symmetry mismatch between the monoclinic β-phase and the trigonal α-phase (see Fig. 5) observed also by other authors [9]. We see this as a strong support for our hypothesis that coherent strain in the system Ga_2O_3 on (0001) $α-Al_2O_3$ is able to stabilize $α-Ga_2O_3$. Considering the example of structural transition in conventional semiconductors or

metals by Bruinsma and Zangwill [6] that upon further growth undergo a kind of martensitic transformation accompanied by plastic relaxation we find our system to be essentially different. In our system the misfit dislocations are located at the interface between the relaxed $α-Ga_2O_3$ and the fully strained $β-Ga_2O_3$ and not as expected at the interface between sapphire and $α-Ga_2O_3$. Plastic relaxation in the thin two dimensional grown layer is impossible, since no shear stresses are present in the easy glide planes ((0001), {11-20} {1-100}). Growth of the layer then proceeds through homogeneous nucleation of three dimensional islands (as described in e.g. [10]). Due to the symmetry mismatch, islands grow in terms of domain matching epitaxy [11], i.e. in six distinct in plane orientations, but plastically relaxed.
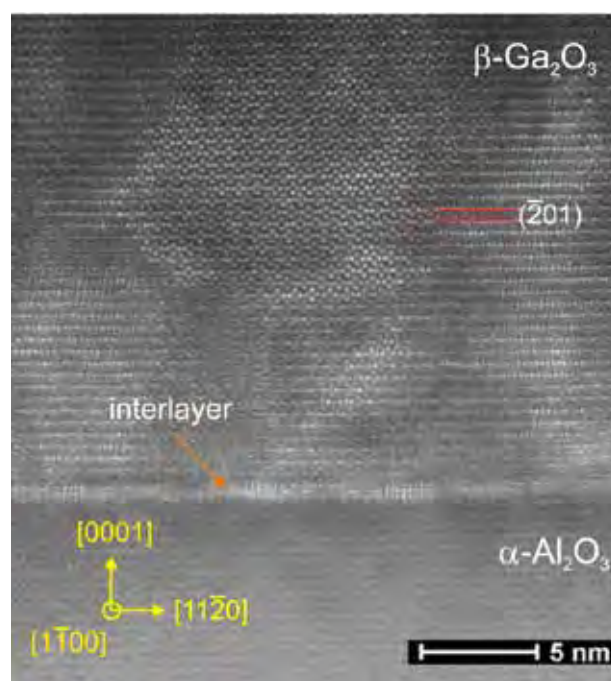
*Fig. 3*
Typical HAADF STEM (High Angle Annular Dark Field Scanning Transmission Microscope) image of a MOVPE grown Ga_2O_3 layer on top of c-plane sapphire. Two different patterns are observable, corresponding to different orientated grains. At the $β-Ga_2O_3/α-Al_2O_3$ interface the 3 monolayer thick coherent $α-Ga_2O_3$ is visible.

Simulation & Characterization: Electron Microscopy
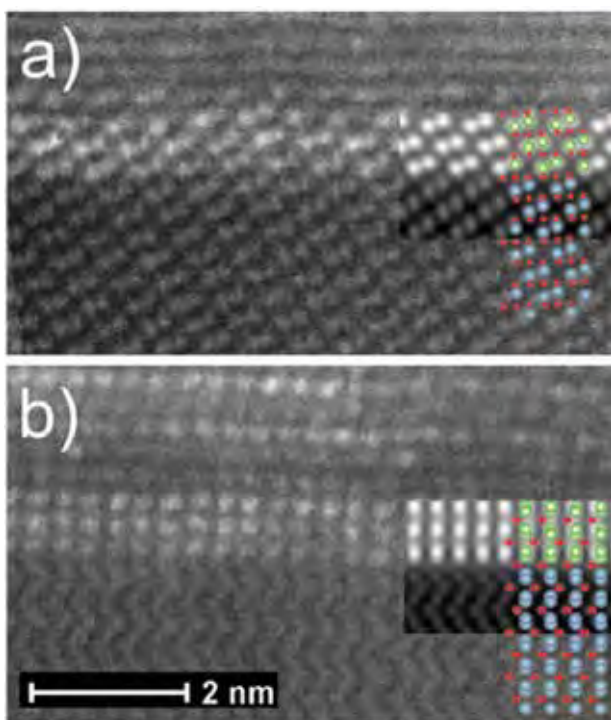
Fig. 4

Interface region in the <11-20> and <1-100> projection together with structural model and the STEM simulation of a three monolayer thick α-Ga₂O₃ layer.
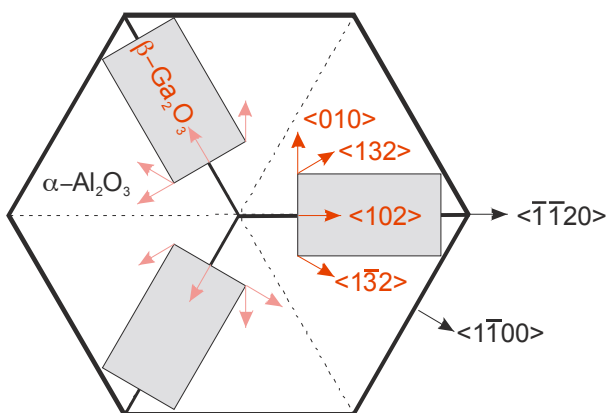
Fig. 5

Epitaxial relation between α-Al₂O₃ and of β-Ga₂O₃. The symmetry mismatch between the trigonal α-Al₂O₃ and monoclinic β-Ga₂O₃ leads to the formations of six rotational domains.

Structure of charge imbalanced interfaces between $K_xNa_{1-x}NbO_3$ and rare earth scandates

Interfaces between two insulating *perovskite*-type *oxide* materials (general formula: ABO_3) are known to exhibit a variety of properties which do not exist in the constituent bulk materials. For example, in the $LaAlO_3/SrTiO_3$ system, the formation of a two-dimensional electron gas (2DEG) at the interface has been observed [12] and devices, such as field-effect transistors have been demonstrated [13]. An even more interesting goal would be the realization of a 2DEG at the interface between a ferroelectric, polar oxide and a non-polar one. This would allow switching of the 2DEG by polarization reversal in the ferroelectric layer sharing the interface. However, understanding and exploitation of such interface effects demands next to a well-defined growth process also a detailed interface characterization.

A prerequisite for the realization of a 2DEG between a ferroelectric perovskite films and an insulating oxide substrate with charged-imbalanced interfaces is an atomically abrupt interface with an effective positive charge. However, as known from heterovalent semiconductor interfaces, interdiffusion and exchange of ions across the interface may lead to an electrically neutral interface. In collaboration with the group "Ferroelectric Oxide Layers" we studied thin, coherent films of $K_xNa_{1-x}NbO_3$ that have been epitaxially grown by liquid-delivery spin metal-organic chemical vapor deposition (MOCVD) and pulsed laser deposition (PLD) on several substrates (partially provided by the "Oxides/Fluorides" group of IKZ). We performed quantitative high-resolution scanning transmission electron microscopy high angle annular dark field imaging (STEM-HAADF, also known as STEM Z-contrast).

Our investigations reveal that structures of $NaNbO_3$ layers on rare-earth scandate substrates ($DyScO_3$ and $TbScO_3$) always exhibit an intermixing of ions of group A (Na and Dy/Tb) at the interface between film and substrate. As an example, a STEM-HAADF image of a $NaNbO_3$ film on a $DyScO_3$ substrate in the $[1-10]_o$ projection is shown in Fig. 6(a). Due to the high atomic number of Dy (Z = 66, indicated by blue balls) these ions are clearly visible and cause a high intensity in the HAADF image. In contrast, Na ions (Z = 11, indicated by yellow balls) provoke only a very low intensity. However, at the interface the intensity of atomic columns of group A ions cannot be attributed to the intensity of a pure Na column nor to that of a pure Dy column. Furthermore, if the structure is observed along the $[001]_o$ projection (see Fig. 6(b)) we found a regular arrangement of intermixed group A ions at the interface with a twofold periodicity along the $[1-10]_o$ direction. From these results we conclude that the A position at the interface is given by an intermixing of Na and Dy. The intermixing phenomenon with in-plane ordering of the group A ions has been observed

for structures grown by MOCVD (deposition at high oxygen partial pressure) as well as for PLD (deposition at low oxygen partial pressure) meaning that a possible presence of oxygen vacancies is not the driving force for the intermixing.

Instead, the intermixing of group A ions can be explained at least tentatively by considering the polar discontinuity at the interface between substrate and film. Due to the surface preparation before epitaxial growth rare-earth scandate substrates are ScO_2 terminated. Then the first monolayer of the film has to be NaO. These two adjacent layers have nominally the same charge (-1) resulting in a -1/-1 interface. This polar discontinuity at the interface can be at least reduced by a partial exchange of Na^{1+} ions by Dy^{3+} ions. In the case of 50/50 intermixing, as one might suppose from the in-plane ordering with the twofold periodicity of group A ions, this would lead to a charge neutral interlayer. A similar intermixing effect (although without the in-plane ordering) has been found for $K_xNa_{1-x}NbO_3$ films grown on TiO_2 terminated $SrTiO_3$ substrates. Also for this system the intermixing can be explained in terms of reducing the polar discontinuity at the interface between substrate and film.

So far epitaxially grown layers, i.e. $NaNbO_3$ layers on rare-earth scandate substrates and $K_xNa_{1-x}NbO_3$ films grown on $SrTiO_3$, exhibit interfaces which have negatively charged monolayers at the interface (e.g. 0/-1 interfaces), which would induce hole gases that are however immobile. We are therefore aiming to realize heterostructures where e.g. $NaNbO_3$ films are deposited on SrO-terminated $SrTiO_3$ substrates resulting nominally in a 0/+1 interface which in turn possibly leads to formation of a 2DEG.
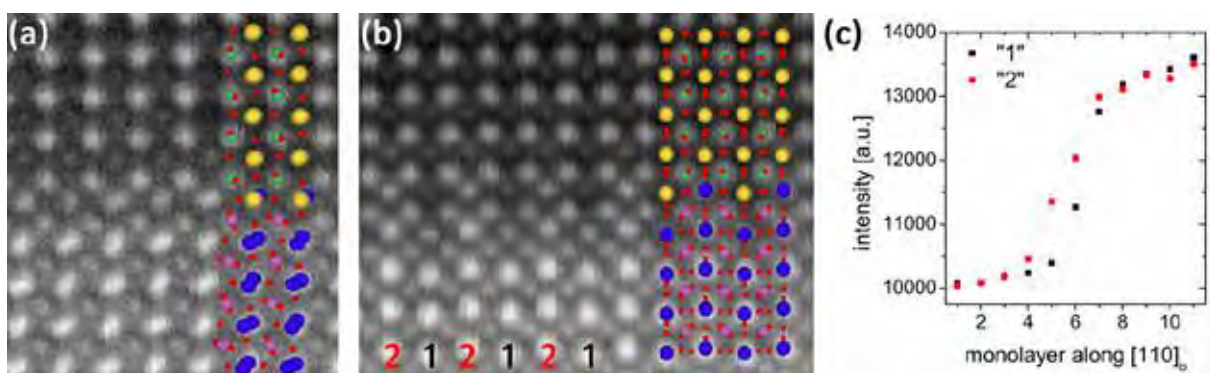
Fig. 6

STEM-HAADF images of the interface between a $NaNbO_3$ thin film grown on a $DyScO_3$ substrate seen along the (a) $[1\text{-}10]_o$ and (b) $[001]_o$ projection. Blue, purple, red, yellow and green balls denote Dy, Sc, O, Na and Nb atoms, respectively. (c) Intensity profiles across the interface of group A ions along the positions "1" and "2" (as indicated in image (b)).

Simulation & Characterization: **Electron Microscopy**

References

[1] T. Schulz, A. Nirschl, P. Drechsel, F. Nippert,
   T. Markurt, M. Albrecht, A. Hoffmann;
   Appl. Phys. Lett. 105 (2014) 181109

[2] J. Iveland, L. Martinelli, J. Peretti, J. S. Speck,
   C. Weisbuch;
   Phys. Rev. Lett. 110 (2013) 177406

[3] M. Binder, A. Nirschl, R. Zeisel, T. Hager,
   H.-J. Lugauer, M. Sabathil, D. Bougeard,
   J. Wagner, J. B. Galler;
   Appl. Phys. Lett. 103 (2013) 071108

[4] F. Bertazzi, M. Goano, X. Zhou, M. Calciati,
   G. Ghione, M. Matsubara, E. Bellotti;
   Appl. Phys. Lett. 106 (2015) 061112

[5] L. M. Foster, H. C. Stumpf;
   J. Am. Chem. Soc. 73 (1951) 1590

[6] R. Bruinsma, A.Zangwill;
   J. Physique 47 (1986) 2055

[7] S. Froyen, S.-H. Wei, A. Zunger;
   Phys. Rev. B 38 (1988) 10124

[8] R. Schewski, G. Wagner, M. Baldini, D. Gogova,
   Z. Galazka, T. Schulz, T. Remmele, T. Markurt,
   H. von Wenckstern, M. Grundmann, O. Bierwagen,
   P. Vogt, M. Albrecht;
   Appl. Phys. Express 8 (2015) 011101

[9] R. Huang, H. Hayashi, F. Oba, I. Tanaka;
   J. Appl. Phys. 101 (2007) 063526

[10] M. Becker, S. Christiansen, M. Albrecht,
   H.P. Strunk, H. Wawra;
   J. Crystal Growth 310 (2008) 3261

[11] J. Narayan, B. C. Larsion;
   J. Appl. Phys. 93 (2003) 278

[12] A. Ohtomo, H. Y. Hwang;
   Nature 427 (2004) 423

[13] B. Förg, C. Richter, J. Mannhart;
   Appl. Phys. Lett. 100 (2012) 053506

Simulation & Characterization:
Chemical & Thermodynamic Analysis

Head   PD Dr. habil. Detlef Klimm
Team   Dr. R. Bertram

Überblick

Auch im aktuellen Berichtszeitraum waren die Aktivitäten der unserer Querschnittgruppe hauptsächlich der Unterstützung der Züchtergruppen des Instituts gewidmet. In der Regel werden chemische (durch ICP-OES) oder thermische Analysen (z.B. durch DTA) auf Nachfrage durchgeführt. Ab diesem Jahr erfolgte jedoch eine engere Kooperation mit der Gruppe Galliumarsenid, weil das durch diese Gruppe betriebene Projekt TEMPO in beträchtlichem Umfange chemische Analysen erfordert. Dieses Projekt untersucht im Rahmen der EU-Verordnungen Reach – Registration, Evaluation, Authorisation and Restriction of Chemicals – und CLP- Classification, Labelling, Packaging- die Löslichkeit und das Gefährdungspotential von GaAs; weiter gehende Informationen finden sich im Bericht der Gruppe Galliumarsenid. Darüber hinaus war unsere Gruppe in verschiedene Aktivitäten zur Entwicklung von Referenzmaterialien zur chemischen Analytik involviert. Als Beispiele seien Y:ZrO$_2$ (durch die BAM organisierter internationaler Ringversuch) und Referenzgläser für Rastersonden (Geo.X unter Federführung des Naturkundemuseums Berlin) genannt. Zirkoniumdioxid (ZrO$_2$) ist wegen seiner herausragenden physikalischen und chemischen Eigenschaften ein bedeutender industrieller Werkstoff. So besitzt es einen extrem hohen Schmelzpunkt (2700°C), hohe Beständigkeit gegenüber Säuren und Basen, gutes elektrisches und thermisches Isolationsvermögen, sowie eine hohe Oberflächenhärte. Unter allen Oxidkeramiken zeigen solche auf ZrO$_2$-Basis die höchste Bruchzähigkeit; daher sind diese Materialien für eine Reihe von Hochtechnologien unverzichtbar, z.B. zur Herstellung piezoelektrischer Komponenten, Kondensatoren, Katalysatoren, Feststoff-Brennstoffzellen, oder als Zahnersatz. Für einige Anwendungen können schon Spuren von Verunreinigen die relevanten Eigenschaften und damit die Eignung signifikant beeinflussen; sogar die Kornstruktur von Keramiken wird durch die dort erfolgende Konzentrierung mancher Verunreinigungen modifiziert. Die exzellente Biokompatibilität von ZrO$_2$-Keramik kann nur genutzt werden, wenn Spurenverunreinigungen quantitativ spezifiziert sind. Folglich sind geeignete Referenzmaterialien zur Verwendung als Standards unverzichtbar. Die entsprechenden Anforderungen erwuchsen einer Initiative der H. C. Starck GmbH, Laufenburg, einem wichtigen Hersteller von High-Tech-Keramiken auf ZrO$_2$-Basis.

Seit Ende des Jahres 2014 erweitert eine „Laser-Flash-Apparatur" LFA 427 (NETZSCH, Deutschland) die experimentellen Möglichkeiten der Gruppe; sie gestattet die Messung der Wärmediffusivität oberhalb Zimmertemperatur bis 1575°C (Abbildung 1). Dazu muss bemerkt werden, dass unzureichender Wärmetransport weg von der Phasengrenze durch den aus einer Schmelze wachsenden Kristall (z.B. beim Czochralski-Prozess) eine häufige Ursache von Wachstumsinstabilitäten darstellt [1,2]. In der Vergangenheit erfolgten thermische Leitfähigkeitsmessungen für das IKZ wiederholt durch Dritte auf kommerzieller Basis. Dabei musste aber konstatiert werden, dass einige Materialien wie verschiedene TCOs und SrTiO$_3$ während der Messungen mit der umgebenden Atmosphäre reagieren. Zur Ermittlung zuverlässiger Resultate ist es daher essenziell, alle Messbedingungen zuverlässig selbst kontrollieren zu können.

Overview

Continuously, the efforts of the group are devoted to the scientific support of the crystal grower's groups of our institute. Usually chemical analysis (by ICP-OES) or thermoanalytic measurements (e.g. DTA) are performed on demand. In this year, however, a closer collaboration with the "Gallium Arsenide" group was established, because the project TEMPO addressed by this group requires a substantial workload of chemical analysis. The project investigates the solubility of gallium arsenide to be considered in the frame of the EU's Reach and CLP regulations. More information can be found in the "Gallium Arsenide" report. Besides, the group is involved in several activities that aim on the development of standard reference materials, such as Y:ZrO$_2$ (international round-robin, organized by BAM) or reference glasses (Geo.X, organized by Naturkundemuseum Berlin). Zirconium dioxide (ZrO$_2$) is an important industrial material with outstanding physical and chemical properties, including a high melting point (2700 °C), high resistance against acids and bases, low electric and thermal conductivity, high surface hardness. It has the highest fracture toughness of the oxide ceramics, and has therefore become essential in various fields of modern technology (manufacturing piezoelectricity components, capacitor, catalysts, solid electrolyte fuel battery, dentistry materials, etc.). In some applications, trace impurities can strongly affect the relevant properties and usefulness of zirconium dioxide, even grain boundary processes are affected by the concentration of trace elements.

The excellent biocompatibility of ZrO_2 ceramics is only useful if trace impurities of the material can be characterized quantitatively. Consequently, standard reference materials are for the validation of analytical methods indispensable. The requirements for better and reliable characterization of ZrO_2 were raised by H. C. Starck GmbH, Laufenburg, who is an important producer of advanced ceramics made of this material.

By the end of 2014, the experimental facilities where extended by a "Laser Flash Apparatus" LFA 427 (NETZSCH, Germany) which allows the measurement of thermal diffusivities between room temperature and 1575 °C (Figure 1). It should be noted that insufficient heat transport from the phase boundary through a crystal grown from the melt e.g. in a Czochralski process is a common reason for unstable growth [1,2]. In the past, measurements of the thermal conductivity were repeatedly performed by third parties on a commercial basis. We had to recognize, however, that some crystalline substances such as several TCOs and $SrTiO_3$ tend to react with the surrounding atmosphere during measurements. To achieve reliable results, it is essential to control all measurement conditions.

In the LFA 427 Laser Flash Apparatus the sample's bottom surface is exposed to the short pulse (typically <1 ms) of a Nd:YAG laser which generates heat. This heat dissipates to the top surface. The time dependent detector signal there is evaluated numerically according to different appropriate models and gives the thermal diffusivity a(T) which is related to the thermal conductivity by $\lambda(T) = a(T) \rho(T) c_p(T)$, where is the mass density and c_p is the specific heat capacity.

Results

This report focusses on some recent thermodynamic studies on $MgGa_2O_4$. Some details on the Czochralski growth are reported in the "Oxides/Fluorides" chapter of this annual report and in a first publication [3]. Although 2/3 of this material's cations are Ga^{3+}, and the melting point (1930°C) is 110 K higher compared to Ga_2O_3, it possesses higher stability upon the crystal growth process, with less significant evaporation. It is well known that that $MgGa_2O_4$ crystallizes in an inverse spinel structure [4], and it will be discussed here for the first time why just this crystal structure and entropic effects which are related to it might be responsible of the stabilization of $MgGa_2O_4$.
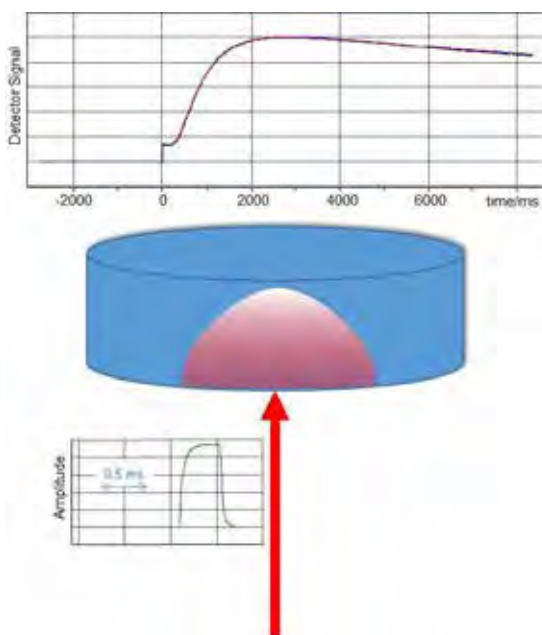
Fig. 1

The Principle of a LFA (Laser Flash Apparatus): The sample disc (blue) resides in a homogeneous temperature field and is illuminated from the bottom by a submillisecond laser pulse. The created additional heat dissipates to the sample's top surface where time-dependent signal is measured over several seconds by an infrared detector.
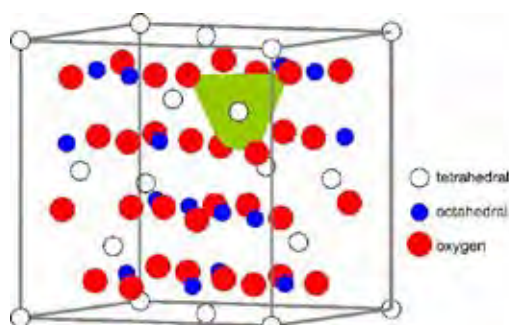
Fig. 2

One unit cell of the spinel structure contains 8 formula units $(A_{1-x}B_x)^{tet}(B_{2-x}A_x)^{oct}O_4$. Here the "normal" case (x=0) is shown.

In the cubic spinel structure where oxide ions set up a cubic dense packing, 1/8 of the tetrahedral sites and ½ of the octahedral sites are occupied by the metal ions. In the archetype spinel $MgAl_2O_4$, Mg^{2+} is tetrahedrally and Al^{3+} is octahedrally coordinated. In Figure 2 this means that Mg^{2+} sits on the white, and Al^{3+} on the blue positions. For some other spinels such as $MgGa_2O_4$, however, the 3-valent ion occupies the tetrahedral sites. The 50% remaining 3-valent ions and the 2-valent ions occupy the octahedral sites. Both extrema are called "normal" or "inverse", respectively. Crossovers are possible and are expressed by the "degree of inversion" of the spinel, which ranges from x = 0 (normal) to x=1 (inverse).

It turns out that x usually depends on the temperature T, because thermal activation of ion jumps between sites leads to randomization. Usually upon heating the inversion degree approaches for all spinels statistical ordering which is obtained for x = 2/3 (Figure 3).
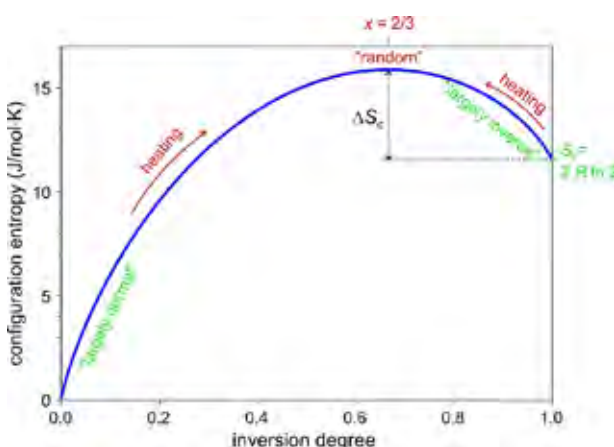
Fig. 3

The configuration entropy S_c of an AB_2O_4 spinel is minimum in the normal atomic distribution and significantly higher for the inverse configuration. At very high T, both configurations tend towards the statistical (random) distribution of A^{2+} and B^{3+} over the tetrahedral and octahedral sites.

Obviously, the degree of ion ordering and hence configuration entropy S_c changes with x, and can be expressed by

$$S_c = -R \left[x \ln x + (1-x) \ln(1-x) + x \ln \frac{x}{2} + (2-x) \ln \left(1 - \frac{x}{2}\right) \right]$$

for AB_2O_4 spinels [5]. The function $S_c(x)$ is plotted in Figure 3 and demonstrates the configuration entropy gain from inverse to random of ΔS_c = 4.35 J/(mol·K). It was discussed elsewhere that entropic contributions to the Gibbs free energy of spinel phases can be so large that even phases with positive formation energy, such as $Mg_3Ga_2GeO_8$ in the $MgGa_2O_4$–Mg_2GeO_4 system, or other intermediate oxides are stabilized [4,6].

A larger entropy results in a larger specific heat capacity, and vice versa,

$$\Delta S = \int \frac{c_p}{T} dT$$

and increments of cp can be measured by differential scanning calorimetry (DSC) where a larger c_p results in a shift of the DSC curve to the endothermal direction.
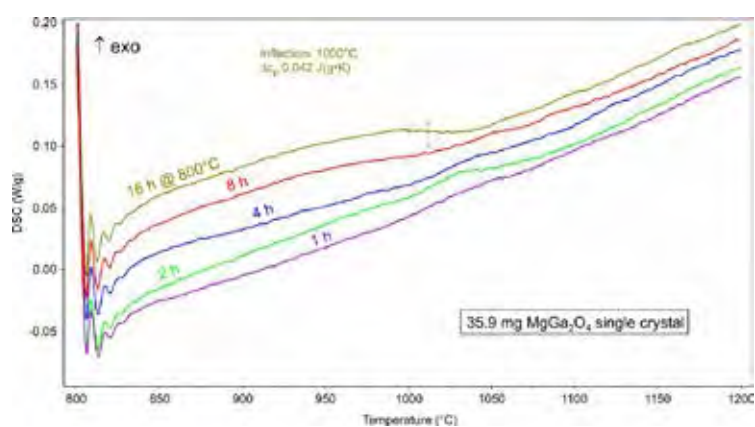
Fig. 4

5 subsequent DSC heating runs from 800°C with 30 K/min to 1200°C. Prior to each heating run, a holding period between 16 hours (top) to 1 hour (bottom) was introduced.

Figure 4 shows DSC curves where one piece of a $MgGa_2O_4$ single crystal was heated quickly (30 K/min, for a large signal) from 800°C to 1200°C. At the higher temperature the Mg^{2+} and Ga^{3+} ions can assumed to be in a random distribution which is reached quickly due to thermally activated diffusion steps. The inverse spinel structure which is stable at 800°C can be reached only if sufficient time is available. From Figure 4 it is obvious that for the shorter holding times at 800°C the inverse spinel is not obtained, and consequently no significant thermal effect is observed upon heating. Only after a long term annealing at 800°C the inverse spinel is formed, and randomization near 1000°C is connected with a DSC curve shift to the endothermal direction, because c_p rises.

The growing specific heat capacity results from the configuration entropy that becomes larger upon randomization of the spinel phase. It is not yet clear if additional contributions such as redistribution of charge contributes to the entropy.

It is intended to continue work on this topic because it is not only interesting from the theoretical point of view. The described entropic stabilization of a phase might be relevant for the development of future crystalline materials. Possibly here exists an analogy to novel "high-entropy" metallic alloys which show extremely structural, mechanical, and not at least chemical properties and are a hot topic of contemporary research [7].

References

[1] D. Schwabe, R. Uecker, M. Bernhagen, Z. Galazka;
J. Crystal Growth 335 (2011) 138–147

[2] C. Guguschev, D.J. Kok, Z. Galazka, D. Klimm,
R. Uecker, R. Bertram, M. Naumann, U. Juda,
A. Kwasniewski, M. Bickermann;
CrystEngComm 17 (2015) 3224–3234,
DOI: 10.1039/C5CE00095E

[3] Z. Galazka, D. Klimm, K. Irmscher, R. Uecker,
M. Pietsch, R. Bertram, M. Naumann, M. Albrecht,
A. Kwasniewski, R. Schewski, M. Bickermann;
Phys. Status Solidi A 212 (2015) 1455–1460, DOI:
10.1002/pssa.201431835

[4] K. Leinenweber, A. Navrotsky;
Phys. Chem. Minerals 16 (1989) 497–502

[5] H.S.C. O'Neill, A. Navrotsky;
American Mineralogist 68 (1983) 181–194

[6] D. Klimm, D. Schulz, S. Ganschow, Z. Galazka,
R. Uecker; Mater. Res. Soc. Symp. Proc. 1394 (2012),
DOI: 10.1557/opl.2012.257

[7] Ming-Hung Tsai, Jien-Wei Yeh;
Mater. Res. Lett. 2 (2014) 107–123

Simulation & Characterization:
Crystal Machining

Head   Dr. Uta Juda
Team   M. Imming, V. Lange, Th. Wurche

Überblick

Die Arbeit der Gruppe Kristallbearbeitung konzentriert sich vorrangig auf folgende Aufgaben: Der wichtigste Komplex ist die Probenpräparation für die routine-mäßige züchtungsbegleitende Diagnostik der im Haus gezüchteten Kristalle. Durch das breite Spektrum an zu bearbeitenden Materialien mit unterschiedlichen me-chanischen Eigenschaften und Dimensionen entstehen vielseitige Anforderungen an die Probengeometrie und an die Oberflächenqualität.

Eine andere Aufgabe ist die Herstellung von kristallo-graphisch genau orientierten Kristallkeimen und Sub-straten für den Einsatz in der Kristallzüchtung.

Ein weiterer Schwerpunkt liegt in der Entwicklung von Schneid- und Oberflächenpräparationstechnologien und -vorschriften, vor allem für neue am Institut ge-züchtete Kristallmaterialien, um auch hierbei den An-forderungen der Züchtung und der Materialdiagnostik gerecht zu werden.

Darüber hinaus werden auch anspruchsvolle Service- und Forschungsaufträge für die Industrie, für Hoch-schulen und außeruniversitäre Forschungseinrichtun-gen übernommen, die von der Lieferung bearbeiteter Proben bis hin zur Entwicklung von Technologien und die Erarbeitung der damit verbundenen Dokumen-tationen reicht.

Die Präparation von Halbleitermaterialien oder von Kristallen für optische Anwendungen, für die Diagnos-tik oder für den Einsatz als Substrate für die Epitaxie erfordert meist eine hohe Präzision in der Bearbeitung. Unabhängig von Material oder Verwendungszweck durchläuft jede Probe bzw. jeder Wafer bis zur Fertig-stellung verschiedene Arbeitsschritte wie Schneiden, Formatieren und Oberflächenpräparation mittels un-terschiedlicher Schleif-, Läpp- und Polierprozesse. Die dazu in unserer Gruppe zur Verfügung stehenden Methoden umfassen:

- *röntgenografisches Orientieren von Kristallen*
- *Trennschleifen mit verschiedenen Verfahren (Diamantdraht- und Diamant-Innentrennsägen)*
- *Flachschleifen mit Diamantwerkzeugen*
- *Läppen mit verschiedenen Läppmitteln (Aluminium-oxid, Ceriumoxid, Siliciumcarbid, Borcarbid, Diamant) in verschiedener Korngrößen und Suspensionen*
- *mechanisches und chemo-mechanisches Polieren*

- *Oberflächencharakterisierung mittels Lichtmikros-kopie, Atomkraftmikroskopie (AFM), Konfokalmikros-kopie (CFM) und Rasterelektronenmikroskopie (REM)*
- *Bestimmung von Wafergeometrie und Oberflächen-parametern wie Waferdicke, Durchbiegung, Ebenheit, Parallelität und Oberflächenrauigkeit*

Sowohl die vorhandene anlagentechnische Ausstattung als auch die hohe fachliche Kompetenz aller Mitarbeiter auf dem Gebiet der gesamten Probenpräparation er-möglichen es, kurzfristig und in hoher Qualität auf unterschiedliche Probenanforderungen zu reagieren.

Overview

The work of the group Crystal machining is focused on the following tasks: The most important complex is the sample preparation for routine characterization and material diagnostics of the in-house grown crystals. Special requirements on sample geometry and surface parameters such result from the wide spectrum of ma-terials with a wide range of mechanical properties and sample sizes.

Another major task is the preparation of crystallogra-phically oriented seed crystals and substrates with a very precise orientation for use in crystal growth.

A further complex is the development of cutting and surface preparation technologies and instructions for new materials grown at the institute in order to meet the requirements for crystal growth and material dia-gnostics.

Fourthly, ambitious service and research orders from industry, universities and other research institutes are fulfilled reaching from the supply of machined samples up to the development of technologies and related do-cumentations.

The preparation of crystals for semiconductor and op-tical applications, for diagnostics or as substrates for epitaxial processes requires high-precision machining. Whatever the application or material, each sample or wafer undergoes several stages during manufacture, which include formatting, slicing the wafer from the crystal and preparing the surface using different grin-ding, lapping and polishing techniques. The methods used in our group include:

Simulation & Characterization: **Crystal Machining**

- crystal orientation using x-ray techniques
- crystal cutting and wafering by different methods (single and multi diamond wire and inner diameter diamond sawing)
- wafer grinding with diamond tools
- wafer lapping with various abrasives (aluminum oxide, cerium oxide, silicon carbide, boron carbide, diamond) in different particle sizes and suspensions
- mechanical and chemo-mechanical polishing
- surface characterization by light microscopy, atomic force microscopy (AFM) confocal microscopy (CFM) and scanning electron microscopy (REM)
- determination of standard wafer geometry and surface parameters like thickness, bow, evenness, parallelism and roughness.

The available equipment and also high experience and competence of all staff members in the field of sample preparation enable us to achieve the varying requirements in short time and with high quality.

Results

One of the major tasks was the development of polishing and etching methods for nitrides and oxides grown at our institute, with main focus on Aluminum Nitride (AlN), Strontium Titanate (SrTiO$_3$) and Gallium Oxide (Ga$_2$O$_3$). The aim of this work is to prepare epi-ready surfaces for epitaxial growth using a suitable chemo-mechanical polishing (CMP) method including a high quality mechanical pre-polishing. CMP is a process of polishing and planarization of wafer surfaces with slurries containing abrasive particles and reactive chemicals. It represents the final step in wafer preparation. The important tasks of CMP are the removal of scratches, surface and sub-surface damages caused by the precedent mechanical polishing as well as the reduction of residual roughness and unevenness of the surface without leaving disturbing residual surface layers. A basic requirement for successful CMP is also a high-quality mechanical pre-polish because only few microns of the material should be removed by CMP, otherwise further geometric restraints cannot be maintained.

In 2013 the experiments focused on the polishing of Al-polar AlN surfaces have already been successful. As a result, scratch-free Al-polar surfaces of high quality with a roughness value of 0.05 nm (root mean square, RMS) over large areas could be. In order to proof whether the surface has epi-ready quality these samples were used as substrates for homo-epitaxial layer deposition. In the last time a good quality was obtained which suggests an excellent CMP. Based on these results and depending on the availability of samples, the mechanical and chemo-mechanical polishing of Al-polar surfaces will be optimized and also applied to other planes of AlN crystals. First experiments with m-plains were carried out.

Also an ambitious challenge has been the development of a preparation technology for some oxides again to achieve an epi-ready state. Different experiments on polishing with colloidal silica slurries aluminium oxide and cerium oxide were performed with varying process parameters like pressure, velocity of plate- and carrier rotation, polishing time, mixture of polishing fluid, flow rate of the slurry and the type of polishing pad. Also in these experiments it was found that the pH-value of the polishing slurry is a parameter which should not be underestimated. It becomes apparent that polishing works both in alkaline and acidic slurries, but it has a significant influence at the polishing time. First results show surfaces without scratches and no significant edge roll off.
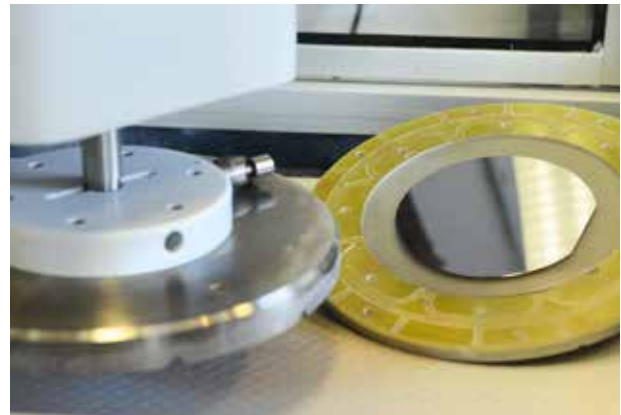
Appendix
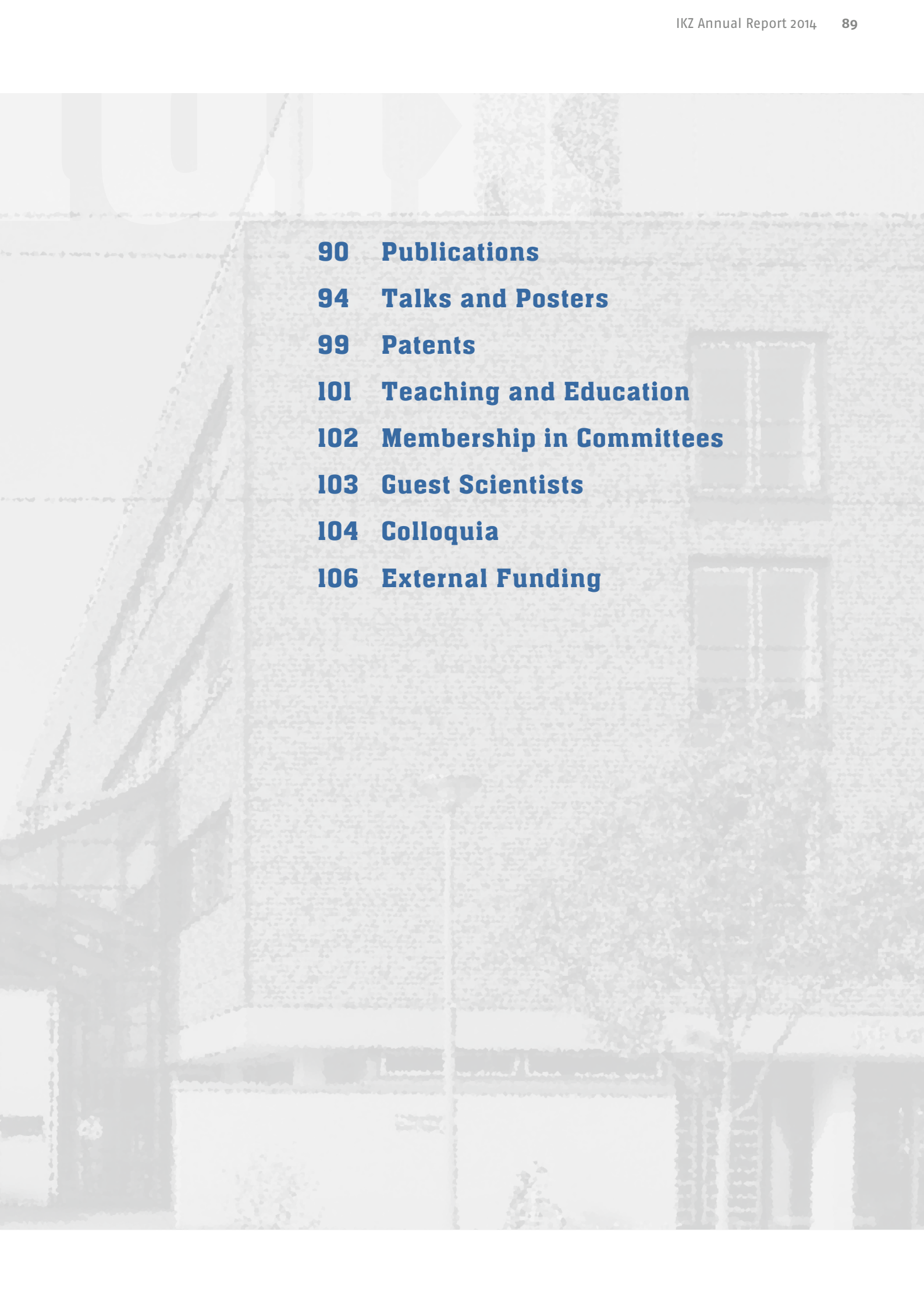
Appendix: **Publications**

Articles in books

M. Bickermann, T. Paskova; *Vapor Transport Growth of Wide Bandgap Materials;* in: P. Rudolph, Handbook of Crystal Growth, Handbook of Crystal Growth, Bulk Crystal Growth; 2nd Edition, Vol. 2 a (2014) 621-669

Z. Galazka; *Growth Measures to Achieve Bulk Single Crystals of Transparent Semiconducting and Conducting Oxides;* in: P. Rudolph, Handbook of Crystal Growth, Bulk Crystal Growth; 2nd Edition, Vol. 2 a (2014) 209 − 240

D. Klimm; *Phase Equilibria;* in: T. Nishinaga, Handbook of Crystal Growth, Fundamentals; 2nd Edition, Vol. 1 a (2014) 86 − 136

W. Miller; *Simulation of Epitaxial Growth by Means of Density Functional Theory, Kinetic Monte Carlo, and Phase Field Methods;* in: T. Nishinaga, Handbook of Crystal Growth, Fundamentals ; 2nd Edition, Vol. 1 a (2014) 522 − 559

A. Muiznieks, J. Virbulis, A. Lüdge, H. Riemann, N. Werner; *Floating Zone Growth of Silicon;* in: P. Rudolph, Handbook of Crystal Growth, Bulk Crystal Growth; 2nd Edition, Vol. 2 a (2014) 241 − 279

J. Winkler, M. Neubert; *Automation of Crystal Growth from Melt;* in: P. Rudolph, Handbook of Crystal Growth, Bulk Crystal Growth; 2nd Edition, Vol. 2 b (2014) 1143 − 1184

Articles in international peer reviewed journals

M. F. Acosta, S. Ganschow, D. Klimm, S. Serrano-Zabaleta, A. Larrea, R. I. Merino; *Directional solidification of the eutectic LiF−LiYF$_4$ using Bridgman and micro-pulling down techniques: Microstructural study and some properties;* J. Eur. Ceram. Soc. **34** (2014) 2051 − 2059

M. Albrecht, L. Lymperakis, J. Neugebauer; *Origin of the unusually strong luminescence of a-type screw dislocations in GaN;* Phys. Rev. B **90** (2014) 241201(R)

M. Albrecht, R. Schewski, K. Irmscher, Z. Galazka, T. Markurt, M. Naumann, T. Schulz, R. Uecker, R. Fornari, S. Meuret, M. Kociak; *Coloration and oxygen vacancies in wide band gap oxide semiconductors: Absorption at metallic nanoparticles induced by vacancy clustering − A case study on indium oxide;* J. Appl. Phys. **115** (2014) 053504

M. Baldini, D. Gogova, K. Irmscher, M. Schmidbauer, G. Wagner, R. Fornari; *Heteroepitaxy of Ga$_{2(1-x)}$In$_{2x}$O$_3$ layers by MOVPE with two different oxygen sources;* Cryst. Res. Technol. **49** (2014) 552 − 557

N. M. Barrière, J. A. Tomsick, S. E. Boggs, A. Lowell, C. Wade, M. Baugh, P. von Ballmoos, N. V. Abrosimov, L. Hanlon; *Developing a method for soft gammaray Laue lens assembly and calibration;* Nuclear Instruments & Methods in Physics Research Section A **741** (2014) 47 − 56

D. Braun, V. Scherer, C. Janowitz, Z. Galazka, R. Fornari, R. Manzke; *In-gap states of In$_2$O$_3$ single crystals investigated by scanningtunneling spectroscopy;* Phys. Status Solidi A **211** (2014) 59 − 65

M. Busch, E. Meyer, K. Irmscher, Z. Galazka, K. Gärtner, H. Winter; *Fast atom diffraction from a β−Ga$_2$O$_3$(100) surface;* App. Phys. Lett. **105** (2014) 051603

B. Cai, J. Schwarzkopf, E. Hollmann, M. Schmidbauer, M. O. Abdel-Hamed, R. Wördenweber; *Anisotropic ferroelectric properties of anisotropically strained epitaxial NaNbO$_3$ films;* J. Appl. Phys. **115** (2014) 224103

J. R. de Moraes, D. Klimm, V. L. Mazzocchi, C. B. Ramos Parente, S. Ganschow, S. L. Baldochi; *Thermal analysis and phase relations in the pseudobinary system La$_2$W$_2$O$_9$ − Li$_2$W$_2$O$_7$;* Cryst. Growth Des. **14** (2014) 5593−5598

U. Demirbas, R. Uecker, D. Klimm, B. Sumpf, G. Erbert; *Intra-cavity frequency-doubled Cr:LiCAF laser with 265mW continuous-wave blue (395−405 nm) output;* Opt. Commun. **320** (2014) 38 − 42

N. Deßmann, S.G. Pavlov, V. N. Shastin, R. Kh. Zhukavin, V. V. Tsyplenkov, S. Winnerl, M. Mittendorff, N. V. Abrosimov, H. Riemann, H.-W. Hübers; *Time-resolved electronic capture in n-type germanium doped with antimony;* Phys. Rev. B **89** (2014) 035205_1 − 035205_8

N. Dropka, A. Glacki, Ch. Frank-Rotsch; *GaAs − Vertical Gradient Freeze Process Intensification;* Cryst. Growth Des. **14** (2014) 5122 − 5130

N. Dropka, Ch. Frank-Rotsch; *Enhanced VGF-GaAs growth using pulsed unidirectional TMF;* J. Crystal Growth **386** (2014) 146 − 153

V. V. Emtsev, N. V. Abrosimov, V. V. Kozlovskii, G. A. Oganesyan; *Vacancy-donor pairs and their formation in irradiated n-Si;* Semiconductors **48** (2014) 1438−1443

V.V. Emtsev, N.V. Abrosimov, V.V. Kozlovskii, G.A. Oganesyan; *Electrical properties of diluted n- and p-Si$_{1-x}$Ge$_x$ at small x;* Semiconductors **48** (2014) 1552 − 1556

M. Feneberg, M. F. Romero, B. Neuschl, K. Thonke, M. Röppischer, C. Cobet, N. Esser, M. Bickermann, R. Goldhahn; *Temperature dependent dielectric function and reflectivity spectra of nonpolar wurtzite AlN;* Thin Solid Films **571** (2014) 502 − 505

Appendix: **Publications**

P. Fielitz, G. Borchardt, S. Ganschow, R. Bertram, R.A. Jackson, H. Fritze, K.-D. Becker; *Tantalum and niobium diffusion in single crystalline lithium niobate;* Solid State Ionics **259** (2014) 14 − 20

Ch. Frank-Rotsch, N. Dropka, A. Glacki, U. Juda; *VGF growth of GaAs utilizing heater-magnet module;* J. Crystal Growth **401** (2014) 702 − 707

O. B. Gadzhiev, P. G. Sennikov, A. I. Petrov, K. Kachel, S. Golka, D. Gogova, D. Siche; *The role of NH_3 and hydrocarbon mixtures in GaN pseudo-halide CVD: a quantum chemical study;* J. Mol. Model **20** (2014) 2473

Z. Galazka, R. Uecker, D. Klimm, K. Irmscher, M. Pietsch, R. Schewski, M. Albrecht, A. Kwasniewski, S. Ganschow, D. Schulz, C. Guguschev, R. Bertram, M. Bickermann, R. Fornari; *Growth, characterization, and properties of bulk SnO_2 single crystals;* Phys. Status Solidi A **211** (2014) 66 −73

Z. Galazka, K. Irmscher, R. Uecker, R. Bertram, M. Pietsch, A. Kwasniewski, M. Naumann, T. Schulz, R. Schewski, D. Klimm, M. Bickermann; *On the bulk β-Ga_2O_3 single crystals grown by the Czochralski method;* J. Crystal Growth **404** (2014) 184 − 191

Z. Galazka, R. Uecker, R. Fornari; *A novel crystal growth technique from the melt: Levitation-Assisted Self-Seeding Crystal Growth Method;* J. Crystal Growth **388** (2014) 61 − 69

R. Gergova, K. S. A. Butcher, P. W. Binsted, D. Gogova; *Initial results for epitaxial growth of InN on gallium oxide and improved Migration-Enhanced Afterglow Epitaxy growth on gallium nitride;* J. Vac. Sci. Technol. B **32** (2014) 031207-1 − 031207-5

A. Glacki, N. Dropka, Ch. Frank-Rotsch, U. Juda, M. Naumann; *Characterization of 4 in VGF-GaAs single crystals grown in a heater-magnet module;* J. Crystal Growth **397** (2014) 6 − 12

C. Guguschev, G. Calvert, S.Podowitz, A. Vailionis, A. Yeckel, R. S. Feigelson; *The application of floating dies for high speed growth of CsI single crystals by edge-defined film-fed growth (EFG);* J. Crystal Growth **404** (2014) 231 − 240

C. Guguschev, D. Klimm, F. Langhans, Z. Galazka, D. Kok, R. Uecker; *Top-seeded solution growth of $SrTiO_3$ crystals and phase diagram studies in the SrO-TiO_2 system;* CrystEngComm **16** (2014) 1735 - 1740

P. Gumann, O. Patange, C. Ramanathan, H. Haas, O. Moussa, M. L. W. Thewalt, H. Riemann, N. V. Abrosimov, P. Becker, H.-J. Pohl, K. M. Itoh, D. G. Cory; *Inductive measurement of optically hyper-polarized phosphorous donor nuclei in an isotopically enriched Silicon-28 crystal;* Phys. Rev. Lett **113** (2014) 267604_1 − 267604_5

W. Guo, J. Kundin, M. Bickermann, H. Emmerich; *A study of the step-flow growth of the PVT-grown AlN crystals by multi-scale modeling method;* CrystEng-Comm **16** (2014) 6564 − 6577

J. Haeberle, M. Richter, Z. Galazka, C. Janowitz, D. Schmeißer; *Resonant photoemission at the 01s threshold to characterize In_2O_3 single crystals;* Thin Solid Films **555** (2014) 53 − 56

C. Hartmann, A. Dittmar, J. Wollweber, M. Bickermann; *Bulk AlN growth by physical vapour transport;* Semicond. Sci. Technol. **29** (2014) 084002

W. S. Hwang, A. Verma, H. Peelaers, V. Protasenko, S. Rouvimov, H. Xing, A. Seabaugh, W. Haensch, C. Van de Walle, Z. Galazka, M. Albrecht, R. Fornari, D. Jena; *High-voltage field effect transistors with wide-bandgap β-Ga_2O_3 nanomembranes;* Appl. Phys. Lett. **104** (2014) 203111

K. Irmscher, M. Naumann, M. Pietsch, Z. Galazka, R. Uecker, T. Schulz, R. Schewski, M. Albrecht, R. Fornari; *On the nature and temperature dependence of the fundamental band gap of In_2O_3;* Phys. Status Solidi A **211** (2014) 54 − 58

D. Klimm; *Electronic materials with a wide band gap: recent developments;* IUCrJ **1** (2014) 281 − 290

E. Korhonen, F. Tuomisto, O. Bierwagen, J. S. Speck, Z. Galazka; *Compensating vacancy defects in Sn- and Mg-doped In_2O_3;* Phy. Rev. B **90** (2014) 245307

D. Linke, N. Dropka, F. Kiessling, R.-P. Lange, M. König, J. Krause, D. Sontag; *Characterization of a 75 kg mc-Si ingot grown in a KRISTMAG®-type G2-sized DS furnace;* Sol. Energy Mater. Sol. Cells **130** (2014) 652 − 660

K. L. Litvinenko, S. G. Pavlov, H.-W. Hübers, N. V. Abrosimov, C. R. Pidgeon, B. N. Murdin; *Photon assisted tunneling in pairs of silicon donors;* Phys. Rev. B **89** (2014) 235204_1 − 235204_5

V. Lopes-Oliveira, L. K. S. Herval, V. Orsi Gordo, D. F. Cesar, M. P. F. de Godoy, Y. Galvão Gobato, M. Henini, A. Khatab, M. Sadeghi, S. Wang, M. Schmidbauer; *Strain and localization effects in InGaAs(N) quantum wells: Tuning the magnetic response;* J. App. Phys. **116** (2014) 233703

M. Martens, F. Mehnke, C. Kuhn, C. Reich, V. Kueller, A. Knauer, C. Netzel, C. Hartmann, J. Wollweber, J. Rass, T. Wernicke, M. Bickermann, M. Weyers, M. Kneissl; *Performance characteristics of UV-C AlGaN-based lasers grown on on sapphire and bulk AlN substrates;* Photonics Technology Letters IEEE **26** (2014) 342 − 345

Appendix: **Publications**

Yu. I. Mazur, V. G. Dorogan, L. D. de Souza , D. Fan, M. Benamara, M. Schmidbauer, M. E. Ware, G. G. Tarasov, S-Q. Yu, G. E. Marques, G. J. Salamo; *Effect of AlGaAs cladding layers on the luminescence of GaAs/GaAs$_{1-x}$Bi$_x$ /GaAs heterostructures;* Nanotechnology **25** (2014) 035702

W. Miller, A. Popescu, G. Cantù; *Solidification of multicrystalline silicon–simulation of micro-structures;* J. Crystal Growth **385** (2014) 127 – 133

R. Mitdank, S. Dusari, C. Bülow, M. Albrecht, Z. Galazka, S. F. Fischer; *Temperature-dependent electrical characterization of exfoliated β-Ga$_2$O$_3$ micro flakes;* Phys. Status Solidi A **211** (2014) 543 – 549

A. Mogilatenko, H. Kirmse, O. Bierwagen, M. Schmidbauer, M.-Y. Tsai, I. Häusler, M. E. White, J. S. Speck; *Effect of heavy Ga doping on defect structure of SnO$_2$ layers;* Phys. Status Solidi A **211** (2014) 87 – 92

M. Nazarzadehmoafi, S. Machulik, F. Neske, V. Scherer, C. Janowitz, Z. Galazka, M. Mulazzi, R. Manzke; *Schottky contact by Ag on In$_2$O$_3$ (111) single crystals;* Appl. Phys. Lett. **105** (2014) 162104

M. Neubert, J. Winkler; *Nonlinear model-based control of the Czochralski process IV: Feedforward control and its interpretation from the crystal grower's view;* J. Crystal Growth **404** (2014) 210 – 222

S. G. Pavlov, N. Deßmann, V. N. Shastin, R. Kh. Zhukavin, B. Redlich, A. F. G. van der Meer, M. Mittendorff, S. Winnerl, N. V. Abrosimov, H. Riemann, H.-W. Hübers; *Terahertz stimulated emission from Silicon doped by hydrogenlike acceptors;* Phys. Rev. X **4** (2014) 021009_1 – 021009_7

P. Petrov, W. Miller; *Fast kinetic Monte Carlo simulation and statistics of quantum dot arrays;* Surf. Sci. **621** (2014) 175 – 183

J. Philippen, C. Guguschev, D. Klimm; *Single crystal fiber growth of cerium doped strontium yttrate, SrY$_2$O$_4$: Ce^3+;* arXiv preprint (2014) arXiv:1401.7578

G. Pica, G. Wolfowicz, M. Urdampilleta, M. L. W. Thewalt, H. Riemann, N. V. Abrosimov, P. Becker, H.-J. Pohl, J. J. L. Morton, R. N. Bhatt, S. A. Lyon, B. W. Lovett; *Hyperfine Stark effect of shallow donors in silicon;* Phys. Rev. B **90** (2014) 195204_1 – 195204_10

H.-J. Rost, R. Menzel, H. Riemann, M. Wuenscher, S. Haufe; *Improvement of the growth stability for large diameter Si-float zone crystals by controlling the gas flow;* Phys. Status Solidi A **211** (2014) 2471–2474

E. Rotunno, M. Albrecht, T. Markurt, T. Remmele, V. Grillo; *Three dimensional analysis of composition in solid alloys by variable probe in scanning transmission electron microscopy;* Ultramicroscopy **146** (2014) 62 – 70

M. Sawicka, G. Muziol, H. Turski, A. Feduniewicz-Żmuda, M. Kryśko, S. Grzanka, E. Grzanka, J. Smalc-Koziorowska, M. Albrecht, R. Kucharski, P. Perlin, C. Skierbiszewski; *Semipolar (20ˉ21) GaN laser diodes operating at 388 nm grown by plasma-assisted molecular beam epitaxy;* J. Vac. Sci. Technol. B **32** (2014) 02C115

D. G. Schlom, L.-Q. Chen, C. J. Fennie, V. Gopalan, D. A. Muller, X. Pan, R. Ramesh, R. Uecker; *Elastic strain engineering of ferroic oxides;* MRS Bull. **39** (2014) 118 – 130

M. Schmidbauer, J. Sellmann, D. Braun, A. Kwasniewski, A. Duk, J. Schwarzkopf; *Ferroelectric domain structure of NaNbO$_3$ epitaxial thin films grown on (110) DyScO$_3$ substrates;* Phys. Status Solidi RRL **8** (2014) 522 –526

J. Schmidtbauer, R. Bansen, R. Heimburger, T. Teubner, T. Boeck; *MBE Growth of Germanium Nanowires along ⟨110⟩;* J. Cryst. Growth **406** (2014) 36 – 40

T. Schulz, A. Duff, T. Remmele , M. Korytov, T. Markurt, M. Albrecht, L. Lymperakis, J. Neugebauer, C. Chèze, C. Skierbiszewski; *Separating strain from composition in unit cell parameter maps obtained from aberration corrected high resolution transmission electron microscopy imaging;* J. Appl. Phys. **115** (2014) 033113 – 033122

T. Schulz, A. Nirschl, P. Drechsel, F. Nippert, T. Markurt, M. Albrecht, A. Hoffmann; *Recombination dynamics in In$_x$Ga$_{1-x}$N quantum wells – Contribution of excited subband recombination to carrier leakage;* Appl. Phys. Lett. **105** (2014) 181109

J. Schwarzkopf, D. Braun, M. Schmidbauer, D. Braun, R. Wördenweber; *Ferroelectric domain structure of anisotropically strained NaNbO$_3$ epitaxial thin films;* J. Appl. Phys. **115** (2014) 204105

T. Sekiguchi, A. M. Tyryshkin, S. Tojo, E. Abe, R. Mori, H. Riemann, N. V. Abrosimov, P. Becker, H.-J. Pohl, J. W. Ager, E. E. Haller, M. L. W. Thewalt, J. J. L. Morton, S. A. Lyon, K. M. Itoh; *Host isotope mass effects on the hyperfine interaction of group-V donors in silicon;* Phy. Rev. B **90** (2014) 121203(R)_1 – 121203(R)_5

J. Sellmann, J. Schwarzkopf, A. Kwasniewski, M. Schmidbauer, D. Braun, A. Duk; *Strained ferroelectric NaNbO$_3$ thin films: Impact of pulsed laser deposition growth conditions on structural properties;* Thin Solid Films **570** (2014) 107 – 113

Appendix: **Publications**

A. J. Sigillito, H. Malissa, A. M. Tyryshkin, H. Riemann, N. V. Abrosimov, P. Becker, H.-J. Pohl, M. L. W. Thewalt, K. M. Itoh, J. J. L. Morton, A. A. Houck, D. I. Schuster, S. A. Lyon; *Fast, low-power manipulation of spin ensembles in superconducting microresonators;* Appl. Phys. Lett. **104** (2014) 222407_1 – 222407_4

T. Suski, T. Schulz, M. Albrecht, X. Q. Wang, I. Gorczyca, K. Skrobas, N. E. Christensen, A. Svane; *The discrepancies between theory and experiment in the optical emission of monolayer In(Ga)N quantum wells revisited by transmission electron microscopy;* Appl. Phys. Lett. **104** (2014) 182103 – 182106

G. Wagner, M. Baldini, D. Gogova, M. Schmidbauer, R. Schewski, M. Albrecht, Z. Galazka, D. Klimm, R. Fornari; *Homoepitaxial growth of β-Ga$_2$O$_3$ layers by metal-organic vapor phase epitaxy;* Phys. Status Solidi A **211** (2014) 27 – 33

G. Wolfowicz, M. Urdampilleta, M. L. W. Thewalt, H. Riemann, N. V. Abrosimov, P. Becker, H.-J. Pohl, J. J. L. Morton; *Conditional control of donor nuclear spins in Silicon using stark shifts;* Phys. Rev. Lett. **113** (2014) 157601_1 – 157601_5

M. Woll, M. Burianek, D. Klimm, S. Gorfman, M. Mühlberg; *Characterization of (Bi$_{0.5}$Na$_{0.5}$)$_{1-x}$Ba$_x$TiO$_3$ grown by the TSSG method;* J. Crystal Growth **401** (2014) 351 – 354

Articles in conference proceedings

R. Bansen, R. Heimburger, J. Schmidtbauer, T. Teubner, T. Boeck; *Solution Growth of Crystalline Si on Glass;* Conference Proceedings of the European Photovoltaic Energy Conference and Exhibition (29th EU PVSEC) (2014) 1908 – 1911

N. Dropka, Ch. Frank-Rotsch; *Enhanced VGF growth of single- and multi-crystalline semiconductors using pulsed TMF;* Proceedings of the International Scientific Colloquium "Modelling for Electromagnetic Processing" (MEP 2014), Leibniz University of Hannover (2014) 79 – 85

E. Korhonen, F. Tuomisto, O. Bierwagen, J. S. Speck, M. E. White, Z. Galazka; *Vacancy complexes in Sb-doped SnO$_2$;* AIP Conf. Proceedings **1583** (2014) 368

D. Gogova, G. Wagner, M. Baldini, M. Schmidbauer, K. Irmscher, R. Schewski, Z. Galazka, M. Albrecht, R. Fornari; *Structural properties of Si-doped β-Ga$_2$O$_3$ layers grown by MOVPE;* J. Crystal Growth, Proceedings of 17th International Conference on Crystal Growth and Epitaxy (ICCGE-17) **401** (2014) 665 – 669

D. Klimm, J. Philippen, T. Markurt, A. Kwasniewski; *Ce^{3+}:CaSc$_2$O$_4$ Crystal Fibers for Green Light Emission: Growth Issues and Characterization;* MRS Proceedings, Symposium Solid-State Chemistry of Inorganic Materials (Mater. Res. Soc. Symp. Proc.) **1655** (2014)

R. Menzel, H. Riemann, N. Abrosimov; *Numerical model for Si single crystal growth from melt in a Si granular bed;* Proceedings of the International Scientific Colloquium „Modelling for Electromagnetic Processing" (MEP2014), Leibniz University of Hannover (2014) 465 – 469

S. Richter, M. Werner, M. Schley, F. Schaaff, H. Riemann, H.-J. Rost, F. Zobel, R. Kunert, P. Dold, Ch. Hagendorf; *Influence of slim rod material properties to the Siemens feed rod and the float zone process;* Proceedings of the 4th International Conference on Crystalline Silicon Photovoltaics (SiliconPV 2014) Energy Procedia **55** (2014) 596 – 601

R. Uecker; *The historical development of the Czochralski method;* J. Crystal Growth, Proceedings of 17th International Conference on Crystal Growth and Epitaxy (ICCGE-17) **401** (2014) 7 – 24

M. Wünscher, R. Menzel, H. Riemann, A. Lüdge; *Combined 3D and 2.5D modeling of the floating zone process with Comsol Multiphysics;* J. Crystal Growth, The 7th International Workshop on Modeling in Crystal Growth **385** (2014) 100 – 105

Other publications

R. Bertram, S. Ganschow; Dotierungen in Saphir-Kristallen; Zeitschrift für anorganische und allgemeine Chemie **640** (2014) 2406

R. Bertram, S. Ganschow; Chemische Analyse von Saphir-Kristallen; GIT Labor-Fachzeitschrift **58** (2014) 42 – 43

Appendix: **Talks and Posters**

Invited talks at national and international conferences

M. Albrecht; *Strain relaxation and dislocation formation in epitxial growth of AlGaN on GaN(0001);* ISGN 5, 5th International Symposium on Growth of III-Nitrides; Atlanta, Georgia, USA; May 2014

M. Albrecht; *Aberration Corrected High Resolution TEM Characterisation of III-Nitrides Materials and Devices;* Conferences on Modern Materials and Technologies, Forum on New Materials; Montacatini, Italy; June 2014

M. Albrecht; *Atomic Resolution Transmission Electron Microscopy Studies of III-Nitride Nanostructures;* START 2014; Kiev, Ukraine; June 2014

M. Albrecht; *The anti-surfactant effect of Si in GaN epitaxy;* The International Workshop on Nitride Semiconductors; Wrocław, Poland; August 2014

M. Bickermann; *Seeded Bulk AlN Growth by the Physical Vapor Transport Method;* IWN2014-Konferenz; Wroclaw, Polen; August 2014

M. Bickermann; *Growth of AlN bulk crystals for AlGaN-based devices:* M. Bickermann, A. Dittmar, C. Hartmann, K. Irmscher, S. Kollowa,, A. Kwasniewski, T. Schulz, F. Langhans, T. Neugut, U. Juda, J. Wollweber, A. Knauer, M. Weyers, C. Reich, F. Mehnke, C. Kuhn, M. Martens, T. Wernicke, M. Kneissl; E-MRS Frühjahrs-tagung (Symposium W); Lille, Frankreich; May 2014

T. Boeck; *Growth of Si- and Ge-Nanocrystals;* 22. DGK Jahrestagung; Berlin; March 2014

Ch. Frank-Rotsch; *Enhancement of GaAs VGF process by using traveling magnetic fields;* E-MRS Spring Meeting; Lille, France; May 2014

Ch. Frank-Rotsch; *HP-Ge crystal growth for GERDA and growth of 4-inch germanium crystals by VGF in a hea-ter-magnet-module:* Ch. Frank-Rotsch, N.V. Abrosimov, M. Czupalla, J. Fischer, K. Imscher, U. Juda, W. Miller; 2nd workshop on germanium detectors and technolo-gies, Muenster University Center (MUC), The University of South Dakota; USA; September 2014

Ch. Frank-Rotsch; Panel Discussion on Crystal Growth (60'), Conveners: Dongming Mei, Christiane Frank-Rotsch, Guojian Wang, Elaine Roth; 2nd workshop on germanium detectors and technologies, 14-17 Sep-tember 2014, Muenster University Center (MUC), The University of South Dakota, USA

Z. Galazka; *Bulk single crystals and properties of trans-parent semiconducting oxides;* 2014 MRS Fall Meeting & Exhibit; Boston, Massachusetts, USA; November/December 2014

Z. Galazka; *Czochralski growth, characterization and properties of β-Ga$_2$O$_3$ single crystals;* TCO 2014; Leipzig, Germany; September/October 2014

Z. Galazka; *Bulk Single Crystals of Transparent Semi-conducting Oxides: Growth and Properties;* 6th In-ternational Workshop on Crystal Growth Technology; Berlin, Germany; June 2014

D. Gogova; *Gallium Oxide – A Newly Rediscovered Wide Bandgap Semiconductor:* D. Gogova, G. Wagner, M. Baldini, K. Irmscher, M. Albrecht, R. Schewski, M. Schmidbauer, A. Kwasniewski, Z. Galazka; Collaborative Conference on Crysral Growth, Recent Advances in Growth of Wide Bandgap Materials Workshop; Pukhet, Tailand; November 2014

C. Hartmann; *Growth and Characterization of Bulk AlN Crystals:* C. Hartmann, J. Wollweber, S. Kollowa, A. Dittmar, K. Irmscher, F. Langhans, M. Naumann, A.Kwasniewski, M. Bickermann; ISGN-5, 5th Inter-national Symposium on Growth of III-Nitrides; Atlanta, Georgia, USA; May 2014

K. Irmscher; *Point defect characterization of bulk AlN crystals: Tri-carbon defect related UV absorption;* K. Irmscher, C. Hartmann, S. Kollowa, A. Dittmar, M. Naumann, F. Langhans, T. Neugut, A. Kwasniewski, M. Pietsch, J. Wollweber, M. Bickermann; Materials Research Society Fall Meeting; Boston USA; November/December 2014

D. Klimm; *Strain engineering with perovskite layers – the quest for substrate crystals;* 22. Annual Conference of the German Crystallographic Society (DGK); Berlin; March 2014

T. Markurt; *A Predictive Model for Plastic Strain Relaxation in (0001)-Oriented III-Nitride Wurtzite Film;* Materials Research Society Fall Meeting; Boston, USA; November/December 2014

N.V. Abrosimov; *Monoisotopic single crystalline Silicon: crystal growth and application;* X International Confe-rence "Silicon 2014"; Irkutsk, Russia; July 2014

M. Neubert, J. Winkler; *Schmelzkristallzüchtung – von der Systemanalyse zur modellbasierten Regelung;* DKT 2014, DGKK Jahrestagung; Halle, Germany; March 2014

J. Schmidtbauer; *MBE Growth Behavior of Si and Ge Nanowires in Comparison;* EMN Open Access Week; Chengdu, China; September 2014

T. Schulz; *Composition and ordering in nominal InN/GaN superlattices – towards understanding their optical properties;* The International Workshop on Nitride Semiconductors; Wrocław, Poland; August 2014

J. Schwarzkopf; *Epitaxial growth of strained, ferroelec-tric oxide films;* DKT 2014; Halle, Germany; March 2014

D. Siche; *The role of chemical vapour transport for the growth of wide bandgap compound semiconductors at IKZ;* Naturwissenschaftstag der BTU; Senftenberg, Germany; June 2014

Appendix: **Talks and Posters**

Invited seminars at national and international institutions

R. Bansen; *Solution Growth of Crystalline Si on Glass*; IMEC; Leuven, Belgium; April 2014

R. Bansen; *Solution Growth of Crystalline Si*; R. Bansen, C. Ehlers, Th. Teubner, T. Boeck; Fraunhofer ISE; Freiburg, Germany; July 2014

R. Bansen, T.Boeck; *Solution Growth of Si on glass*; CHEETAH webinar; February 2014

R. Bansen, T.Boeck; *Si on low cost substrates*; CHEETAH webinar; May 2014

R. Bansen, T.Boeck; *Deposition of Si onto ultra-thin Si substrates*; CHEETAH webinar; November 2014

M. Bickermann; *Das Leibniz-Institut für Kristallzüchtung (IKZ) und Aktivitäten im Bereich AlN*; Kurzvortrag im Seminar der AG R. Zahn (Halbleiterphysik); Institut für Physik, TU Chemnitz, Germany; June 2014

M. Bickermann; *Aktivitäten in Forschung (am IKZ) und Lehre (an der TUB)*; Vortrag auf der 2. Klausurtagung der Hochschullehrer des Instituts für Chemie der TU Berlin; Döllnsee/Schorfheide (Templin), Germany; February 2014

M. Bickermann; *Aktivitäten in Forschung (am IKZ) und Lehre (an der TUB)*; Vortrag auf der 3. Klausurtagung der Hochschullehrer des Instituts für Chemie der TU Berlin; Döllnsee/Schorfheide (Templin), Germany; July 2014

D. Gogova; *MOVPE Growth and Characterization of β-phase Gallium Oxide Epitaxial Layers*; D. Gogova, G. Wagner, M. Baldini, K. Irmscher, M. Albrecht, R. Schewski, M. Schmidbauer, Z. Galazka; Seminar at PDI; Berlin, Germany; November 2014

C. Hartmann; *Aluminiumnitrid Volumenkristallzüchtung mittels physikalischen Gasphasentransports*; Fraunhofer Institut für Angewandte Festkörperphysik Freiburg (IAF) im FMF Seminar „Spezielle Probleme der Festkörperphysik und der Materialforschung"; Freiburg, Germany; Januar 2014

C. Hartmann; *Züchtung und Charakterisierung von Aluminiumnitrid – Volumenkristallen*; Kolloquium – TU Clausthal, Institut für Energieforschung und Physikalische Technologien; Clausthal, Germany; September 2014

K. Irmscher; *Point defects in AlN*; Kolloquim AG Zahn, TU Chemnitz, Germany, June 2014

K. Irmscher; *A highly abundant tri-carbon defect dominates the detrimental ultraviolet absorption at 4.7 eV in AlN*; Kolloqium AG Kneissl, Technische Universität Berlin, Germany, November 2014

K. Kachel; *Cyano based GaN growth*; Naturwissenschaftstag der BTU; Senftenberg, Germany; June 2014

F. Ringleb; *CIGS-Mikrokonzentrator-Solarzellen*; F. Ringleb, J. Schmidtbauer, R. Bansen, T. Boeck; Helmholtz-Zentrum Berlin für Materialien und Energie, Berlin, Germany; May 2014

F. Ringleb; *Herstellung und Charakterisierung von In-Mikrotröpfchen als Precursormaterial für Chalcopyritsolarzellen*; F. Ringleb, Th. Teubner, T. Boeck; Freie Universität Berlin, Berlin, Germany; October 2014

J. Sellmann; *Impact of PLD-growth conditions on the structural and piezo/ferroelectric properties of strained alkaline niobates*; Universität Leipzig, Institut für Experimentelle Physik II; Leipzig, Germany; June 2014

G. Wagner; *Epitaxial growth of β-Ga$_2$O$_3$ by metal-organic vapor-phase epitaxy*; Institutskolloquium Ferdinand-Braun Institut, Leibniz-Institut für Höchstfrequenztechnik; Berlin, Germany; March 2014

G. Wagner; *Epitaxial growth of β-Ga$_2$O$_3$ by metal-organic vapor-phase epitaxy*; Institutskolloquium, Technische Universität Berlin, Institut für Festkörperphysik; Berlin, Germany; June 2014

Oral contributions at national and internationals conferences and workshops

M. Bickermann; *Vom AlN-Kristall zum UV-C-Laser: Erste Ergebnisse zu Wafering, Epitaxie und Bauelementherstellung auf AlN-Substraten des IKZ*; Hauptvortrag im Arbeitskreis „Massive Halbleiterkristalle", DGKK, Universität Freiberg/Sachsen, Germany; October 2014

N. Dropka; *Enhanced VGF-GaAs and DS-Si growth using pulsed down-outward TMF*; N. Dropka, Ch. Frank-Rotsch; International Scientific Colloquium: Modelling for Electromagnetic Processing (MEP 14); Hanover, Germany; September 2014

N. Dropka; *Enhanced VGF-GaAs growth using pulsed unidirectional TMF*; N. Dropka, Ch. Frank-Rotsch; DKT 2014 – DGKK Jahrestagung; Halle, Germany; March 2014

N. Dropka; *Enhanced growth of single- and multicrystalline semiconductors using pulsed travelling magnetic fields*; N. Dropka, Ch. Frank-Rotsch; 11th World Congress on Computational Mechanics (WCCM XI), 5th European Conference on Computational Mechanics (ECCM V), 6th European Conference on Computational Fluid Dynamics (ECFD VI); Barcelona, Spain; July 2014

Appendix: **Talks and Posters**

T. Ervik; *Dislocation developments in multicrystalline silicon ingots solidified under the influence of travelling magnetic fields:* T. Ervik, U. Juda, J. Walter, F. M. Kießling; DGKK-Arbeitskreis Herstellung und Charakterisierung von massiven Halbleitern; Freiberg, Germany; October 2014

T. Ervik; *Dislocation developments in a multicrystalline silicon ingot solidified under the influence of travelling magnetic fields:* T. Ervik, U. Juda, J. Walter, F. M. Kießling; E-MRS Spring Meeting 2014; Lille, France; May 2014

T. Ervik; *Dislocation formation in quasi-mono-crystalline silicon for solar cells:* T. Ervik, G. Stokkan, T. Buonassisi, Ø. Mjøs , O. Lohne; DKT 2014 – DGKK Jahrestagung; Halle, Germany; March 2014

A. Glacki; *Prozessintensivierung der VGF-GaAs Züchtung mithilfe von Wandermagnetfeldern:* A. Glacki, Ch. Frank-Rotsch, U. Juda, A. Kwasniewski, M. Naumann; DGKK-Arbeitskreis Herstellung und Charakterisierung von massiven Halbleitern; Freiberg, Germany; October 2014

C. Guguschev; *SrTiO$_3$ crystal growth activities at the IKZ;* Deutsch-Französischer Oxidkristall-/Dielektrika-/Laserkristall-Workshop; Idar-Oberstein, Germany; September 2014

K. Irmscher; *Electrical properties of In$_2$O$_3$ single crystals: distinction between surface and bulk conductivity:* K. Irmscher, M. Pietsch, W. Troeder, Z. Galazka; DPG-Frühjahrstagung 2014; Dresden, Germany; March/April 2014

F. Kießling; *Direct and sensitive analysis of metals contaminating the edge zone of directionally solidified silicon:* S. Meyer, W. Kwapil, A. Zuschlag, Frank M. Kießling, M. Schumann, St. Riepe; DKT 2014 – DGKK Jahrestagung; Halle, Germany; March 2014

F. Kießling; *Influence of Crucible and Coating Materials on the Quality of Directionally Solidified Silicon:* St. Riepe, S. Meyer, F. M. Kießling, M. Schummann, W. Kwapil; DKT 2014 – DGKK Jahrestagung; Halle, Germany; March 2014

S. Kollowa; *Si-dotierte AlN-Volumenkristalle:* S. Kollowa , A. Dittmar, C. Hartmann, K. Irmscher, F. Langhans, M. Pietsch, T. Schulz, J. Wollweber, M. Bickermann; DGKK-Arbeitskreis Massive Halbleiterkristalle; Freiberg, Germany; November 2014

M. Neubert, J. Winkler; *Schmelzkristallzüchtung – von der Systemanalyse zur modellbasierten Regelung;* Deutsche Kristallzüchtungstagung; Halle, Germany; March 2014

F. Ringleb, T. Boeck; CIGS/CZTS – *Approaches towards new Microconcentrator Solar Cells;* CHEETAH webinar; November 2014

H.-J. Rost; *Improvement of the growth stability for large diameter Si- Float zone crystals by controlling the gas flow:* H.-J. Rost, R. Menzel, H. Riemann, M. Wuenscher, S. Haufe; EMRS 2014; Lille, France; May 2014

H.-J. Rost; *Influence of slim rod material properties to the Siemens feed rod and the float zone process:* S. Richter, M. Werner, M. Schley, F. Schaaff, H. Riemann, H.-J. Rost, F. Zobel, R. Kunert, P. Dold, C. Hagendorf; 4th International Conference on Silicon Photovoltaics, SiliconPV 2014; Netherlands; March 2014

R. Schewski; *Stabilization of α-Ga$_2$O$_3$ Interlayer in the Growth of β-Ga$_2$O$_3$ on Sapphire by PLD, MBE and MOCVD:* R. Schewski, G. Wagner, D. Gogova, M. Baldini, T. Remmele, T. Markurt, T. Schulz, O. Bierwagen, P. Vogt, H. von Wenckstern, M. Grundmann, M. Albrecht; MRS Fall Meeting & Exhibit; Boston, Massachusetts, USA; November/December 2014

R. Schewski; *MOCVD grown homoepitaxial β-Ga$_2$O$_3$ layer studied by Transmission Electron Microscopy:* R. Schewski, G. Wagner, M. Baldini, D. Gogova, T. Markurt, T. Schulz, T. Remmele, Z. Galazka, R. Uecker, M. Albrecht; MRS Fall Meeting & Exhibit; Boston, Massachusetts, USA; November/December 2014

R. Schewski; *MOCVD grown homo and heteroepitaxial β-Ga$_2$O$_3$ layer studied by transmission electron microscopy:* R. Schewski, M. Albrecht, G. Wagner, M. Baldini, D. Gogova, Z. Galazka, R. Uecker; DPG Spring Meeting; Dresden, Germany; March/April 2014

J. Schmidtbauer; *MBE Growth and Characterization of Ge Nanowires*; Projekttreffen Kooperationsprojekt Yerevan State University PDI-IKZ, Yerevan State University; Yerevan, Armenia; April 2014

J. Schwarzkopf; *Ferroelectric domains in anisotropically strained (K,Na)NbO$_3$ thin films;* University of Groningen, Faculty of Mathematics and Natural Sciences; Netherlands; June 2014

J. Schwarzkopf; *Epitaxial growth of strained (K,Na)NbO$_3$ films;* University Potsdam, Institute of Physics & Astronomy; Potsdam, Germany; October 2014

J. Schwarzkopf; *Ferroelectric domains in anisotropically strained (K,Na)NbO$_3$ thin films;* MRS Spring Meeting; San Francisco, USA; April 2014

J. Schwarzkopf; *Impact of compressional and tensile biaxially-anisotropic strain on the ferroelectric properties of epitaxial NaNbO$_3$ and SrTiO$_3$ films:* R. Wördenweber, J. Schwarzkopf, B. Cai, Y. Dai, D. Braun, J. Schubert, E. Hollmann; Joint IEEE International Symposium on the Applications of Ferroelectrics, International Workshop on Acoustic Transduction Materials and Devices & Workshop on Piezoresponse Force Microscopy (ISAF/IWATMD/PFM); Pennsylvania, USA; May 2014

Appendix: **Talks and Posters**

J. Sellmann; *Epitaxial PLD growth of strained piezoelectric $K_xNa_{1-x}NbO_3$ thin films and superlattices;* DPG–Frühjahrstagung 2014; Dresden, Germany; March/April 2014

J. Sellmann; *Film ratio dependece of piezo/ferroelectric properties in strained $K_{0.5}Na_{0.5}NbO_3$–based superlattices on $DyScO_3$;* E–MRS Fall Meeting 2014; Warsaw, Poland; September 2014

G. Wagner; *Ga_2O_3 and $(Ga_{1-x}Inx)_2O_3$ layers on beta-$Ga_2O_3(100)$ grown by metal organic vapour phase epitaxy;* TCO 2014; Leipzig, Germany; September/October 2014

G. Wagner; *Homo– and heteroepitaxial growth of beta-Ga_2O_3 layers by MO–VPE;* E–MRS Fall-meeting; Warschau, Poland; September 2014

R. Zwierz; *Microwave plasma enhanced vapour growth of single crystalline GaN layers;* DKT 2014 – DGKK Jahrestagung; Halle, Germany; March 2014

Poster presentations at national and international conferences

H. Ch. Alt, A. Kersch, H. E. Wagner, A. Glacki, Ch. Frank-Rotsch; *The 2060 cm^{-1} absorption band in gallium arsenide;* Defects in Semiconductors Gordon Research Conference; Waltham, Massachusetts, USA; August 2014

M. Baldini, M. Albrecht, D. Gogova, K. Irmscher, R. Schewski, M. Schmidbauer, G. Wagner; *$(Ga_{1-x}In_x)_2O_3$ layers grown by metal organic vapour phase epitaxy;* CIMTEC 2014, 6th Forum on New Materials; Montecatini Terme, Italy; June 2014

R. Bansen, C. Ehlers, J. Schmidtbauer, Th. Teubner, T. Boeck; *Solution Growth of Crystalline Si on Glass;* 29th EU PVSEC; Amsterdam, Netherlands; September 2014

R. Bertram, S. Ganschow; *Dotierungen in Saphir-Kristallen;* 17. Vortragstagung Fachgruppe Festkörperchemie und Materialforschung; Dresden, Germany; September 2014

S.Dadgostar, E.H. Hussein, W.T. Masselink, F. Hatami, J. Schmidtbauer, T. Boeck; *Structural properties of AlGaP films on GaP grown by gas–source molecular–beam empitaxy;* DPG–Tagung; Berlin, Germany, March 2014

S. Dadgostar, F. Hatami, W.T. Masselink, J. Schmidt-bauer, T. Boeck; *Self–assembled growth of InxGa1–xAs quantum dots on GaP by gas–source molecular–beam epitaxy;* DPG–Tagung; Berlin, Germany; March 2014

K. Kachel, N. Jankowski, S. Golka, Ch. Nenstiel, R. Zwierz, D. Siche, M. Bickermann; *Growth of GaN Layers with Controlled Carbon Doping by PHVPE;* IWN 2014, Int. Workshop on Nitride Semiconductors; Wroclaw, Poland; August 2014

D. Klimm; *Thermal analysis for crystal growth beyond 2000°C: Case studies;* 40 Years of GEFTA (Gesellschaft für Thermische Analyse); Berlin, Germany; September 2014

D. Klimm; *Growth and Characterization of Ce^{3+} doped Calciumferrate(III) Type Crystals;* 23th IUCr Congress; Montreal, Canada; August 2014

D. J. Kok, K. Irmscher, M. Naumann, C. Guguschev, Z. Galazka, R. Uecker; *Temperature dependence of the band gap of $SrTiO_3$: implications for the radiative heat transport at growth temperatures;* DKT 2014 – DGKK Jahrestagung; Halle, Germany; March 2014

D. J. Kok, K. Irmscher, M. Naumann, C. Guguschev, Z. Galazka, R. Uecker; *Temperature dependent optical properties of $SrTiO_3$;* MRS Fall meeting; Boston, USA; November/December 2014

S. Kollowa, A. Dittmar, C. Hartmann, K. Irmscher, F. Langhans, M. Pietsch, T. Schulz, J. Wollweber, M. Bickermann; *Silicon Doped AlN Bulk Crystals Grown by Physical Vapor Transport;* IWN 2014; Wroclaw, Polen; August 2014

S. Kollowa, A. Dittmar, C. Hartmann, F. Langhans, J. Wollweber, M. Bickermann; *Approach for Silicon Doping of AlN Bulk Crystals Grown by Physical Vapor Transport;* IWN 2014; Wroclaw, Polen; August 2014

E. Korhonen, F. Tuomisto, D. Gogova, G. Wagner, M. Baldini, Z. Galazka; *Vacancy defects in homo– and heteroepitaxial Ga_2O_3 thin films;* Int. Workshop Positron Studies Defects (PSD–14); Kyoto, Japan; September 2014

F. Langhans, C. Hartmann, T. Markurt, M. Naumann, M. Albrecht, A. Dittmar, S. Kollowa, T. Neugut, J. Wollweber, M. Bickermann; *Untersuchung von dekorierten Versetzungen in homoepitaktisch gewachsenen AlN Volumenkristallen;* DKT 2014; Halle, Germany; March 2014

R. Menzel, H. Riemann, N. Abrosimov, M. Renner; *Silizium Granulat Eigentiegelverfahren – Ergebnisse erster Experimente und numerischer Simulation;* Deutsche Kristallzüchtungstagung 2014 – Fraunhofer CSP; Halle, Germany; March 2014

R. Menzel, H. Riemann, N. Abrosimov; *Numerical model for Si single crystal growth from melt in a Si granular bed;* Modelling for Electromagnetic Processing" (MEP2014), Leibniz University of Hannover, Germany; September 2014

Appendix: **Talks and Posters**

S. Meyer, W. Kwapil, A. Zuschlag, Frank M. Kießling, M. Schumann, St. Riepe; *Direct and sensitive analysis of metals contaminating the edge zone of directionally solidified silicon;* DKT 2014 – DGKK Jahrestagung; Halle, Germany; March 2014

S. Richter, M. Werner, M. Schley, F. Schaaff, H. Riemann, H.-J. Rost, F. Zobel, R. Kunert, P. Dold, C. Hagendorf; *The influence of chemical purity of slim rods to the Siemens process and float zone crystallization;* DKT 2014; Halle, Germany; March 2014

J. Schwarzkopf, D. Braun, A. Kwasniewski, P. Müller, M. Schmidbauer; *Influence of lattice strain on ferro-electric domain formation in $K_xNa_{1-x}NbO_3$ thin films grown by MOCVD;* EMRS Fall Meeting; Warsaw, Poland; September 2014

C.E. Tommaseo, G. Wagner, M. Baldini; *XAFS analyses of homo- and heteroepitaxial grown $\beta-Ga_2O_3$ films on $\beta-Ga_2O_3$ and Al_2O_3 substrates;* BESSY User Meeting; Berlin, Germany; December 2014

Appendix: **Patents**

Granted

H. Riemann, H.-J. Rost
Vorrichtung zum tiegelfreien Zonenschmelzen von Halbleitermaterialstäben
DE 196 10 650.8

S. Ganschow, R. Bertram, D. Klimm, P. Reiche, R. Uecker
Verfahren und Anordnung zur Herstellung von ZnO-Einkristallen
DE 10 2004 003 596.2

Ch. Frank-Rotsch, P. Rudolph, R.-P. Lange, O. Klein, B. Nacke
Vorrichtung und Verfahren zur Herstellung von Kristallen aus elektrisch leitenden Schmelzen
DE 10 2007 028 548.7
08784553.3 (DK, ES, FR, NO)
KRIST*MAG*®

R.-P. Lange, M. Ziem, D. Jockel, P. Rudolph, F. Kießling, Ch. Frank-Rotsch, M. Czupalla, B. Nacke, H. Kasjanow
Vorrichtung zur Herstellung von Kristallen aus elektrisch leitenden Schmelzen
DE 10 2007 028 547.9
08784554.1 (DK, ES, FR, NO)
KRIST*MAG*®

Ch. Frank-Rotsch, P. Rudolph, R.-P. Lange, D. Jockel
Vorrichtung und Verfahren zur Herstellung von Kristallen aus elektrisch leitenden Schmelzen
DE 10 2007 046 409.8
KRIST*MAG*®

P. Rudolph, M. Ziem, R.-P. Lange
Vorrichtung zum Züchten von Einkristallen aus elektrisch leitfähigen Schmelzen
DE 10 2007 020 239.5
KRIST*MAG*®

R. Fornari, S. Ganschow, D. Klimm, M. Neubert, D. Schulz
Verfahren und Vorrichtung zur Herstellung von Zinkoxid-Einkristallen aus einer Schmelze
DE 10 2007 006 731.5

P. Rudolph, M. Ziem, R.-P. Lange, D. Jockel
Vorrichtung zur Herstellung von Kristallen aus elektrisch leitenden Schmelzen
DE 10 2008 035 439.2

F. Büllesfeld, U. Sahr, W. Miller, P. Rudolph, U. Rehse, N. Dropka
Verfahren zum Erstarren einer Nichtmetall-Schmelze
DE 10 2008 059 521.7
09 749 132.8 (DK, ES, IT, NO, R, GB)

R. Fornari
Vorrichtung und Verfahren zur Züchtung von III-Nitrid-Volumenkristallen
08 161 254.1 (DE, PL, FR, GB, SE)

P. Rudolph, R.-P. Lange, M. Ziem
Vorrichtung zur Herstellung von Sililziumblöcken
DE 10 2009 045 680.5

N. Dropka, P. Rudolph, U. Rehse
Verfahren und Anordnung zur Herstellung von Kristallblöcken von hoher Reinheit und dazugehörige Kristallisationsanlage
DE 10 2010 028 173.5

H. Riemann, N. Abrosimov, J. Fischer, M. Renner
Verfahren und Vorrichtung zur Herstellung von Einkristallen aus Halbleitermaterial
EP 2 504 470 (NO, ES, NL, FR, DK, GB, BE, IT)

N. Dropka, Ch. Frank-Rotsch, M. Ziem, P. Lange
Verfahren und Vorrichtung zur gerichteten Kristallisation von Kristallen aus elektrisch leitenden Schmelzen
DE 10 2012 204 313.6

N. Dropka, Ch. Frank-Rotsch, P. Rudolph, R.-P. Lange, U. Rehse
Kristallisationsanlage und Kristallisationsverfahren zur Herstellung eines Blocks aus einem Material, dessen Schmelze elektrisch leitend ist
DE 10 2010 041 061.6

O. Klein, F. Kießling, M. Czupalla, P. Rudolph, R.-P. Lange, B. Lux, W. Miller, M. Ziem, F. Kirscht
Verfahren und Vorrichtung zur Züchtung von Kristallen aus elektrisch leitenden Schmelzen, die in der Diamant- oder Zinkblendestruktur kristallisieren
DE 10 2009 027 436.7

Pending

U. Rehse, P. Rudolph, W. Miller, N. Dropka, F. Büllesfeld, U. Sahr
Method for the solidification of a non-metal melt
WO02012060802A3 (CN, US, TW)

R. Fornari, F. Kießling, P. Rudolph, V. Trautmann
Kristallisationsanlage und Kristallisationsverfahren
DE 10 2009 046 845.5

H. Riemann, N. Abrosimov, J. Fischer, M. Renner
Verfahren und Vorrichtung zur Herstellung von Einkristallen aus Halbleitermaterial
DE 10 2010 052 522.7
10801372.3 (EP), 13/511,751 (US), 2012-540285 (JP)

T. Boeck, R. Fornari, R. Heimburger, G. Schadow, J. Schmidtbauer, H.-P. Schramm, T. Teubner
Kristallisationsverfahren zur Erzeugung kristalliner Halbleiterschichten
DE 10 2010 044 014.0

F. Kießling, Ch. Frank-Rotsch, N. Dropka, P. Rudolph
Verfahren zur gerichteten Kristallisation von Ingots
DE 10 2011 076 860.2

Appendix: **Patents**

Z. Galazka, R. Uecker, R. Fornari
**Method and apparatus for growing indium oxide
(In$_2$O$_3$) single crystals and indium oxide (In$_2$O$_3$) single
crystal**
PCT/EP2012/057447

M. Wünscher, N. Werner
**Modellprädikative Regelung des Zonenschmelz-
verfahrens**
DE 10 2012 108 009.7
PCT/EP2013/067893

M. Wünscher, H. Riemann
**Vorrichtung für das tiegelfreie Zonenziehen von
Kristallstäben**
DE 10 2012 022 958.8
PCT/DE2013/000627

N. Dropka, Ch. Frank-Rotsch, P. Lange, P. Krause
**Kristallisationsanlage und Kristallisationsverfahren
zur Kristallisation aus elektrisch leitenden Schmelzen
sowie über das Verfahren erhältliche Ingots**
DE 10 2013 211 769.8
PCT/EP2014/059684

D. Linke
Vorrichtung zum Züchten von Ingots
DE 10 2013 220 130.3

A. Dittmar, C. Hartmann, J. Wollweber, U. Degenhardt,
F. Stegner
**Keimhalter einer Einkristallzüchtungsvorrichtung,
Einkristallzüchtungsvorrichtung und Komposit-
werkstoff**
DE 10 2014 017 021.7

Registered Trademark

KRIST*MAG*®

Appendix: **Teaching and Education**

Prof. Dr. Matthias Bickermann
- *Kristallzüchtung II: Methoden und Anwendungen;* Technische Universität Berlin, Institut für Chemie, WS 2013/14, WS 2014/15,
- *Kristallzüchtung I:* Grundlagen und Methoden; Technische Universität Berlin, Institut für Chemie, SS 2014
- ART.06 Kunst und Wissenschaft Chemie/Alchemie/ Kunst; S. Bürkle, M. Lerch, M. Bickermann, A. Grohmann, A. Gross, Technische Universität Berlin, WS 2013/14 und WS 2014/15

PD Dr. Detlef Klimm
- *Phasendiagramme;* Humboldt-Universität zu Berlin, Institut für Chemie, WS 2013/14, WS 2014/15
- *Thermische Analyse und thermische Eigenschaften;* Humboldt-Universität zu Berlin, Institut für Chemie, SS 2014
- *Versuch „Phasendiagramme"* im Fortgeschrittenen-Praktikum Physik; Humboldt-Universität zu Berlin, WS 2013/14, SS 2014, WS 2014/15
- *Festkörperchemie;* Humboldt-Universität zu Berlin, Institut für Chemie; Vertretung Prof. Pinna, WS 2013/14, WS 2014/15

apl. Prof. Dr. Dietmar Siche
- *Crystal Growth;* BTU Cottbus, SS 2014

Doctoral theses (ongoing)

Roman Bansen
Herstellung und Charakterisierung von polykristallinem Silicium auf Glas

Dorothee Braun
Ferro- und piezoelektrische Charakterisierungen von bleifreien Perowskitschichten

Christian Ehlers
Wachstum von Si/Ge-Nanostrukturen auf amorphen und kristallinen Substraten

Krzysztof Kachel
GaN-Kristallzüchtung aus der Gasphase ohne chemischen Ga-Transport

Stefan Kayser
Charakterisierung mono- und multikristalliner Halbleiter wie SiGe, Si_xGe_{1-x} und GaAs mit LPS- und SPL-Methoden

Dirk Kok
Einfluss der Züchtungsbedingungen auf die Realstruktur von $SrTiO_3$

Sandro Kollowa
Dotierung und Kompensation bei der Sublimationszüchtung von AlN-volumenkristallen

Frank Langhans
Untersuchung zur Wachstumskinetik und Oberflächenmorphologie bei der Sublimationszüchtung von AlN-Volumenkristallen

Toni Markurt
Elektronenmikroskopische Charakterisierung von InGaN –basierten Quantenstrukturen

Stefan Mohn
Elektronenmikroskopische Charakterisierung von heteropolaren Nitrid-Nitrid und Nitrid-Oxid Grenzflächen

Robert Schewski
Wachstum und Relaxation von Gruppe III Sesquioxiden

Jan Sellmann
Einfluss von epitaktischem Strain auf die funktionellen Eigenschaften von dünnen Perowskit-Schichten

Natalia Stolyarchuk
Investigation of III-Nitride/Oxide Interfaces at Atomic Scale

Doctoral theses (completed)

Alexander Glacki
VGF growth of 4'' GaAs single crystals with traveling magnetic fields
Humboldt-Universität Berlin, Institut für Physik

Nico Werner
Analysis and Automation of the crucible-free Floating Zone (FZ) Growth of Silicon Crystals
Technische Universität Berlin, Fakultät III – Prozesswissenschaften

Radoslaw Zwierz
Plasma- Enhanced Growth of GaN Single Crystallline Layers from Vapour Phase
Brandenburgische Technische Universität Cottbus

Diploma, Master and bachelor theses (completed)

Stefanie Krämer, Bachelor
Abscheidung von kristallinen SnO_2-Schichten auf TiO_2-, Al_2O_3 (1-102)- und Al_2O_3 (0001)-Substrat mittels Dip-Coating-Verfahren; Universität Potsdam, Fachbereich Chemie

Jan Leuschner, Bachelor
Wolfram als Diffusionssperre für die AlN-Kristallzüchtung; Technische Universität Berlin, Fachbereich Chemie

Philipp Müller, Diplom
Strukturelle Untersuchungen an verspannten Kaliumniobatschichten; Technische Universität Berlin, Physikalische Ingenieurswissenschaft

Appendix: **Membership in Committees**

Committees

Rainer Bertram
- DIN – Deutsches Institut für Normung e.V. – NA 062 – Normenausschuss Materialprüfung (NMP), member

Dr. Christiane Frank-Rotsch
- Deutsche Gesellschaft für Kristallzüchtung und Kristallwachstum (DGKK), secretary
- International Organization for Crystal Growth (IOCG), member of the council
- European Network of Crystal Growth (ENCG), member of the council

PD Dr. Detlef Klimm
- International Union of Crystallography, Commission on Crystal Growth and Characterization of Materials, member

Dr. Wolfram Miller
- European Network of Crystal Growth (ENCG), member of the executive committee

Editoral committees

Prof. Dr. Matthias Bickermann
- Progress in Crystal Growth and Characterization of Materials, Elsevier B.V., associate editor

PD Dr. Detlef Klimm
- Special issue Crystal Research & Technology, guest editor

Conference committees

Dr. Martin Albrecht
- International Workshop on Nitride Semiconductors (IWN2014), Wroclaw 2014, Poland, program committee

Prof. Dr. Matthias Bickermann
- 11th International Conference on Ceramic Materials and Components for Energy and Environmental Applications (CMCEE-11), 2016, Vancouver, Canada, co-organisator of session "Crystalline materials and devices for electro-optical and biomedical applications"

- International Workshop on Bulk Nitride Semiconductors (IWBNS), member of international advisory committee

Dr. Christiane Frank-Rotsch
- Fifth European Conference on Crystal Growth (ECCG5), 2015, Bologna, Italy, member of advisory board

- 18th International Conference on Crystal Growth and Epitaxy (ICCGE-18), 2016, Nagoya, Japan, member of advisory board

PD Dr. Detlef Klimm
- 23th IUCr Congress, Montreal 2014, Canada, co-organisator of session "Recent Development of Widegap Materials; Semiconductor and Oxides"
- E-MRS Spring Meeting 2014, Lille, France: Gemeinsam mit M. Neubert, T. Duffar, M. Dudley Organisation Symposium U "Crystal growth related twins and point defects in semiconductors and dielectrics"

apl. Prof. Dr. Dietmar Siche
- First European School on Crystal Growth (ESCG), member of scientific committee

International Workshop on Crystal Growth Technology (IWCGT-6) Berlin 2014 Committee members from IKZ:

Conference Chair:
Prof. Dr. Matthias Bickermann

Steering committee:
Dr. Frank M. Kießling, Dr. Reinhard Uecker

Program committee:
Prof. Dr. Matthias Bickermann, Dr. Michael Neubert

Local organization and program committee:
Sabine Bergmann, Prof. Dr. Matthias Bickermann, Dr. Christiane Frank-Rotsch, Steffen Ganschow, Dr. Christo Guguschev, Andrea Lepper, Dr. Robert Menzel, Uwe Rehse, Dr. Maike Schröder, apl. Prof. Dr. Dietmar Siche

Appendix: **Guest Scientists at IKZ**

01.01. 2014 – 31.12. 2014

Asdrubal Antonio Botero
04.08. – 26.09.2014
National University of Columbia, Bogotá, Columbia

Prof. A.A. Ezhewskii
30.10. – 05.11.2014
Nizhny Novgorod State University, Russia

Prof. Dr. Karen Gambaryan
16.01. – 30.01.2014
Yerevan State University, Department of Physics,
Yerevan, Armenia

Jorge Andrés Guerra Torres
04.11. 2013 – 02.02.2014
Pontificia Universidad Católica del Perú, Peru

Dr. Mutong Niu
01.01. – 31.12.2014
Suzhou Institute of Nano–tech and Nano–bionics,
Chinese Acadmey of Sciences, Suzhou, Jiangsu Province,
Peoples Republic of China

Aleksy Patryn
20.10. – 31.10.2014
Koszalin University of Technology, Russia

Prof. Dr. Petr G. Sennikov
02.01. – 10.01.2014
18.07. – 31.08.2014
12.09. – 19.09.2014
RAS – Institute of Applied Physics, Russia

Dr. Tobias Schulz
01.01. – 31.12.2014
Humboldt–Universität zu Berlin

Prof. Mike Thewalt
13.09. – 16.09.2014
Simon Fraser University, Burnaby, Canada

Appendix: **Colloquia at the IKZ**

Dr. Horst Bettin
Physikalisch–Technische Bundesanstalt (PTB),
Braunschweig
„Die Avogadro–Konstante und das geplante
Einheitensystem", January 2014

PD Dr. Detlef Klimm
IKZ
„Hochtemperatur–Thermodynamik: Redox–Stabilität
von Werkstoffen & Materialien", February 2014

M.Sc. Eng. Tomasz Sochacki
Polish Academy of Science and TopGaN Ltd.,
Institute of High Pressure Physics, Poland
"Halide Vapor Phase Epitaxy of GaN on
ammonothermally grown GaN seeds", February 2014

Dipl.–Phys. Sandro Kollowa
IKZ
„Dotierung mit Silizium und Sauerstoff bei der
Sublimationszüchtung von Aluminiumnitrid–Volumen–
kristallen", February 2014

Prof. Dr. Mathias Schubert
University of Nebraska–Lincoln, Electrical Engineering,
USA
"Generalized Ellipsometry and the Optical Hall effect:
Characterization of Anisotropic Materials from single
crystalline to complex–structured Media", March 2014

Prof. Dr. Lars Arnberg
Norwegian University of Science and Technology,
Materials Science and Engineering, Norway
"Research on crystallisation of solar silicon at NTNU",
March 2014

PD Dr. Martin Schmidbauer
IKZ
"Ferroelectric domains in strained $NaNbO_3$ epitaxial
thin films", March 2014

Prof. Dr. Russell D. Dupuis
Georgia Institute of Technology, Microelectronics/Micro–
systems, Optics and Photonics, Atlanta, Georgia, USA
"AlGaN based UV Lasers and Avalanche Photodiodes",
March 2014

Dr. Holger von Wenckstein
Universität Leipzig, Institut für
Experimentelle Physik II, Abteilung Halbleiterphysik
"Compositional approach to wide band–gap
semiconducting oxides", March 2014

M.Sc. Dirk Kok
IKZ
"Temperature dependence of the band gap of $SrTiO_3$:
implications for radiative heat transport at growth
temperatures", April 2014

Dr. Michael Neubert
IKZ
„Schmelzkristallzüchtung – von der Systemanalyse zur
modellbasierten Regelung", April 2014

Dr. Howard Dawson
Anacortes, Washington, USA
"Rod stress and causes of poly rod fracture during
poly–Si deposition", April 2014

Dr. Torunn Ervik
IKZ
"Dislocations in directionally solidified crystalline
silicon – generation mechanisms and interactions",
May 2014

Dr. Kevin Keller
Technische Universität Bergakademie Freiberg,
Institut für Mineralogie
"Investigation of shock–synthesized rocksalt–type
aluminum nitride", May 2014

PD Dr. Stefan Krischok
Technische Universität Ilmenau, Institut für Physik und
Institut für Mikro– und Nanotechnologien Forscher–
gruppe Oberflächenphysik funktioneller Nanostrukturen
"Surface properties of polar and nonpolar InN and GaN:
In situ studies on MBE grown thin films", May 2014

Dr. Jan Schmidtbauer
IKZ
"MBE Growth and Characterization of Germanium
Nanowires", June 2014

MSc.–Phys. Iryna Buchovska
Department of Pillar LTD, Kiev
"Defect engineering of directionally solidified silicon on
industrial scale", June 2014

Prof. Dr. Ramón Collazo
North Carolina State University, Department of
Materials Science and Engineering; USA
"Identification and control of point defects in
AlGaN and AlN", August 2014

Dr. Keisuke Shigetoh
Toyota Central R&D Labs, Inc; Japan
"Sublimation growth of bulk aluminum nitride in a no–
vel tantalum carbide coating crucible", September 2014

Dr. Andrew A. Allerman
Sandia National Laboratories, Albuquerque,
 New Mexico, USA
"Low–dislocation–density AlGaN templates for UV laser
diodes", September 2014

Prof. Dr. Mike Thewalt
Simon Fraser University, Department of Physics,
Burnaby, Canada
"Highly enriched 28Si – a 'semiconductor vacuum'",
September 2014

Dr. Leo J. Schowalter
Crystal IS Green Island, New York, USA
"AlN substrates from bulk crystals for high performance
UVC LEDs"

Appendix: **Colloquia at the IKZ**

Prof. Dr. Peer Schmidt
Brandenburgische Technische Universität Cottbus–
Senftenberg, Fakultät für Naturwissenschaften
„Flüchtige Bekannte: Analyse der Phasenbildung und
Kristallzüchtung mit Elementen der Gruppen 15 und
16", October 2014

PD Dr. Eduard Lavrov
Technische Universität Dresden, Halbleiterphysik
"Hydrogen in ZnO and TiO_2", October 2014

Prof. Dr. Martina Schmid
Helmholtz–Zentrum Berlin für Materialien und
Energie GmbH
"Nano– and microconcentrators for the next
generation of Chalcopyrite solar cells", October 2014

Dr. Tim Wernicke
Technische Universität Berlin, Institut für Festkörper–
physik, AG Experimentelle Nanophysik und Photonik
"Growth of AlGaN based UV emitters by MOVPE",
November 2014

Dr. Nicolaj Moll
IBM Zürich, Department Cognitive Computing and
Computational Sciences, Quantum Technology Group,
Switzerland
"First–Principles Computations for Surface Science",
November 2014

M.Sc. Phys. Dorothee Braun
IKZ
"Ferroelectric properties in strained (K,Na)NbO3 thin
films", December 2014

M.Sc. Eng. MBA Jason Schmitt
Nitride Solutions Inc., Wichita, Kansas, USA
"Aluminum Nitride, an electronic device and thermal
management material", December 2014

Appendix: **External Funding**

Joint Initiative for Research and Innovation

Effizienter Züchtungsprozess für GaAs im kombinierten Heizer-Magnet-Modul; 2011–2014

Homo- and heteroepitaxy of transparent semiconducting oxide layers of the Ga_2O_3-In_2O_3-Al_2O_3 ternary system on beta-Ga_2O_3 and In_2O_3-Substrates; 2012–2015

Growth of high perfection bulk SrTiO3 single crystals; 2013–2016

International programs

Cost-reduction through material optimisation and Higher EnErgy output of solAr pHotovolatics modules – joining Europe's Research and Development efforts in support of ist PV industry; EU, 2014–2017

Programs of Federal Ministry of Education and Research (BMBF) and Federal Ministry of Economics and Technology (BMWi)

SolarWinS: Einfluss nichtdotierender Verunreinigungen auf die elektrische Aktivität von Kristalldefekten; BMBF, 2011–2014

Entwicklung, Umsetzung und Professionalisierung eines Verwertungskonzepts am Leibniz-Institut für Kristallzüchtung; BMBF, 2011–2014

Entwicklung hochtemperaturstabiler Tiegelkomponenten für die einkristalline Züchtung nitridischer Halbleiter (N-Keramik); BMWi (Zentrales Innovationsprogramm Mittelstand ZIM); 2012–2014

Investigation and surface characterization of InAsSbP-, Si- and Ge-nanostructures for mid-infrared and thermoelectric applications; International Bureau of BMBF, 2013–2014

Erforschung des human- und ökotoxikologisch relevanten Löslichkeits- und Reaktionsverhalens von GaAs sowie verwandter Arsenide und Phosphide im Verbundprojekt TEMPO: Toxikologische, physikalisch-chemische und gesellschaftliche Erforschung innovativer Materialien und Prozesse der Optoelektronik; BMBF, 2013–2016

Induktiv gekoppelter Niederdruck-Plasmareaktor zur Nitrid-Einkristallzüchtung; BMWi (zentrales Innovationsprogramm Mittelstand ZIM); BMBF, 2013–2015

InTerFEL: Zeitaufgelöste und nichtlineare Infrarot- und Terahertz-Spektroskopie mit einem FEL; BMBF, 2014–2017

Entwicklung einer Nitrid-Schaumkeramik als Graphitersatz; BMWi (Zentrales Innovationsprogramm Mittelstand ZIM), 2014–2016

Plasmaabscheidung von GaN-Bauelementen PlanB – Elektronenmikroskopische Analyse und Modellierung der Wachstums- und Relaxationsprozesse von PSD InAlGaN-Schichten auf Saphir und Silizium Substraten; BMBF, 2014–2017

DFG

Lösungsmittelgenerierte Phasenumwandlung zur Erzeugung kristalliner Si-Schichten; 2011–2014

Science of polar homo- and heterointerfaces; 2012–2015

Entwicklung einer Züchtungstechnologie für semi-isolierende GaN-Substrate und Untersuchung der in-situ Kohlenstoffdotierung; 2014–2017

Funding by partners from industry and other institutions

Growth and characterization of new oxide single crystals; CrysTec GmbH, Berlin, DE; 2005–2014

Growth and characterization of new oxide crystals for piezoelectric sensors; Kistler Instrumente AG, Winterthur, CH; 2005–2019

Polysilicon Analysis; REC Silicon Inc. (US), 2010–2014 Asymmetrisch geschnittene Siliziumkristalle für Blaze-Gitter; Helmholtz-Zentrum Berlin für Materialien und Energie, DE; 2011–2014

KILOGRAMM-2; Physikalisch-Technische Bundesanstalt, Braunschweig, DE; 2011–2015

Entwicklung einer 200mm GaN auf Silizium-Wafer-Technologie für die Herstellung von Leuchtdioden und Leistungselektronikbauelementen; Azzurro Semiconductors AG, DE; 2012–2014

Growth and characterization of silicon crystals; Elkem Solar A/S, NO; 2012–2014

Züchtungsexperimente zur Validierung der GFZ-Modellierung; Siltronic AG, Burghausen, DE; 2012–2014

Berlin, September 2015